


Spring 4-15-2019

MECHANISMS OF ORIENTED CELL DIVISION AND THEIR ROLES IN TISSUE DEVELOPMENT

Evan Blake Dewey
University of New Mexico

Follow this and additional works at: https://digitalrepository.unm.edu/biol_etds

 Part of the [Biochemistry Commons](#), [Biology Commons](#), [Cancer Biology Commons](#), [Cell Biology Commons](#), [Developmental Biology Commons](#), and the [Molecular Biology Commons](#)

Recommended Citation

Dewey, Evan Blake. "MECHANISMS OF ORIENTED CELL DIVISION AND THEIR ROLES IN TISSUE DEVELOPMENT." (2019). https://digitalrepository.unm.edu/biol_etds/312

This Dissertation is brought to you for free and open access by the Electronic Theses and Dissertations at UNM Digital Repository. It has been accepted for inclusion in Biology ETDs by an authorized administrator of UNM Digital Repository. For more information, please contact amywinter@unm.edu.

Evan B. Dewey

Candidate

Biology

Department

This dissertation is approved, and it is acceptable in quality and form for publication:

Approved by the Dissertation Committee:

Christopher A. Johnston, Chairperson

Richard M. Cripps

Stephen A. Stricker

Helen J. Hathaway

**MECHANISMS OF ORIENTED CELL DIVISION AND THEIR
ROLES IN TISSUE DEVELOPMENT**

by

EVAN B. DEWEY

Bachelor's of Science, Biochemistry, University of Oregon, 2012

DISSERTATION

Submitted in Partial Fulfillment of the
Requirements for the Degree of

Doctor of Philosophy

Biology

The University of New Mexico
Albuquerque, New Mexico

May, 2019

ACKNOWLEDGMENTS

I would like to thank my advisor, Christopher Johnston for his guidance, inspiration, and support. I would like to thank my committee members, Rich Cripps, Steve Stricker, and Helen Hathaway for their time, positive feedback and encouragement. I would also like to thank the entire Johnston Lab for moral and technical support.

I would also like to thank my family and friends for their help and support during my time as a graduate student, I would not be here without them.

**MECHANISMS OF ORIENTED CELL DIVISION AND THEIR ROLES IN
TISSUE DEVELOPMENT**

By

Evan B. Dewey

Bachelor's of Science, Biochemistry, University of Oregon, 2012

DISSERTATION

Submitted in Partial Fulfillment of the
Requirements for the Degree of

Doctor of Philosophy

Biology

The University of New Mexico
Albuquerque, New Mexico

May, 2019

ABSTRACT

Properly executed cell division is crucial to development, maintenance, and longevity of multicellular organisms. Defects in both symmetric and asymmetric divisions can lead to improper developmental patterning, as well as genomic instability, disruption of tissue homeostasis, and cancer. Our research focuses on how regulators orchestrate proper cell divisions. Mushroom Body Defect (Mud) is one such regulator, and here we describe how Mud is regulated via the Hippo signaling pathway kinase Warts (Wts), showing Wts phosphorylates Mud to enhance interaction with the polarity protein Partner of Inscuteable, promoting spindle orientation activity. We next focus on another regulator, Shortstop (Shot), describing a role for Shot in cell divisions, with both tissue culture and *in vivo* *Drosophila* epithelial models showing spindle assembly, spindle misalignment, and chromosome migration defects in Shot knockdowns (KDs). These activities are mediated not only through traditional Shot roles in stabilization of spindle MTs through crosslinks to actin, but also through direct interaction of Shot to dynein activator subunit actin-related protein 1 (Arp1). We hypothesize Shot interaction with Arp1 functions to crosslink it to spindle MTs, facilitating MT motor protein Dynein activity, promoting its activities in cell division. Live cell imaging experiments show defects in cell division timing under Shot KD conditions, implicating involvement of the spindle assembly checkpoint (SAC). Inhibition of SAC components under Shot KD conditions leading to timing rescue. Shot loss *in vivo* leads increases in apoptosis, in line with previous findings linking mitotic regulators to cell death. Previous studies implicated induction of the jun-N-kinase

(JNK) apoptotic pathway under spindle regulator KD, but Shot KD apoptosis likely does not utilize JNK. When Shot KD-induced apoptosis is inhibited, tumorigenic-like conditions result, underscoring the importance of Shot as a key component in development and maintenance of multicellular organisms. Shot KD-induced apoptosis is likely mediated via p53 and the DNA damage response (DDR), with DNA double strand breaks occurring in Shot KD, and additionally enhanced when coupled to SAC inhibition. Finally, we utilize mRNA sequencing (RNAseq) to describe Shot KD-induced genes involved in DDR, highlighting a distinct mechanism to mitigate loss of a key oriented cell division regulator.

TABLE OF CONTENTS

LIST OF FIGURES	VIII
INTRODUCTION	1
CHAPTER 1.....	11
WARTS PHOSPHORYLATES MUD TO PROMOTE PINS-MEDIATED MITOTIC SPINDLE ORIENTATION IN <i>DROSOPHILA</i> INDEPENDENT OF YORKIE	11
ABSTRACT	12
INTRODUCTION.....	13
RESULTS	16
DISCUSSION.....	36
EXPERIMENTAL PROCEDURES.....	41
CHAPTER 2.....	47
DIVERSE MITOTIC FUNCTIONS OF THE CYTOSKELETAL CROSSLINKING PROTEIN SHORTSTOP SUGGEST A ROLE IN DYNEIN/DYNACTIN ACTIVITY.....	47
ABSTRACT	48
INTRODUCTION.....	49
RESULTS	52
DISCUSSION.....	75
MATERIALS AND METHODS.....	83
CHAPTER 3.....	91
MECHANISMS OF APOPTOSIS INDUCED BY LOSS OF SHORTSTOP IN <i>DROSOPHILA</i> WING DISC EPITHELIAL TISSUE	91
ABSTRACT	92
INTRODUCTION.....	93
RESULTS	95
DISCUSSION.....	101
MATERIALS AND METHODS.....	107
REFERENCES	113

LIST OF FIGURES

INTRODUCTION

FIGURE 1: MECHANISMS OF ORIENTED CELL DIVISION.....	3
---	---

CHAPTER 1

FIGURE 1: WARTS LOCALIZES TO MITOTIC SPINDLE POLES IN MITOTIC S2 CELLS.....	17
---	----

FIGURE 2: THE CORE HIPPO KINASE COMPLEX IS REQUIRED FOR ROBUST PINS-MEDIATED SPINDLE ORIENTATION IN POLARIZED S2 CELLS	20
--	----

FIGURE 3: HIPPO SIGNALING ACTS INDEPENDENTLY OF ITS CANONICAL EFFECTOR, YORKIE, TO CONTROL S2 CELL SPINDLE ORIENTATION.....	23
---	----

FIGURE 4: WARTS DIRECTLY PHOSPHORYLATES MUD WITHIN ITS C-TERMINAL COILED-COIL DOMAIN	25
--	----

FIGURE 5: MUD PHOSPHORYLATION MODULATES ITS DIRECT INTERACTION WITH PINS.....	28
---	----

FIGURE 6: WARTS KINASE IS DISPENSABLE FOR SPINDLE POLE MUD LOCALIZATION BUT NECESSARY FOR ITS CORTICAL ASSOCIATION WITH PINS	30
--	----

FIGURE 7: WARTS IS REQUIRED FOR CORTICAL MUD LOCALIZATION AND SPINDLE ORIENTATION IN WING IMAGINAL DISC EPITHELIAL CELLS	31
--	----

CHAPTER 2

FIGURE 1: SHOT LOCALIZES TO MITOTIC SPINDLE POLES AND DIRECTLY BINDS ARP-1	55
--	----

FIGURE 2: SHOT IS REQUIRED FOR MITOTIC SPINDLE ORIENTATION.....	59
---	----

FIGURE 3: SHOT IS REQUIRED FOR FOCUSING OF MITOTIC SPINDLE POLES.....	62
---	----

FIGURE 4: SHOT IS REQUIRED FOR POLEWARD CONGRESSION OF MITOTIC CHROMOSOMES.....	64
---	----

FIGURE 5: SHOT LOSS ACTIVATES THE SAC TO DELAY MITOTIC EXIT ...	67
---	----

FIGURE 6: SHOT LOSS INDUCES CHROMOSOME SEGREGATION DEFECTS.....	70
---	----

FIGURE 7: SHOT LOSS ACTIVATES APOPTOSIS IN <i>DROSOPHILA</i> EPITHELIA AND LEADS TO DISRUPTION OF TISSUE MORPHOLOGY.....	73
--	----

CHAPTER 3

FIGURE 1: SHOT LOSS CAUSES DSBS IN IMAGINAL WING DISCS; LEVELS OF DSBS, BUT NOT APOPTOSIS, ARE INCREASED WHEN SAC IS DISRUPTED96

FIGURE 2: LOSS OF P53 AFFECTS SHOT RNAI TISSUE; SAS-4 RNAI TISSUE IS UNAFFECTED99

FIGURE 3: DIFFERENTIAL GENE EXPRESSION IN SHOT RNAI AND SAS- 4 RNAI IMAGINAL WING POUCH TISSUE.....101

INTRODUCTION

To successfully reproduce and thrive, multicellular organisms must properly develop and maintain a multitude of complex tissues. Oriented cell divisions both facilitate the formation of novel tissue in development and preserve the integrity of existing tissues in multicellular organisms. In development, undifferentiated cells must divide in such a way to produce new cell types and create a proper body pattern for an organism. Once an organism has reached adulthood, it must maintain its tissues properly through homeostasis. Throughout an organism's lifetime, tissues must replace old, unhealthy, or compromised cells with new cells of the same type through oriented divisions of neighboring, healthy cells of the same type. When defective, oriented divisions can lead to improper development of key tissues/organ systems and result in a malformed organism (Vorhagen and Niessen, 2014; Zhong and Zhou, 2017). In adults, complications from oriented divisions can lead to tumors in various tissues, and in some cases, cause transformation of healthy cells to malignant (cancerous) ones (Bonello and Peifer, 2019; Tellkamp et al., 2014). Given the multitude of consequences from aberrant oriented divisions, a clear understanding of their mechanisms is crucial to preventing both abnormal development and formation of tumors and cancers.

Several different cell types across diverse organisms have been utilized to better understand oriented divisions in both development and adult tissue homeostasis. These include *C. elegans* embryos, *Drosophila* neuroblasts and wing disc sensory organ precursor cells, and *M. musculus* epidermal cells, all of which have helped determine key factors involved in fidelity of oriented cell

divisions. Collectively, these systems have yielded mechanisms common to the process. First, the dividing cell must establish and maintain an axis of polarity. This axis asymmetrically distributes certain components to different parts of the cell membrane, often done through posttranslational modifications to regulate locations of each component (Figure 1A). Once polarity has been established, it must be maintained, usually through spatial restriction of components via posttranslational modification (both through those used in polarity establishment and in some cases through additional ones; Figure 1B). Once the axis of polarity is established and maintained, the cell can begin to divide in such a way that either unevenly distributes polarity factors (as in differentiation in development), or evenly distributes these factors to maintain cell identity (as in tissue homeostasis; Figure 1D). The mitotic spindle must be oriented properly such that each new cell obtains an appropriate amount of DNA along with the specified factors. To do this, the spindle must first be contacted by the membrane components (a process called spindle capture) and subsequently be aligned to polarity components via molecular force (referred to as force generation; Figure 1C). With appropriate establishment and maintenance of polarity coupled to robust spindle capture, force generation and spindle alignment, oriented cell divisions can occur reliably, allowing for success of the developmental and homeostatic processes they underpin. Many components and pathways have been identified that facilitate mechanisms of oriented cell divisions, and two such pathways will be the primary focus of this dissertation.

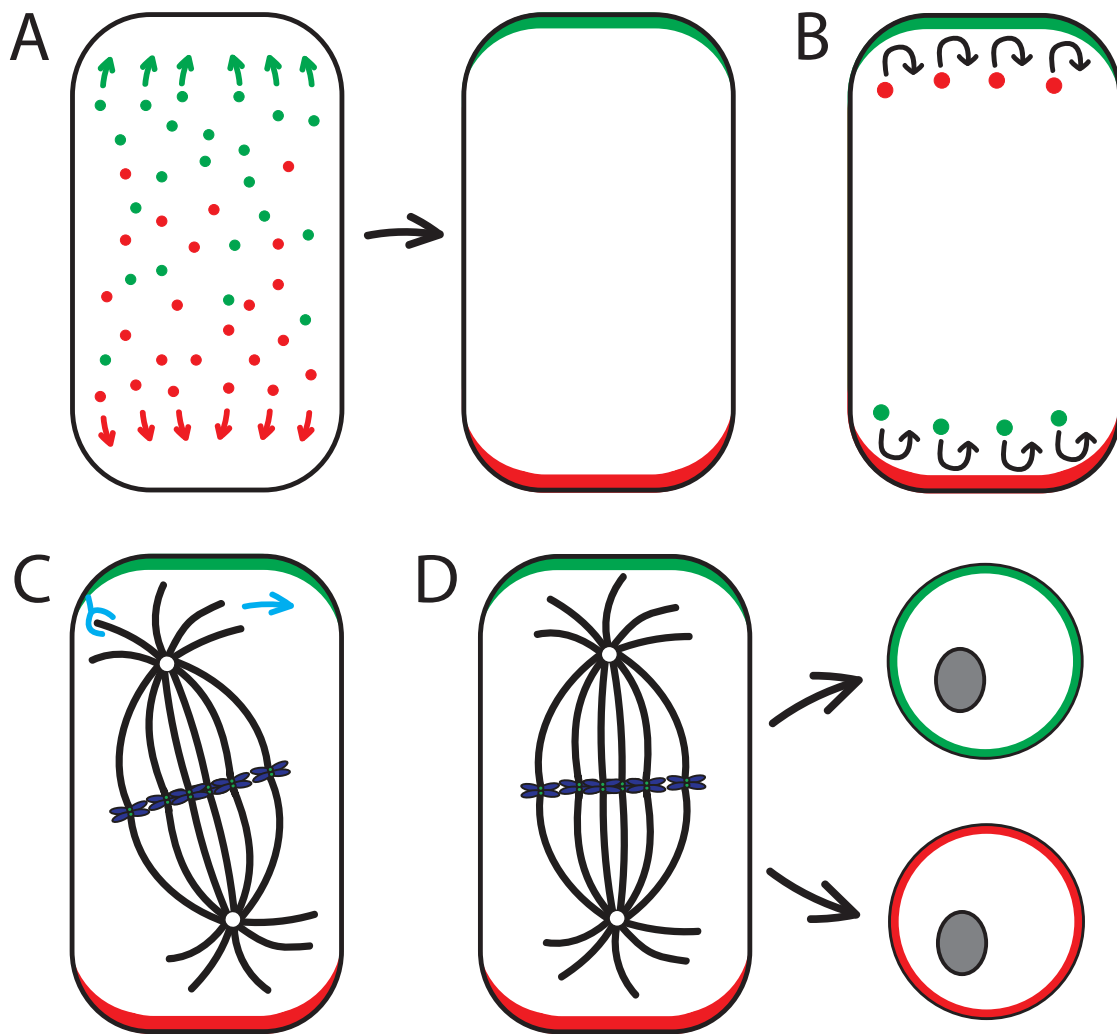


Figure 1. Mechanisms of Oriented Cell Division. (A) Polarity must first be established through proper segregation of fate determinants and polarity cues to particular locations on the cell membrane, a process typically done via posttranslational modification (e.g. phosphorylation). (B) Once polarity is established, it must be maintained. Components must be confined to their respective sides of the membrane, with posttranslational modifications again playing a role in restricting membrane binding at improper locations. (C) After polarity is established and maintained, the spindle must be aligned properly relative to the polarity cues. This is done in two steps: first, spindle capture binds and tethers the spindle to the membrane (blue hook), and second spindle force generation utilizes molecular (specifically microtubule) motors to direct the spindle to the midpoint of the polarity cue (blue arrow). (D) Once the spindle is aligned, the cell can then divide, ensuring that cell fate determinants are distributed properly to each new daughter cell.

Studies in *C. elegans* embryos were among the first to yield significant information about the establishment of polarity and oriented cell divisions. These embryos must divide asymmetrically in order to ensure proper *C. elegans*

development. Many genes involved in these divisions were named for their partitioning defect phenotype, as knockout embryos were unable to effectively establish polarity and partition cell fate determinants to the appropriate areas of the membrane. Without polarity, the spindle was misaligned in the initial asymmetric division, and daughter cells lost their asymmetry and identity (Etemad-Moghadam et al., 1995; Grill et al., 2001; Kempthues et al., 1988). Key to establishing and maintaining polarity in these embryos is a complex involving PAR-3, PAR-6, and PKC-3. This complex, which is known as the anterior PAR complex, initially localizes throughout the membrane, before breaking symmetry and receding to the anterior side of the embryo (Cuenca et al., 2003; Munro et al., 2004). Together this complex functions to restrict posterior components via phosphorylation of PAR-2 by PKC-3 (Hao et al., 2006). Conversely, posterior complex protein PAR-2 also functions with PAR-1 and PAR-5 to exclude the anterior complex protein PAR-3 (Hao et al., 2006; Motegi et al., 2011). Once this polarity has been established and maintained, a force generating complex acts to capture astral microtubules to promote the centering and rotation of centrosomes such that they are positioned along the A-P axis. This complex consists of the proteins $G\alpha$, GPR-1/2, LIN-5, and the minus end directed microtubule motor dynein (Colombo et al., 2003; Gotta et al., 2003; Nguyen-Ngoc et al., 2007; Srinivasan et al., 2003). Dynein functions as the main generator of force, with other proteins in the force generating complex serving to connect dynein (and thus the spindle) to the cortex (Nguyen-Ngoc et al., 2007). The cortically tethered $G\alpha$ interacts with GPR1/2, which binds LIN-5, which further interacts with Dynein

(Couwenbergs et al., 2007; Kotak et al., 2012; Nguyen-Ngoc et al., 2007; Park and Rose, 2008; Srinivasan et al., 2003). When the centrosomes are positioned properly via this force-generating complex, the spindle can then form, with the force-generating complex continuing to maintain spindle alignment to the A-P axis during this process. While G α is uniformly localized throughout the cortex (Gotta and Ahringer, 2001), GPR1/2 and LIN-5 are restricted to the anterior and posterior cortices through a PAR dependent manner (Colombo et al., 2003; Galli et al., 2011; Gotta et al., 2003; Park and Rose, 2008), connecting polarity to spindle orientation. Many of these proteins further play a role in subsequent divisions of the P2 and EMS cells of the embryo, underscoring the importance of these proteins in oriented divisions and cell fate specification throughout *C. elegans* development (Werts et al., 2011).

Drosophila neuroblasts are another area in which oriented cell divisions have been well characterized. Neuroblasts must divide asymmetrically to self-renew and produce a ganglion mother cell that goes on to differentiate into neurons and neuroglia (Dewey et al., 2015c; Doe, 2008; Lu and Johnston, 2013). Many of the components involved in neuroblast divisions are the subject of Chapter 1 of this dissertation. Polarity establishment involves localization of an apical complex consisting of Par-3 (also known as Bazooka), Par-6, and atypical protein kinase C (aPKC) (Petronczki and Knoblich, 2001; Wodarz et al., 1999), plus a basal complex comprising Miranda (Mir), Prospero (Pros), Brain tumor (Brat), and Numb (Betschinger et al., 2006; Lee et al., 2006a). Once the polarity domains are established, aPKC with activation from Par-6 helps restrict basal

components via phosphorylation of Numb and Miranda (Atwood and Prehoda, 2009; Graybill and Prehoda, 2014; Smith et al., 2007). After polarization, two pathways stemming from the protein partner of inscuteable (Pins) function to align the spindle to the apical cortex. Pins is recruited to the membrane via interactions with Insc and G α_i and interacts with proteins discs large (Dlg) and mushroom body defect (Mud) to capture and align the spindle, respectively (Johnston et al., 2009; Nipper et al., 2007; Siller et al., 2006; Yu et al., 2000). Dlg functions in spindle capture by binding both to Pins and the plus end directed microtubule motor kinesin Khc-73, while Mud functions in force generation to align the spindle via its interactions with Pins and minus end directed microtubule motor dynein (Lu and Prehoda, 2013; Wang et al., 2011). Pins was found to bind to Dlg via an Aurora A kinase regulated phosphorylation of its LINKER domain, and to bind Mud via its TPR domain through an unknown regulatory mechanism (Johnston et al., 2009). Regulation of Mud-Pins binding is the primary subject of Chapter 2.

M. musculus epidermal cells provide yet another model for studying oriented cell division. Epidermal cells must divide parallel to the apical-basal axis of the tissue early in development, and switch to perpendicular divisions later in development in order to begin stratification of the epidermis. It is the later divisions that require polarity to asymmetrically distribute cell fate determinants such that the basal daughter cell maintains its identity and the apical daughter inherits proteins that specify differentiation. Here polarity is once again dictated by Par3, Par6, and aPKC, but with structural proteins α -catenin and β_1 -integrin

important to their proper localization (Lechler and Fuchs, 2005; Raghavan et al., 2000). LGN (the Pins homolog in mammals) is once again localized to the apical membrane via $G\alpha_{i3}$ and mInsc (Du and Macara, 2004; Zhu et al., 2011). However, LGN localization via mInsc has been shown to be mutually exclusive to its interaction with NuMA (the Mud homolog in mammals), suggesting potentially distinct roles for Par3-mInsc-LGN and $G\alpha_{i3}$ -LGN-NuMA complexes in oriented cell division (Zhu et al., 2011). Similar to its role in *Drosophila*, mouse LGN functions to bind NuMA to interact with Dynein to properly align the spindle to the apical cortex and perpendicular to the epithelial plane (Lechler and Fuchs, 2005; Poulson and Lechler, 2010; Williams et al., 2011). Less clear is the role that Dlg (with 5 mammalian isoforms) plays in this regulation, with some studies pointing to Dlg1 and Dlg5 as likely candidates (Nechiporuk et al., 2013; Roberts et al., 2007). Yet others propose that due to the near complete decoupling of the spindle from cortical polarity in NuMA depletions, there may not be a role for Dlg at all in these divisions, and instead NuMA may provide both the spindle capture and force generation roles (Williams et al., 2011).

Drosophila imaginal wing discs provide a key model for studying how defects in oriented cell divisions affect epithelial tissue development. Many genetic tools exist to drive knockdown of specific regulators in discrete sections of wing disc tissue, providing a precise and rapid method for analysis. In this manner, genes discovered in other contexts and organisms can be tested for relevancy. Large scale oriented divisions in the wing disc occur along the proximal-distal (PD) axis (Baena-Lopez et al., 2005; Gonzalez-Gaitan et al.,

1994). PD axis growth was found to depend on the atypical cadherins Fat and Daschous, and the atypical myosin Dachs, exerting constriction in a polarized manner to ensure divisions occur in the proper direction (Baena-Lopez et al., 2005; Mao et al., 2011a). Disruptions in the actomyosin cortex as well as knockdowns of the spindle alignment regulator Mud and polarity proteins Scribble and Dlg result in divisions out of the plane of wing disc epithelial tissue (Nakajima et al., 2013). Cells that divide aberrantly delaminate from the tissue and subsequently die, and when death is blocked, these cells undergo an epithelial-to-mesenchymal-like transition, resulting in tumor-like masses (Nakajima et al., 2013). Mechanisms underlying apoptosis in wing disc cells was further explored when knockdowns of centriolar duplication regulators were found to cause widespread cell death (Poulton et al., 2014). Activation of jun-N-terminal kinase (JNK) signaling was found to be critical to apoptosis of these cells, functioning in a stress response to the loss of centrosomes. However, many of these discs were found to continue development normally, thanks mostly to a process called compensatory proliferation, in which neighboring cells that presumably were those not affected by RNAi and retained intact centrosomal duplication processes were able to compensate for cells lost due to apoptosis (Poulton et al., 2014).

Work has also been done in *Drosophila* imaginal wing discs on mechanisms of oriented cell division in *Drosophila* sensory organ precursor cells (SOPs), which undergo a series of asymmetric divisions to generate the trichome hair structures of the adult wing. In the first of these divisions, the pl cell must

orient its division relative to two different axes: 1. the apical-basal axis which is controlled via Pins and 2. the anterior-posterior axis, which is regulated by non-canonical activities of wingless proteins dishevelled (Dsh) and Frizzled (Fz) (David et al., 2005; Gho and Schweisguth, 1998). Dsh is recruited to the membrane via interaction with Fz, and interacts with Mud and Dynein to generate force that aligns the spindle after capture (Segalen et al., 2010). However, the Dsh pathway differs in how it may capture the spindle, and instead of functioning with Dlg and Khc-73, it polarizes F-actin via interactions with the G-protein Rho and actin-polymerizing formin Diaphanous (Dia) (Johnston et al., 2013). This polarized F-actin could work to interact with and capture spindle microtubules (MTs) through an actin-microtubule crosslinking protein.

A key actin-microtubule crosslinker (and the focus of much of this dissertation) is the protein Shortstop (Shot). Shot is the sole actin-microtubule crosslinker in *Drosophila*, and was originally characterized in axon extension in developing embryos (Kolodziej et al., 1995; Lee et al., 2000). Shot is also found in mammals as MACF1 (also known as ACF7), and is not only a critical regulator of cell migration, cell proliferation, embryo development, but is also implicated in human disease (Bouameur et al., 2014; Chen et al., 2006; Jorgensen et al., 2014; Ka et al., 2014; Kodama et al., 2003; Roper and Brown, 2003; Wu et al., 2008). Shot can bind to F-actin through its tandem calponin homology domains and to MTs via its growth arrest specific-like 2 domain (Lee and Kolodziej, 2002a, b). Shot has been found to stabilize and organize MTs *in vivo* via crosslinks to F-actin (Applewhite et al., 2010; Sanchez-Soriano et al., 2010; Sanchez-Soriano et

al., 2009). Shot was found to first localize to the plus (growing) ends of MTs via interaction with the protein EB1 and once localized it bound to the MT lattice in an F-actin dependent manner (Alves-Silva et al., 2012; Applewhite et al., 2010). Regulation of Shot crosslinking activity is through intramolecular inhibition between the N- and C- terminus, with relief of this inhibition coming only in the presence of F-actin (Applewhite et al., 2013). Notably, all of this characterization of Shot was done in interphase contexts, with its role in mitosis previously unexplored.

Each of the chapters of this dissertation has foundations in previous work done on oriented cell division, tissue development, and characterizations of Shot. Chapter 1 describes a novel regulation of the key spindle orientation protein Mud (NuMA in mammals and LIN-5 in *C. elegans*), Chapter 2 describes numerous and previously undescribed roles of Shot in cell division as well as in tissue development, and Chapter 3 determines mechanisms by which Shot causes defects in tissue development. Together, the chapters of this dissertation advance understanding of cell division, its regulators, and their roles in tissue development.

CHAPTER 1

Warts phosphorylates Mud to promote Pins-mediated mitotic spindle orientation in *Drosophila* independent of Yorkie

From Current Biology 25: 2751-2762

Evan B. Dewey, Desiree Sanchez, and Christopher A. Johnston

ABSTRACT

Multicellular animals have evolved conserved signaling pathways that translate cell polarity cues into mitotic spindle positioning to control the orientation of cell division within complex tissue structures. These oriented cell divisions are essential for the development of cell diversity and the maintenance of tissue homeostasis. Despite intense efforts, the molecular mechanisms that control spindle orientation remain incompletely defined. Here we describe a role for the Hippo (Hpo) kinase complex in promoting Partner of Inscuteable (Pins)-mediated spindle orientation. Knockdown of Hpo, Salvador (Sav), or Warts (Wts) each result in a partial loss of spindle orientation, a phenotype previously described following loss of the Pins-binding protein Mushroom body defect (Mud). Similar to orthologs spanning yeast to mammals, Wts kinase localizes to mitotic spindle poles, a prominent site of Mud localization. Wts directly phosphorylates Mud *in vitro* within its C-terminal coiled-coil domain. This Mud coiled-coil domain directly binds the adjacent Pins-binding domain to dampen the Pins/Mud interaction, and Wts-mediated phosphorylation uncouples this intramolecular Mud interaction. Loss of Wts prevents cortical Pins/Mud association without affecting Mud accumulation at spindle poles, suggesting phosphorylation acts as a molecular switch to specifically activate cortical Mud function. Finally, loss of Wts in *Drosophila* imaginal disc epithelial cells results in diminished cortical Mud and defective planar spindle orientation. Our results provide new insights into the molecular basis for dynamic regulation of the cortical Pins/Mud spindle

positioning complex and highlight a novel link with an essential, evolutionarily-conserved cell proliferation pathway.

INTRODUCTION

During cell division the mitotic spindle apparatus directs the localization of the actomyosin contractile ring and cleavage furrow ingression; thus, spindle positioning serves as an essential determinant of cell division orientation. Two fundamental aspects of animal development arise from this principle. First, spindle orientation directs the asymmetric segregation of cell fate determinants during stem cell divisions, providing a means of balancing self-renewal and differentiation. For example, uncoupling of spindle orientation from the cortical polarity axis in *Drosophila* neuroblasts can contribute to an overproliferation of these neural stem cells, disrupting proper CNS development and resulting in severe tissue overgrowth phenotypes (Cabernard and Doe, 2009; Lee et al., 2006a). Second, the establishment and maintenance of complex tissue structures relies on spindle orientation in order to balance cell divisions that lead to tissue expansion versus stratification. For example, spindle orientation defects in the mouse epidermis result in defective stratification, yielding tissue structures that are incapable of proper fluid and electrolyte regulation (Lechler and Fuchs, 2005). Despite being linked to several developmental disorders and having recently emerged as a possible contributor to tumorigenesis (Gonzalez, 2007), the molecular details of spindle orientation process remain incomplete.

The conserved Partner of Inscuteable (Pins) protein regulates spindle orientation in diverse cell types from model organisms spanning metazoan evolution and represents perhaps the best-characterized regulator of spindle positioning (Bellaïche et al., 2001; Colombo et al., 2003; Du et al., 2001; Lee et al., 2006b; Schaefer et al., 2001). Pins is thought to control spindle orientation through two synergistic pathways: (1) its tetratricopeptide repeat (TPR) domains directly bind Mushroom body defect (Mud) to activate dynein-dependent spindle forces, and (2) its phosphorylated 'Linker' domain directly binds Discs large (Dlg) to capture microtubule plus ends through the kinesin motor protein Khc-73 (Johnston et al., 2009; Lu and Johnston, 2013). Mud/dynein-mediated forces generate rapid spindle oscillations to position the metaphase spindle prior to anaphase onset (Colombo et al., 2003; Kotak et al., 2012). Mud is a spindle pole/centrosomal protein that becomes cortically polarized in a Pins-dependent manner. Loss of Pins in *Drosophila* neuroblasts, which induces spindle orientation defects, prevents cortical Mud enrichment without affecting its spindle pole localization (Bowman et al., 2006; Siller et al., 2006). Mud at spindle poles contributes to spindle assembly processes, whereas cortical Mud localization is essential for proper spindle positioning. Furthermore, cortical targeting of dynein-mediated forces appears to be sufficient for spindle orienting activity (Kotak et al., 2012). Together, these results suggest distinct Mud functions are elicited through differential subcellular localizations and highlight the importance of cortical localization in Mud-mediated spindle orientation. Recent studies have demonstrated Ran- and CDK1-dependent pathways that prevent cortical Mud

association; however, the molecular mechanisms that promote the formation of cortical Pins/Mud remain largely undefined (Kiyomitsu and Cheeseman, 2012; Kotak et al., 2013).

Using a combination of biochemical, cellular, and genetic methods, we define a role for the Hippo kinase complex, an eminent regulator of cell growth and proliferation (Zhao et al., 2011), in Pins/Mud-mediated spindle orientation. The core complex components Hippo (Hpo), Salvador (Sav), and Warts (Wts) are each required for spindle orientation to a cortically polarized Pins cue. RNAi directed against individual Hpo components results in a partial loss of spindle orientation, a unique phenotype previously described following selective loss of the Mud/dynein arm of Pins signaling. Wts localizes to mitotic spindle poles and directly phosphorylates Mud *in vitro* within its terminal coiled coil (Mud^{CC}) domain. We also show that Mud^{CC} directly interacts with the adjacent Pins-binding domain (Mud^{PBD}) to regulate its Pins binding capacity. Wts phosphorylation prevents this putative intramolecular interaction, suggesting Wts functions to enhance Pins/Mud complex formation. Consistent with this, loss of Wts prevents Pins-mediated cortical Mud accumulation without perturbing its accumulation at spindle poles. Finally, Wts-directed RNAi results in defective Mud localization and a loss of planar spindle orientation in *Drosophila* imaginal wing disc epithelial cells. Together, our results demonstrate a novel mode of regulating Pins/Mud-dependent spindle orientation through the Hippo tumor suppressor pathway, highlighting an important intersection between cell cycle and spindle orientation pathways.

RESULTS

Warts and Mud localize to spindle poles in mitotic S2 cells.

To identify molecular pathways that promote polarized cortical Mud localization, we reasoned that proteins localized to mitotic spindle poles with cell cycle-dependent activity would represent attractive candidates. The Hippo kinase complex localizes to spindle pole bodies (SPB) in *S. cerevisiae* (the yeast equivalent of centrosomes), and its activity increases throughout mitosis to ultimately induce anaphase onset and mitotic exit through the Mitotic Exit Network (MEN) signaling system (Hotz and Barral, 2014; Menssen et al., 2001). Interestingly, Cdc15 (the yeast Hippo ortholog) activity is necessary for proper orientation of the mother SPB into the nascent bud cell; however, this effect is mediated through asymmetric activity of centrosomal Kar9, a protein with no apparent metazoan ortholog (Hotz et al., 2012). MEN activity is dependent on spindle pole body activity of Dbf2, the yeast equivalent of Wts. Studies using both mouse and human cell culture systems have confirmed that components of the Hippo complex, in particular the Wts kinase orthologs LATS1/2, also localize to spindle poles/centrosomes where they control centrosome disjunction, chromosome segregation, and cell cycle progression (Guo et al., 2007; Mardin et al., 2011; Mardin et al., 2010; Morisaki et al., 2002; Toji et al., 2004; Yabuta et al., 2011). We have thus focused herein on the role of Hippo signaling in oriented cell division using *Drosophila* as a model system.

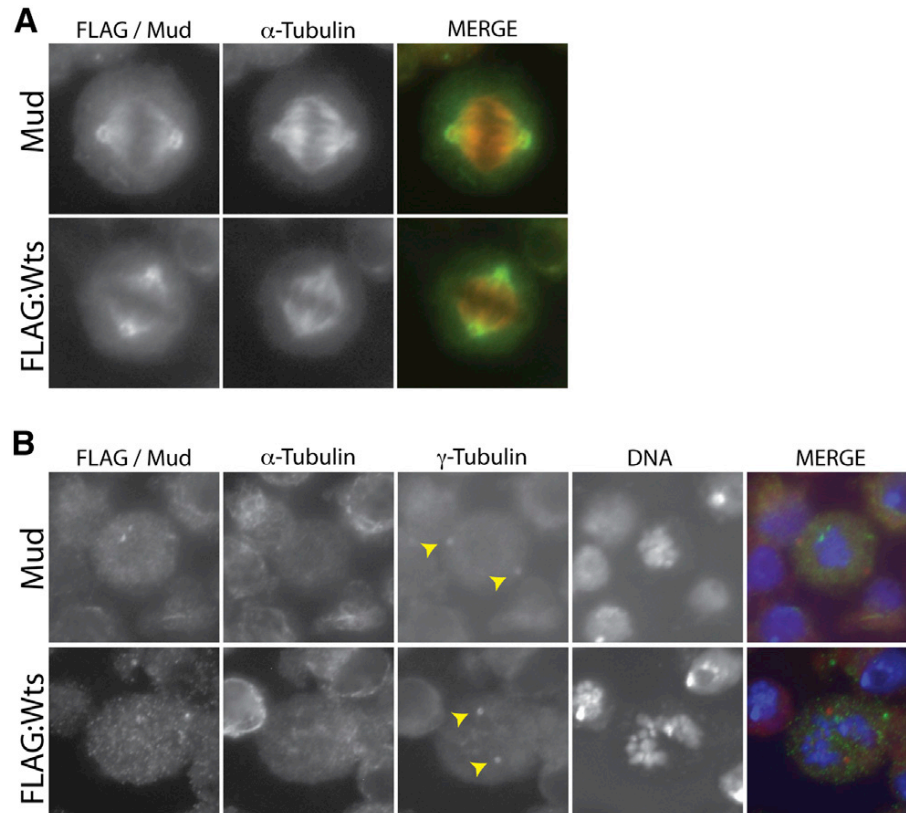


Figure 1. Warts localizes to mitotic spindle poles in mitotic S2 cells. (A) Cells were transfected with full-length Warts tagged with an N-terminal FLAG epitope sequence (FLAG:Wts) and stained with antibodies against FLAG and α -tubulin. To visualize endogenous Mud, we stained untransfected cells with an α -tubulin and Mud antibodies. (B) To depolymerize spindle microtubules, cells were treated with colchicine (12.5 μ M) for 2 hours prior to fixation and antibody staining. Yellow arrowheads indicate both γ -tubulin-positive centrosomes, to which neither Wts nor Mud show significant localization. α -tubulin staining indicates successful depolymerization of spindle microtubules; note this channel is not shown in the merge panel.

We first examined the cellular localization of Wts, the key kinase output in Hippo signaling, in *Drosophila* S2 cells. We cloned full-length Wts from an S2 cDNA library, indicating this gene is endogenously transcribed, and expressed low amounts as a FLAG-tagged transgene. As shown in Figure 1, FLAG-Wts localized to mitotic spindle poles, including proximal regions of their emanating

microtubules. This localization in S2 cells is identical to that seen with endogenous Mud (Figure 1). We further examined Mud and Wts localization following colchicine-induced microtubule depolymerization. Colchicine treatment resulted in primarily cytoplasmic localization of both Mud and Wts with no significant localization at γ -tubulin positive centrosomes, consistent with localization specifically to spindle poles and proximal spindle microtubules. These results are in agreement with previous studies of Mud localization (Izumi et al., 2006). We conclude that Wts kinase localization resembles that of Mud both spatially and temporally at mitotic spindle poles.

Hippo kinase signaling is required for Pins-mediated spindle orientation.

We next investigated whether the Hippo complex regulates spindle positioning in S2 cells using an ‘induced polarity’ reconstitution assay (Johnston et al., 2009). Cells were transfected with the cell adhesion molecule Echinoid (Ed) fused to Pins at its intracellular C-terminus (Ed:Pins), which localizes specifically to sites of cell-cell contact, thus generating Ed-dependent cortical polarization of Pins in an otherwise non-polarized cell. Spindle orientation is then measured relative to these induced polarity crescents within small, otherwise isolated clusters (2-3 cells) containing one contiguous patch of Ed:GFP signal (Figure 2A). As previously reported, the mitotic spindle exhibits robust alignment to the center of this Ed:Pins crescent, whereas cells expressing Ed alone display random spindle orientation (Figure 2C). Also consistent with our previous studies, treatment of cells with RNAi directed against Mud resulted in a partial loss of Ed:Pins-mediated spindle orientation, intermediate between the effects of Ed:Pins and Ed

(Figure 2B,C). This partial loss-of-function phenotype contrasts with the complete dysfunction induced by Dlg^{RNAi} , and is the result of attenuated dynein-mediated spindle forces (Johnston et al., 2009). Individual RNAi treatments against Hpo, Sav, or Wts each caused a partial loss of spindle orientation phenotype that was statistically indistinguishable from Mud^{RNAi} , which can be seen in representative images (Figure 2B) as well as when expressed as a cumulative percent across the entire sample of cells collected (Figure 2C). To control for potential off-target effects, we designed two additional RNAi sequences for each Hippo component that targeted distinct regions of their coding sequences. These alternative RNAi treatments all produced phenotypes identical to the initial results, suggesting that off-target effects were unlikely (Figure S1). We also quantified spindle orientation relative to the outer edge of the Ed:Pins crescent; whereas control cells preferentially orient spindles to the crescent center, a tighter coupling between spindles and the crescent edge is observed following RNAi against Hpo, Sav, or Wts, a result that also mirrors the effects of Mud^{RNAi} (Figure 2D). This phenotype is consistent with residual activity of the spindle-capturing Dlg/Khc-73 pathway, which can operate in the absence of the Mud/Dynein pathway, and suggests that the core Hippo complex is dispensable for Dlg/Khc-73 function (Johnston et al., 2009). Thus, these results suggest that the Hpo/Sav/Wts complex functions specifically within the Pins/Mud/dynein spindle orientation pathway and serves as a positive modulator of its activity.

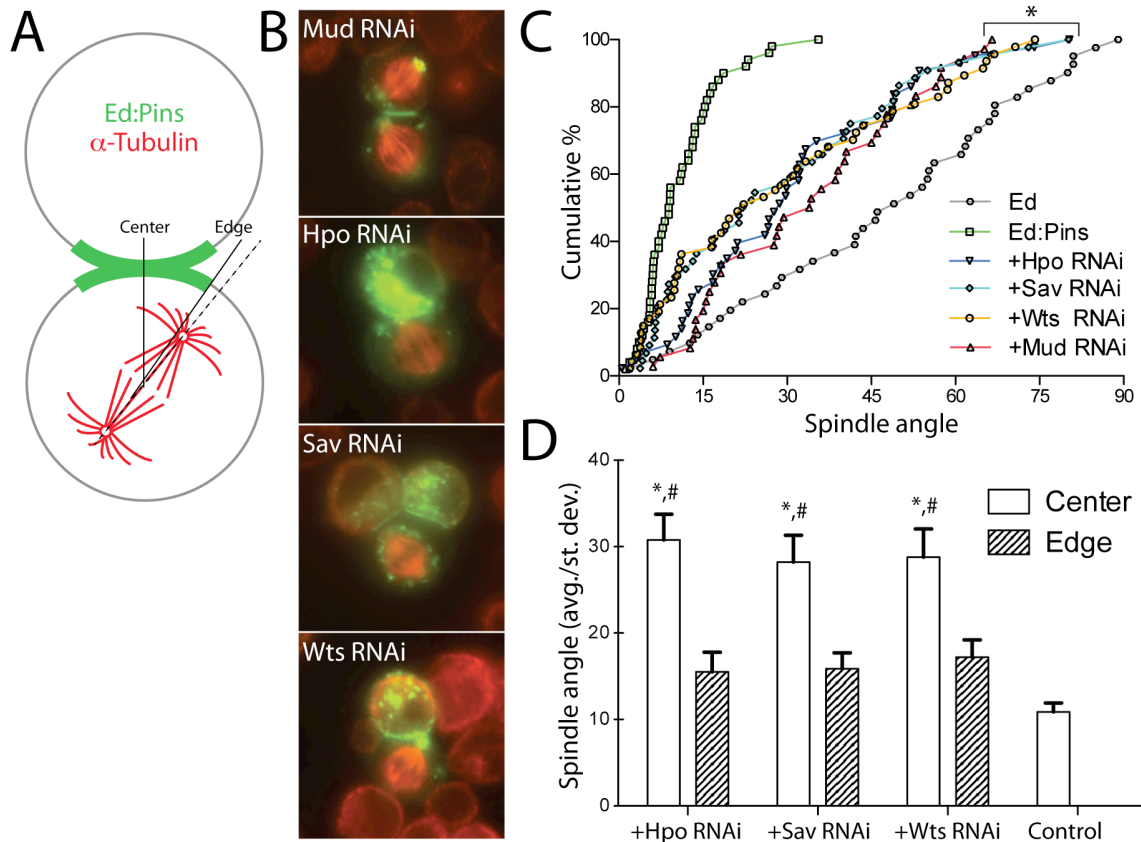


Figure 2. The core Hippo kinase complex is required for robust Pins-mediated spindle orientation in polarized S2 cells. (A) Schematic overview of induced polarity assay. Cells are transfected with Pins fused to the truncated intracellular C-terminus of the adhesion protein Echnoid (Ed), which also contains GFP for visualization. Cell adhesion induces polarized Ed-based crescents, relative to which mitotic spindle orientation is measured. (B) S2 cells were transfected with Ed:GFP:Pins and subsequently treated with dsRNAi against indicated protein. Cells were fixed and stained with an α -tubulin antibody. In addition to the contact-induced cortical crescent, Ed:GFP:Pins often forms cytoplasmic puncta that can accumulate at peri-centrosomal regions. This localization can still occur in the presence of each RNAi treatment, suggesting that neither the Hippo complex nor Mud are required for this non-cortical localization. Also, previous studies have shown spindle orientation to be independent of the amount of puncta present (Johnston et al., 2009). (C) Spindle angles from at least 30 individual cells for each genotype are plotted as the cumulative percentage of cells at or below a given angle of spindle orientation. Each RNAi causes a phenotype intermediate between fully active Ed:Pins and the Ed alone negative control. Each RNAi condition was statistically different from both Ed and Ed:Pins but not one another (*, $p < 0.05$ ANOVA with Tukey's *post-hoc* test). (D) Spindle angles were measured relative to the Ed:Pins crescent edge (grey filled bars) and center (open bars) for each condition. Fully active Ed:Pins (Control) positions spindles more closely to the center, whereas Hpo, Sav, and Wts RNAi preferentially orient spindles to the edge similar to Mud RNAi. *, $p < 0.05$ for 'center' versus 'edge' values within respective genotypes; #, $p < 0.05$ for given RNAi 'center' compared to Control 'center', ANOVA followed by Tukey's *post-hoc* test. The absence or presence of peri-centrosomal Ed:Pins puncta was similar across all conditions examined and did not show any significant correlation with spindle angle measurements, demonstrating they neither interfere with nor contribute to the spindle orientation process. See also Figure S1.

Wts is a member of the NDR (nuclear Dbf2-related) protein kinase family, which also includes the evolutionarily-conserved NDR1/2 kinase, Tricornered (Trc) (Hergovich et al., 2006). Despite strong primary sequence homology and identical consensus phosphorylation target motifs, Trc participates in functions distinct from Wts. Trc localizes to the cytoplasm and cell cortex and maintains extended cellular structures, such as epidermal hair and dendritic branches in sensory neurons (Emoto et al., 2004). As knockdown of kinases could have pleiotropic effects, we reasoned that Trc would serve as an ideal negative control. Indeed, Trc^{RNAi} treatment did not significantly alter Ed:Pins-mediated spindle orientation (10.4 ± 6.2 , n=49 compared to 11.0 ± 14.5 , n=47 with Trc^{RNAi}), consistent with a Wts-specific regulation of Pins/Mud function in S2 cells.

Hippo signaling controls spindle orientation independent of Yorkie.

The canonical phosphorylation target of Wts kinase is the transcriptional regulator, Yorkie (Yki), which normally promotes cell cycle progression through upregulation of genes such as c-myc and cyclin-E (Huang et al., 2005; Wu et al., 2003). Yki phosphorylation, however, prevents its nuclear translocation and function, resulting in cytoplasmic retention thereby explaining the growth suppressive effects of canonical Hpo pathway (Oh and Irvine, 2008). As Wts^{RNAi} treatment would be predicted to increase Yki activity, we designed two approaches to assess whether elevated Yki function may contribute to spindle orientation defects following loss of Wts. First, we simultaneously treated cells with both Wts^{RNAi} and Yki^{RNAi} to determine if Yki^{RNAi} could suppress Wts^{RNAi}-mediated effects. However, as shown in Figure 3B, combined RNAi against Wts

and Yki did not differ from Wts^{RNAi} alone. Treatment of cells with Yki^{RNAi} alone did not perturb Ed:Pins function either, indicating Yki is also not necessary for spindle orientation. Combined treatment with Wts^{RNAi} and Mud^{RNAi} did not differ from treatment with either alone (Figure 3B), adding further support that Wts functions together with Mud to regulate spindle orientation. Second, we overexpressed a constitutively active, 'phosphodead' Yki mutant (Yki^{S168A}) and monitored for a potential dominant phenotype. Yki^{S168A} expression did not significantly affect Ed:Pins-mediated spindle orientation, however. As a complementary approach, we also overexpressed the Yki target gene cyclin-E as another means of mimicking the possible effects of enhanced Yki activity. As with Yki itself, cyclin-E overexpression did not significantly alter spindle orientation (Figure 3A,B). Conditions leading to reduced Wts or Mud function again resulted in precise alignment to crescent edges, whereas cells with compromised Yki function remained oriented preferentially to the middle of Ed:Pins crescents (Figure 3C). These results collectively suggest that the effects of Wts^{RNAi} on spindle orientation are Yki-independent and likely act through an alternative, 'non-canonical' pathway.

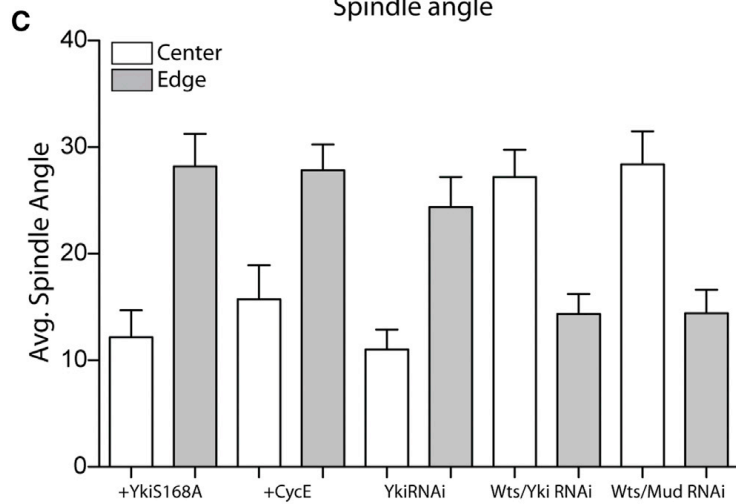
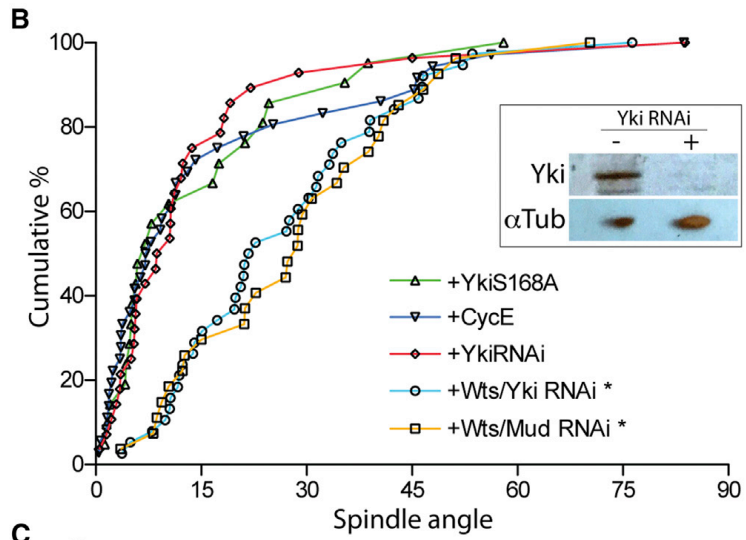
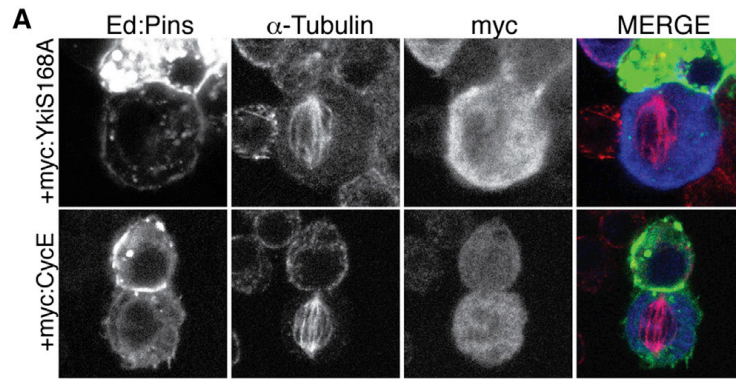


Figure 3. Hippo signaling acts independently of its canonical effector, Yorkie, to control S2 cell spindle orientation. (A) Cells were transfected with Ed:GFP:Pins together with either Yorkie-S168A (YkiS168A) or cyclin-E (CycE) as N-terminal c-myc tag fusion constructs. Cells were fixed and stained with antibodies against α -tubulin and the c-myc epitope. (B) Cumulative percentage plots for indicated genotypes. Neither CycE nor YkiS168A affect Ed:Pins function; RNAi against Yki was also without effect. Combined treatment of Wts and Yki RNAi or Wts and Mud RNAi resulted in spindle orientation similar to either Wts or Mud RNAi alone. *Inset*: western blot (20 μ g total S2 cell lysate protein) indicating robust knockdown of Yki protein expression in cells treated with Yki^{RNAi}. *, $p < 0.05$ compared to Ed:Pins, ANOVA followed by Tukey's *post-hoc* test. (C) Spindle angles were measured relative to the Ed:Pins crescent edge (*grey filled bars*) and center (*open bars*) for each condition. In each genotype, edge and center measurements were statistically separated, $p < 0.05$, ANOVA followed by Tukey's *post-hoc* test.

Warts directly phosphorylates Mud at its C-terminal coiled-coil domain.

Spindle pole localization at metaphase, the phenocopy of Mud^{RNAi} treatment, and the lack of Yki-dependent effects all lead us to explore the hypothesis that Wts functions directly within the Mud pathway. Wts is a serine/threonine kinase that preferentially phosphorylates the consensus sequence motif H-x-R/K-x-x-S/T (where 'H' represents Histidine, 'R/K' represent Arginine/Lysine, and 'x' represents any amino acid) (Hao et al., 2008). Although basic residues at the -2 and/or -3 positions are characteristic of several protein kinase families, the histidine at -5 is the signature preference of the Wts recognition motif, although its presence may not be absolutely mandatory. Using the Eukaryotic Linear Motif (ELM; <http://elm.eu.org/>) program, we performed *in silico* analyses of Pins/Mud pathway components (Lu and Johnston, 2013), revealing a single, strongly predicted Wts phosphorylation site within Mud itself. This site lies within the C-terminal Mud coiled-coil domain (Mud^{CC}) at serine-1868 (S1868; Figure 4A). To directly examine this prediction experimentally, we cloned and purified the Mud^{CC}

domain to homogeneity (Figure 4D) and qualitatively examined phosphorylation using an [γ - 32 P]-ATP radiometric kinase assay with purified Wts. As shown in Figure 4B, Wts directly phosphorylated Mud^{CC}. A single alanine substitution at the predicted phosphorylation site (S1868A) completely abolished the detected signal. These results demonstrate that S1868 in the Mud^{CC} domain is a direct *in vitro* substrate of Wts kinase.

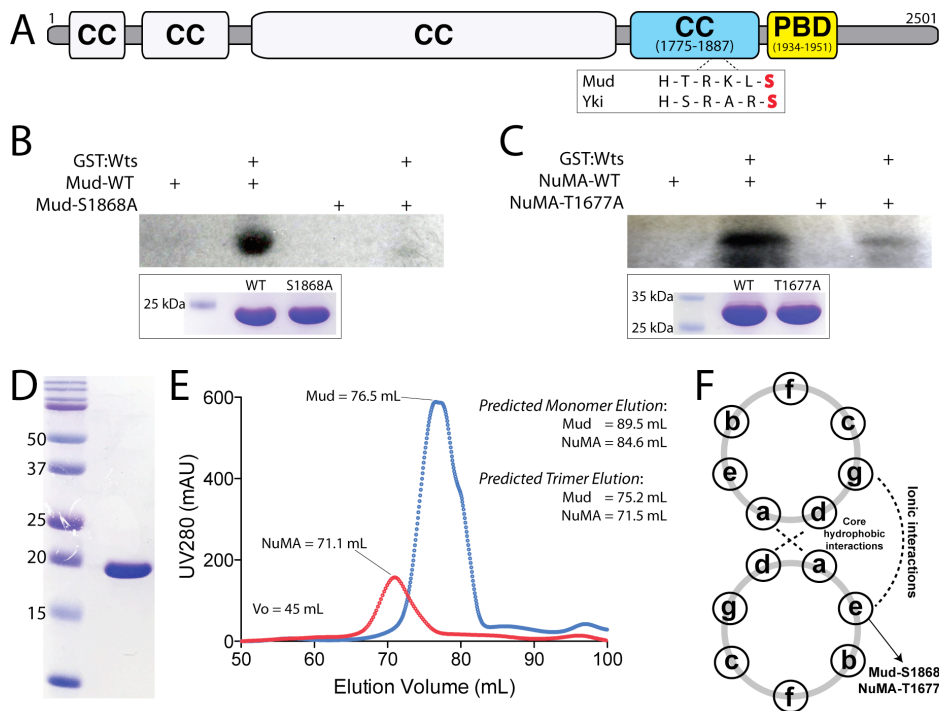


Figure 4. Warts directly phosphorylates Mud within its C-terminal coiled-coil domain. (A) The domain architecture of Mud consists primarily of coiled coil (CC) domains. The most C-terminal of these (Mud^{CC}; blue) contains a single consensus phosphorylation motif for Wts kinase that closely resembles that found in Yki. Immediately following this domain is the minimal Pins-binding domain (Mud^{PBD}; yellow). (B) Mud^{CC}, wild-type (MudCC-WT) or a single S1868A mutant (MudCC-S1868A), were incubated in the absence or presence of GST:Wts kinase together with [γ - 32 P]-ATP. Radioactive phosphate incorporation was assessed by autoradiography using Kodak BioMax-MS radioisotope film. *Inset below*: Coomassie stain of reaction inputs showing equal levels of Mud protein between phosphorylation conditions. (C) Identical experiments carried out with the NuMA^{CC} domain and the corresponding T1677A mutant. (D) Coomassie stained gel indicating homogenous purity of the Mud^{CC} protein purification. (E) Both Mud^{CC} and NuMA^{CC} domains elute from a size-exclusion column at volumes consistent with trimers. Predicted elution volumes were calculated from a standard curve performed on the HiLoad Superdex 200 column (GE Healthcare). (F) Schematic of coiled-coil heptad repeat residue interactions. Both S1868 in Mud^{CC} and T1677 in NuMA^{CC} are predicted to reside at 'e' positions, which participate in ionic interactions in an ideal coiled-coil. See also Figure S2.

The mitotic functions of Mud, particularly those of the cortical Pins/Mud complex, appear to be evolutionarily conserved, yet the overall primary sequence conservation across Mud orthologs is remarkably low (Bowman et al., 2006; Siller et al., 2006). Sequence comparison between orthologous Mud^{CC} domains specifically, however, reveals that Wts phosphorylation is likely to be a conserved regulatory mechanism (Figure S3). NuMA, the mammalian Mud ortholog, contains numerous predicted phosphorylated sites (Yang et al., 1992), and the NuMA C-terminal coiled-coil domain (NuMA^{CC}) in several vertebrates (including humans) retains both the S/T phospho-acceptor residue and the conserved R/K in the -3 position (Figure S1). The histidine at the -5 position preferred within the Wts motif is not conserved, although other Wts substrates have been identified that violate this sequence rule as well (Chiyoda et al., 2012). Radiometric kinase assays demonstrated that NuMA is indeed a direct Wts substrate, with a single T1677A mutation greatly reducing phosphorylation (Figure 4C). Furthermore, MARCOIL sequence analysis (Max-Planck Institute for Developmental Biology) revealed that the coiled-coil register is identical between Mud^{CC} and NuMA^{CC}, with the phosphorylated S/T residue residing at a surface exposed 'E-position' in both (Figure 4F), and, like Mud^{CC}, NuMA^{CC} is predicted to exist as a trimer. Size exclusion chromatography confirmed the trimeric nature of both Mud^{CC} and NuMA^{CC} purified proteins (Figure 4E). These results highlight structural conservation between fly and human orthologs of this key coiled-coil domain. Among *Drosophila* Mud isoforms themselves, it is interesting to note that the Mud^{PBD} and Mud^{CC} domains are mutually inclusive. Specifically, the solitary

Mud^{PBD}-containing isoform, expressed in neuroblasts and likely other cells undergoing Pins-dependent oriented divisions, contains Mud^{CC}, whereas the other two distinguished isoforms exclude Mud^{CC} by sequence truncation or alternative splicing (Siller et al., 2006).

Phosphorylation of Mud^{CC} prevents its self-association with Mud^{PBD}.

To understand the impact of Wts on Mud function, we next explored how phosphorylation might affect Mud structure. The Mud^{CC} domain was originally identified as part of the Pins binding region and immediately precedes the minimal Pins binding sequence subsequently described (Bowman et al., 2006; Siller et al., 2006; Zhu et al., 2011), referred to as Mud^{PBD} herein (Figure 4A). Sequence analysis of the Mud^{CC} and Mud^{PBD} domains revealed significantly opposing surface charge potentials, with predicted isoelectric points of 9.4 and 4.4, respectively (ExPASy Bioinformatics Resource Portal), leading us to speculate that these adjacent domains may exist in an intramolecularly bound conformation. To test this model, we purified the isolated Mud^{PBD} as GST-fusion protein, immobilized it on glutathione agarose beads, and performed 'pulldown' assays with purified Mud^{CC} as an isolated, soluble Mud fragment. Indeed, Mud^{CC} interacted directly with Mud^{PBD} as an *in trans* complex (Figure 5A,B). We then examined whether Wts might modulate this interaction. Phosphorylation of Mud^{CC} by Wts abolished its ability to bind Mud^{PBD} (Figure 5A). These results suggest that Mud exists in an intramolecular conformation through Mud^{CC}-Mud^{PBD} association, a structural feature which is negatively regulated by Wts kinase activity (Figure 5D).

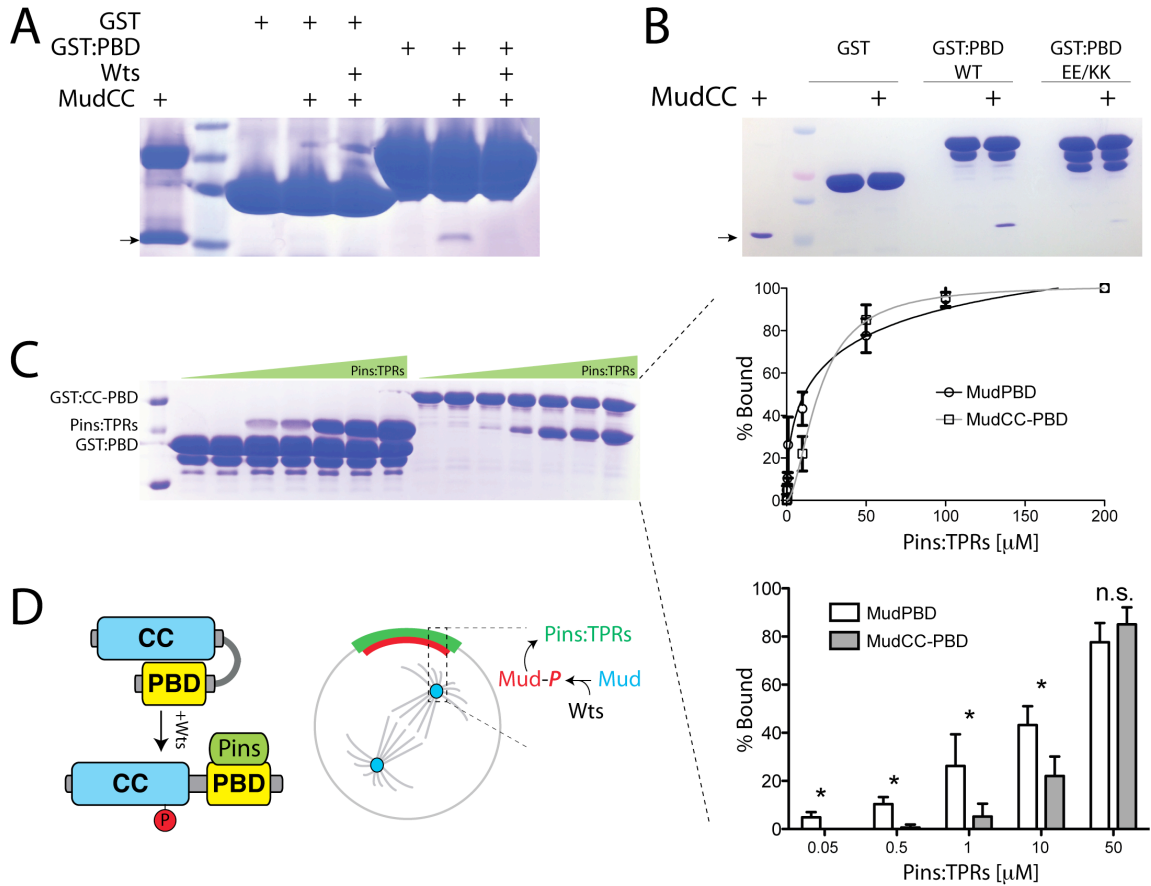


Figure 5. Mud phosphorylation modulates its direct interaction with Pins. (A) Mud^{CC} was incubated in the absence or presence of Wts kinase to allow phosphorylation. Proteins were then incubated with GST or GST fused to Mud^{PBD} (GST:PBD), resolved by SDS-PAGE and coomassie stained to determine bound proteins. Wts inhibits the ability of GST:PBD to co-precipitate Mud^{CC}. The higher molecular weight band in lane 1 is an impurity that sometimes proved difficult to remove during Mud^{CC} purification. (B) Mud^{CC} was incubated with GST or GST:PBD, either as wild-type (WT) sequence or a E1939K/E1941K double mutant (EE/KK). The mutant PBD is severely impaired in its ability to bind Mud^{CC}. The arrow in panels A and B indicates Mud^{CC}. (C) Mud^{PBD} alone or in tandem with the coiled-coil (Mud^{CC-PBD}) were fused to GST and incubated with increasing concentrations of the TPR domains of Pins (Pins:TPRs). Bands representing Pins:TPRs were quantified using densitometry analysis (ImageJ) and plotted as percent bound (*right insets*). Inclusion of the coiled-coil domain (*i.e.* Mud^{CC-PBD}) significantly reduced interaction with Pins:TPRs at concentrations up to 10 μ M. (D) Model for Wts-mediated Mud regulation. Self-association between Mud^{CC} and Mud^{PBD} domains prevents Pins binding at low concentrations. Wts phosphorylation of Mud^{CC} allows for high affinity Pins binding at the cell cortex. Whether the cortical and spindle pole Mud pools are directly connected remains to be determined, as is the precise mechanism for cortical Mud translocation. Statistical analyses were performed using ANOVA with Tukey's *post-hoc* test.

We next considered whether Mud^{PBD} binds Mud^{CC} using similar sequence elements used to bind the TPR domains of Pins (Zhu et al., 2011). Based on the crystal structure of the LGN/NuMA complex (the mammalian Pins/Mud orthologs), we designed a double charge-reversal (E1939K/E1941K; “EEKK”) mutation in Mud^{PBD}. These two residues are strictly conserved between Mud and NuMA, contribute significantly to the LGN/NuMA interaction, and represent strong candidate amino acids to respond to introduction of a negatively charged phosphate on Mud^{CC}. As shown in Figure 5B, this Mud^{PBD} mutant was dramatically impaired in its ability to bind Mud^{CC}. These results are consistent with an electrostatic model of Mud^{CC}-Mud^{PBD} association and suggest that this intramolecular Mud interaction could mask key Pins binding residues, possibly serving as a mode of Mud autoinhibition.

To test whether the intramolecular Mud interaction affects its ability to directly interact with Pins *in vitro*, we examined binding of Pins^{TPR} to either Mud^{PBD} alone or the Mud^{CC-PBD} tandem domain cassette as GST fusion proteins. Binding of Pins^{TPR} to Mud^{PBD} was detectable at low Pins concentrations and fit to a normal Langmuir binding model. In contrast, interaction with Mud^{CC-PBD} was significantly reduced specifically within a low Pins^{TPR} concentration regime, with the binding curve displaying a slightly steeper slope than seen with Mud^{PBD} alone (Figure 5C). These data indicate that the proximal Mud^{CC} domain suppresses the formation of the Pins/Mud^{PBD} complex at low concentrations and may shape the overall dynamics of the interaction. We speculate this may function to prevent unproductive Pins binding at sites of low expression such as the spindle proximal

cytoplasm, thus aiding in the productive formation of a cortical Pins/Mud complex (Figure 5D).

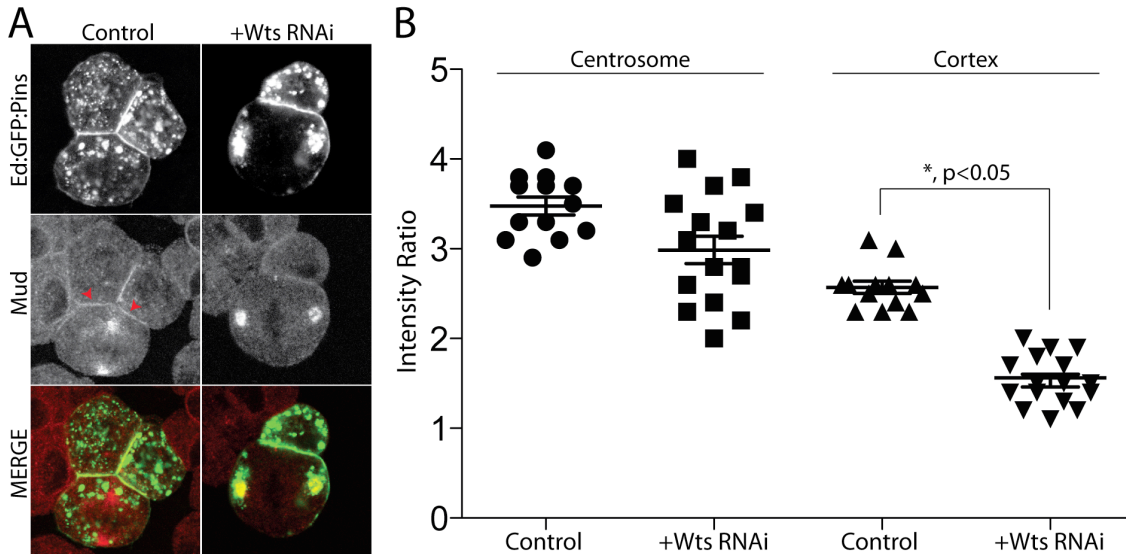


Figure 6. Warts kinase is dispensable for spindle pole Mud localization but necessary for its cortical association with Pins. (A) Cells were transfected with Ed:GFP:Pins and treated without (Control) or with RNAi against Warts (+Wts RNAi). Cells were fixed and stained for endogenous Mud. (B) The relative intensities of cortical and spindle pole localized Mud were calculated relative to cytoplasmic signal using ImageJ software. Wts^{RNAi} reduces cortical Mud accumulation without affecting its localization to spindle poles. Statistical analysis was performed using ANOVA with Tukey's *post-hoc* test.

Warts is required for cortical but not spindle pole Mud localization.

To understand how the Wts/Mud interaction might impinge upon Mud function within a cellular context, namely with respect to its association with Pins, we visualized endogenous Mud localization in S2 cells. In cells with induced Ed:Pins cortical polarity, Mud localizes strongly to both spindle poles as well as accumulating at the cortical Pins crescent (Figure 6), similar to that seen *in vivo* (Bowman et al., 2006; Lechler and Fuchs, 2005; Siller et al., 2006). Treatment with Wts^{RNAi} resulted in a significant reduction in cortical Mud signal; however, its

localization to spindle poles was largely unaffected by Wts loss-of-function (Figure 6). Together with the *in vitro* binding experiments above, these data indicate that Wts-mediated Mud phosphorylation serves as a positive cortical localization signal.

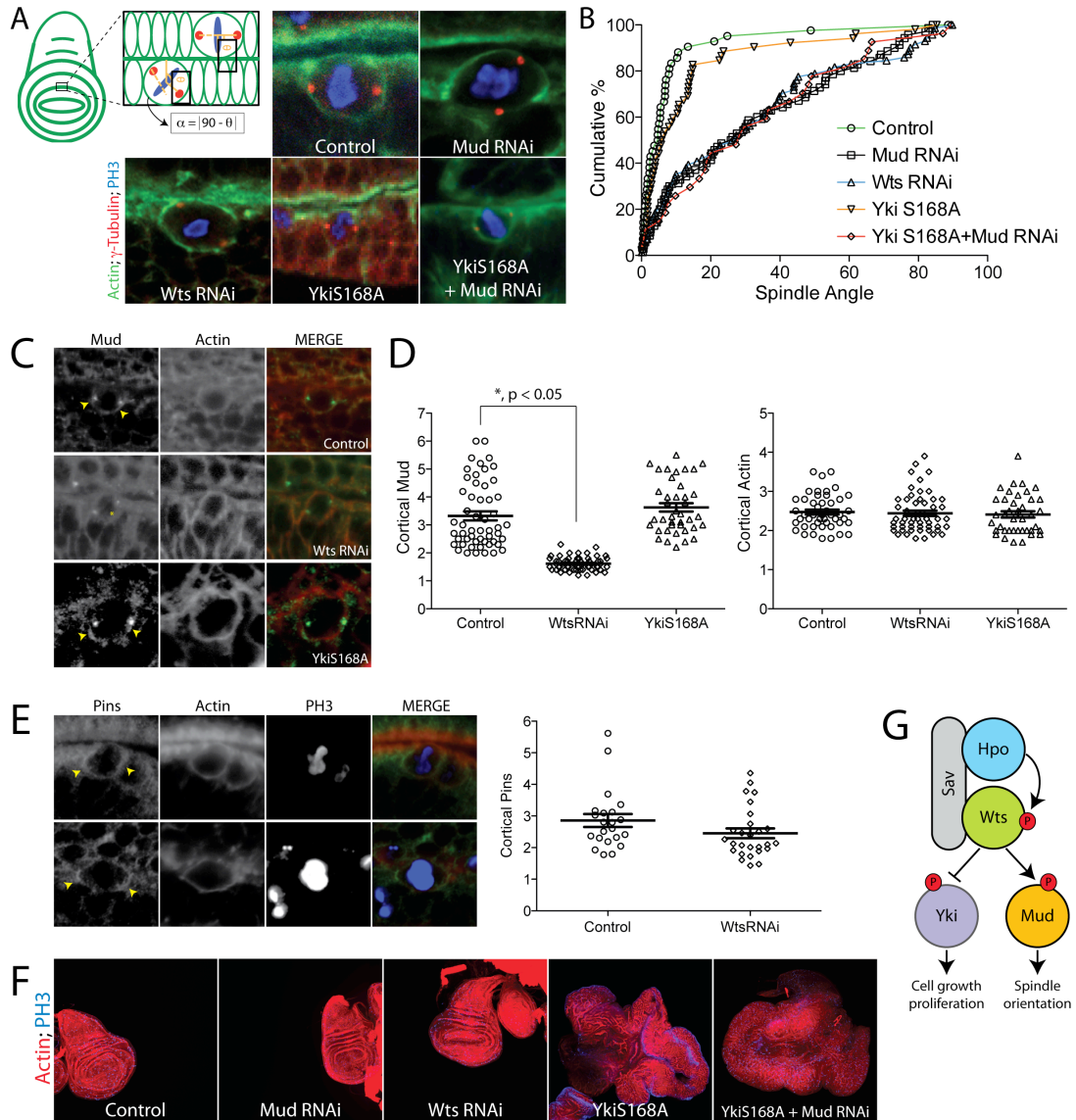


Figure 7. Warts is required for cortical Mud localization and spindle orientation in wing imaginal disc epithelial cells. (A) Spindle orientation in individual epithelial cells of third instar larval imaginal wing discs were measured relative to actin rich folds. Representative images show spindle positioning in indicated genotypes. Discs were dissected and stained with antibodies against γ -tubulin (to mark centrosomes), phosphohistone-H3 (PH3), and phalloidin (to label actin). (B) Cumulative percentage plots for all collected measurements. Expression of Yki^{S168A} does not significantly alter spindle orientation, whereas RNAi against Hpo, Sav, or Wts results in nearly identical loss of spindle orientation as Mud^{RNAi} expression. A second 'Wts-VDRC' RNAi causes statistically equal spindle orientation defects. Asterisks indicate conditions significantly different from control. (C) Expression of Wts^{RNAi}, but not Yki^{S168A}, causes loss of cortical Mud accumulation (*yellow arrowhead indicates sharp cortical Mud signal; yellow asterisk indicates delocalized Mud signal*). (D) Cortical Mud and actin intensity ratios relative to cytoplasmic signal were calculated for each condition. (E) Pins localizes to the cell cortex of dividing wing disc cells with preferential accumulation near spindle poles (*yellow arrowheads*). Quantifications are shown below images: in contrast to Mud, expression of Wts^{RNAi} does not significantly affect cortical Pins localization. (F) Whole wing discs from L3 staged larvae were imaged at identical magnification for each genotype and maximum intensity projections of z-stacks were generated in Zen software (Carl Zeiss). Although neither Mud^{RNAi} nor Hpo, Sav, or Wts^{RNAi} caused dramatic effects on disc size, expression of Yki^{S168A} induced significant overgrowth. Animals expressing both Mud^{RNAi} and Yki^{S168A} had a significantly reduced overgrowth compared to Yki^{S168A} alone. Discs from the alternate Wts-VDRC animals were overgrown to a similar degree as double mutant discs. *, p < 0.05 compared to Control; #, p < 0.05 compared to YkiS168A, ANOVA with Tukey's *post-hoc* test. (G) Model for dual Warts functionality in wing discs: an inhibitory phosphorylation of Yki restricts cell proliferation, whereas an activating phosphorylation of Mud promotes proper spindle orientation. See also Figures S3 and S4.

Warts facilitates Mud-dependent spindle orientation in *Drosophila* wing disc epithelia.

The Hippo signaling pathway is well known to regulate cell proliferation and tissue size *in vivo* through its inhibitory action on Yki (Zhao et al., 2011). Recent studies suggest that this pathway also controls the orientation of cell division in the *Drosophila* imaginal wing disc, a tissue in which planar polarized Fat-Dachsous, an upstream activator of Hpo (Feng and Irvine, 2007; Grusche et al., 2010), instructs directional tissue growth by controlling orientation of individual cell divisions (Mao et al., 2006; Mao et al., 2011b). Mechanisms proposed for this function include proliferation-induced cell crowding and modulation of the actin cytoskeleton, leading to mechanical forces that alter cortical tension and cell

shape globally throughout the tissue (Mao et al., 2013; Repiso et al., 2013). Both of these models implicate tissue-level mechanics that determine mitotic orientations and have been suggested to operate through canonical Wts/Yki activity (Rauskolb et al., 2014). Our results in small, Ed-induced S2 cell clusters, a minimal reconstitution system less constrained by tissue-dependent signaling, suggests Wts may exert cell intrinsic effects as well, independent of Yki-dependent growth. Such activity could operate via regulation of Mud, which has recently been shown to regulate oriented divisions in wing disc epithelia as well (Nakajima et al., 2013). We expressed hairpin *UAS-RNAi* sequences directed against Mud or Wts using the *nubbin-GAL4* (nub^{GAL4}) driver that expresses throughout the wing disc pouch. Mitotic orientations relative to the wing disc axis fluctuate based on cell position within the tissue (Baena-Lopez et al., 2005; Mao et al., 2013); thus, we chose to quantify spindle orientation relative to adjacent actin rich folds typical of late larval discs (Figure 7A). In this paradigm, cells from control animals showed a nearly perfect bias for spindle orientation parallel to the overlaying actin fold. Mud^{RNAi} expression significantly attenuated this bias, resulting in more randomized spindle orientations (Figure 7A,B), consistent with similar studies reported recently (Bell et al., 2015; Nakajima et al., 2013). Expression of RNAi against Hpo, Sav, or Wts each resulted in a nearly identical loss of spindle orientation, suggesting these genes may function in a linear pathway to control oriented epithelial divisions (Figure 7A,B). We also examined spindle orientation in wing discs expressing Wts^{RNAi} driven by two alternative GAL drivers, *apterous-GAL4* and *engrailed-GAL4*. Both of these conditions

resulted in a loss of spindle orientation similar to that seen with *nubbin*-GAL4 (Figure S3). It should be noted that the *nubbin*-GAL4 stock contains UAS-Dicer2 on its X-chromosome; however, its presence did not significantly enhance the effects of Mud^{RNAi} on the spindle orientation phenotype (Figure S4). To test whether Wts^{RNAi} expression alters Mud function, we examined Mud localization in dividing epithelial cells. In control wing discs, Mud localized strongly to both spindle poles as well as the cell cortex, with a bias towards cortical regions above each spindle pole. In contrast, cells from Wts^{RNAi}-expressing discs showed a significant reduction of cortical Mud signal, although Mud localization at spindle poles was not significantly affected (Figure 7C,D). These results mirror those obtained in S2 cells and implicate Wts as an essential determinant of cortical Mud localization and a positive regulator of the Pins/Mud spindle positioning complex in epithelial cells. Cortical actin was not altered under any conditions tested (Figure 7D). We also examined localization of Pins, which although implicated in asymmetric division of wing disc sensory organ precursor cells (Bellaiche et al., 2001; Segalen et al., 2010), has not been directly investigated in disc epithelial cells to our knowledge. Pins was cortically localized and accumulated at regions above spindle poles, similar to that seen with Mud. In contrast to Mud, however, expression of Wts^{RNAi} did not significantly affect Pins cortical association (Figure 7E), consistent with a model in which Wts is required for Mud recruitment to an independently-established cortical Pins cue.

Mud^{RNAi} alone did not cause significant defects in wing disc development (Figure 7F), similar to previous reports (Nakajima et al., 2013; Poulton et al.,

2014). Somewhat surprisingly, Hpo, Sav, and Wts RNAi expressions also did not induce significant tissue overgrowth in wing discs, suggesting that, under the expression conditions used, these constructs were not sufficient to induce excessive Yki activation despite the detrimental effects on spindle orientation (Figure 7F). The lack of overgrowth was independent of GAL4 driver (Figure S3), suggesting the Wts^{RNAi} construct being expressed was not completely penetrant with respect to regulation of tissue size. We therefore tested an alternative RNAi stock (Wts^{RNAi}-VDRC). nub^{GAL4}-mediated expression of this Wts^{RNAi}-VDRC did cause tissue overgrowth, as well as defective spindle orientation similar to the original Wts^{RNAi} stock (Figure 7B,F). That spindle orientation deficits are nearly identical in discs from both Wts RNAi lines despite dramatic differences in tissue growth suggests that, although both are influenced by Wts, these events may operate independent of one another (Figure 7G), although we cannot directly rule out possible differences in RNAi efficacy. To more directly examine the effects of hyperactive Yki on spindle orientation, we overexpressed the constitutively active, Wts-insensitive Yki^{S168A} mutant, which induced a marked overgrowth phenotype (Figure 7F). Despite this misshapen tissue development, however, individual cell divisions remained oriented similar to those in wild-type discs (Figure 7A,B). Cortical Mud localization was also unaffected by Yki^{S168A} expression, again supportive of a Yki-independent Wts/Mud pathway (Figure 7C,D). Thus, Wts appears to regulate both the rate and orientation of cell divisions through distinct downstream effectors with nonequivalent functions in these processes (Figure 7G). Specifically, phosphorylation of Yki imparts an

inhibition of cell proliferation and tissue growth, while Mud phosphorylation acts as an activation of an essential spindle orientation mechanism. To further test this possibility, we examined wing discs of larvae expressing both Mud^{RNAi} and Yki^{S168A}. It should be noted that double mutant animals contain two UAS sequence elements, the same as when each was examined individually due to the selective presence of UAS-Dcr2 in single mutants. The phenotype of these Mud^{RNAi}/Yki^{S168A} double mutant discs appeared to be complementary. That is, discs remained overgrown as seen in the Yki^{S168A} alone; however, co-expression of Mud^{RNAi} induced a spindle orientation defect very similar to Mud^{RNAi} alone (Figure 7). Interestingly, Mud^{RNAi}/Yki^{S168A} double mutant discs experienced a significant ~33% reduction in size compared to Yki^{S168A} single mutant discs that show an overgrowth phenotype alone (Figure 7F), indicating that defective spindle orientation may limit overgrowth potential of this tissue.

DISCUSSION

In this study, we have identified a role for the core Hippo kinase complex in Pins/Mud-dependent spindle orientation (see Figure S5 for summary model). Warts kinase directly phosphorylates Mud within its C-terminal coiled-coil domain, which uncouples self-association with the adjacent Pins-binding domain, thus promoting formation of the Pins/Mud complex *in vitro*. Warts is required for cortical Mud localization and spindle orientation in cultured S2 cells as well as epithelial cells in *Drosophila* imaginal wing discs. Notably, this spindle orientation function of Warts is independent of the canonical pathway effector Yorkie. Thus,

in addition to its well defined role in cell growth and proliferation through Yorkie inhibition, the Hippo pathway can also control the orientation of cell division through a novel Warts effector, Mud. The ability to coordinate the rate and orientation of mitotic events could have important impacts on tissue development and homeostasis.

Controlling the orientation of cell division is an essential underlying mechanism for cell diversification and tissue homeostasis in multicellular animals. Recent years have witnessed an impressive expansion in the identification of spindle orientation regulators (Lu and Johnston, 2013). The highly conserved Pins/Mud complex regulates spindle positioning in diverse cell types across animal taxa (Siller and Doe, 2009); yet, the molecular mechanisms that regulate Pins/Mud activity remain sparsely defined. Using a human cell culture system, Kiyomitsu and Cheeseman recently showed that elevated activity of Ran-GTP localized at condensed metaphase chromosomes inhibited cortical localization of LGN/NuMA (human orthologs of Pins/Mud) (Kiyomitsu and Cheeseman, 2012). This inhibitory signal prevents accumulation at the lateral cortex, indirectly permitting polarized localization that maintains spindle positioning. Kotak, et al. identified CDK1 as an additional negative regulator of cortical NuMA localization. CDK1-mediated phosphorylation reduces cortical NuMA in early phases of the cell cycle to prevent excessive spindle forces, whereas reduction in CDK1 activity at anaphase allows increased NuMA-mediated dynein activation necessary for spindle elongation (Kotak et al., 2013).

As these two pathways dampen cortical Mud localization, what signals then promote the assembly and function of the cortical Pins/Mud complex?

Little is known about how Mud becomes cortically enriched specifically in polarized cells (e.g. with Pins). The Pins-binding protein Canoe (Cno) has been shown to be required for cortical Mud localization, although the molecular mechanism has not been thoroughly addressed (Carmena et al., 2011; Wee et al., 2011). Cno itself localizes with apical Pins in dividing *Drosophila* neuroblasts, which is dependent on a network of monomeric G-proteins. Cno directly interacts with Pins^{TPRs}, which also serve as the binding site for Mud and Inscuteable (Insc). While recent studies have demonstrated that Mud and Insc bind competitively to Pins^{TPRs} (Mauser and Prehoda, 2012; Zhu et al., 2011), it remains to be determined whether similar Pins-binding dynamics exist with between Mud and Cno complex and how the Pins^{TPRs} can accommodate such overlapping demand for its protein-protein interaction capacity. Phosphorylation, particularly in response to cell cycle commands, represents an attractive model for regulating such combinatorial protein interactions.

Another recent study demonstrated that a complex between the centriole duplication protein, Ana2, the dynein light chain molecule, Ctp, was necessary for cortical Mud localization in *Drosophila*. The Ana2/Ctp complex localized at spindle poles, and disrupting its expression prevented polarized cortical Mud association with Pins leading to improper spindle orientation (Wang et al., 2011), a phenotype strikingly similar to that observed herein following knockdown of the

Hpo/Sav/Wts complex. Our *in vitro* binding experiments show that phosphorylation of the Mud coiled-coil domain abolishes a self-association with the Pins-binding domain, allowing for an increased Pins/Mud interaction affinity (Figure 5). Whether Mud phosphorylation affects its association with the Ana2/Ctp complex, directly or indirectly through an additional Mud-binding protein, and how this might impact this proposed mode of cortical Mud localization remains to be investigated.

The Hippo/Warts kinase pathway is a prominent regulator of cell proliferation and growth, yet a considerable amount of attention has been focused on Yki (and its transcriptional control of growth-associated genes) as the terminal pathway effector; noncanonical pathway effectors have only begun to emerge (Hergovich, 2013). Our studies identify Mud as a novel target of Hpo/Wts signaling and provide evidence that Mud-dependent spindle positioning is controlled by this conserved kinase module. Upon mitotic entry, Hpo triggers NEK2-mediated centrosome dysjunction and bipolar spindle assembly (Mardin et al., 2010); our results suggest Hpo signaling persists in later phases of mitosis to regulate the positioning of this bipolar mitotic spindle. Thus, the Hpo complex appears to link cell cycle progression, primarily through regulation of G1/S promoting genes, with dynamic aspects of the mitotic spindle during M-phase. Elevated Hpo signaling at interphase suppresses cell growth and division, suggesting Hpo activation must be tightly regulated both spatially and temporally during M-phase transition. A diverse set of upstream regulators of Hpo function are beginning to be revealed, including cell adhesion and G-protein coupled

receptors, cell polarity complexes, and the actin cytoskeleton (Grusche et al., 2010), and further work will be required to identify possible activators of the spindle-associated Wts activity involved in spindle positioning. Perhaps more clear is the ability of diverse downstream targets of this complex to control unique aspects of the cell cycle. Our results in *Drosophila* wing discs support a model in which distinct Wts targets, Yki and Mud, function together to control tissue development specifically through regulation of the rate and orientation of cell divisions, respectively (Figure 7G).

Wts serves as a negative regulator of cell proliferation yet promotes the activity of an essential spindle orientation pathway; thus, understanding how these events are coordinated with respect to cell cycle progression will be an important question to resolve. Interestingly, discs expressing both Mud^{RNAi} and Yki^{S168A} showed a reduction in overgrowth compared to Yki^{S168A} alone (Figure 7F), suggesting spindle misorientation suppresses tissue growth. Recent studies in *Drosophila* wing discs have shown that loss of genes involved in spindle assembly and orientation, including essential centrosomal proteins as well as Mud, can induce apoptosis resulting in stunted wing development (Nakajima et al., 2013; Poulton et al., 2014). Our results suggest that loss of Mud can also suppress aberrant overgrowth under conditions of constitutive Yki activity. Whether spindle misorientation *per se* is sufficient to induce apoptosis is unclear, as defects in spindle assembly and chromosome segregation were also seen in these discs (Poulton et al., 2014). These results contrast with those obtained in certain model stem cell systems, in which spindle orientation defects are

hypothesized to act synergistically with other overgrowth inducing mutations, including the those involved in the tumorigenesis process (Gonzalez, 2007). The evolutionarily-conserved nature of the Hippo pathway highlights the importance of continued unraveling of its role in both normal development as well as disease.

EXPERIMENTAL PROCEDURES

Fly stocks: The following stocks were obtained from the Bloomington Stock Center: VALIUM20 TRiP lines for *mud*^{RNAi} (stock# 35044), *hpo*^{RNAi} (stock# 33614), *sav*^{RNAi} (stock# 32965) and *wts*^{RNAi} (stock# 34064), *w; PUAS-yki.S168A.V5attP2* (stock# 28818), and the *UAS-Dcr-2.D1, w1118; PGawBnubbin-AC-62* (stock# 25754), *Ap-GAL4* (stock# 46223), and *En-GAL4* (stock# 35064). An additional “KK library” *Wts*^{RNAi} stock was obtained from the Vienna Drosophila Resource Center (VDRC; stock# 106174). The Mud and Yki double mutant was achieved using a *nub-GAL4/nub-GAL4;mud*^{RNAi}/*mud*^{RNAi} line generated using a *Cyo/Br;TM2/TM6* double balancer line (Richard M. Cripps, UNM). Generation of this line resulted in the loss of the *UAS-Dcr-2.D1* allele on the X-chromosome from the original *nub-GAL4* stock. Crossing this *nub-GAL4/nub-GAL4;mud*^{RNAi}/*mud*^{RNAi} line to *w; PUAS-yki.S168A.V5attP2* (for generation of Mud^{RNAi}/YkiS168A double mutants) thus resulted in the presence of two UAS sequence elements. Because single mutant crosses all retained the *UAS-Dcr-2.D1*, conditions in which *UAS-Mud*^{RNAi} or *UAS-YkiS168A* were expressed alone also contained two UAS elements, thereby ensuring wing disc

growth phenotypes were not due to unequal copy numbers of UAS and GAL-4 elements.

Induced S2 cell polarity assay: Schneider S2 cells (Invitrogen; Carlsbad, CA, USA) were grown in Schneider's insect media supplemented with 10% heat-inactivated fetal bovine serum (SIM). Cells were passaged every 3-4 days and maintained at 25°C in the absence of CO₂. For transient transfections, 1 × 10⁶ cells were placed in 6-well culture dishes for 30 minutes in 3 mL of SIM. Cells were then transfected with 0.05-1 µg total DNA using the Effectene® reagent system according to manufacturer protocols (Qiagen, Germantown, MD, USA). Following 24-36 hour incubation, transgene expression was induced by the addition of CuSO₄ (500 µM) for 24 hours.

For the Echinoid-based 'induced polarity' assay, cells were harvested, pelleted, and resuspended in fresh SIM supplemented with CuSO₄. Cells were then placed in a new 6-well dish and rotated at ~175 RPM for 2-3 hours, allowing for stochastic cell collisions that lead to cell-cell contacts and cluster formation (Johnston et al., 2009).

Immunostaining and imaging: Clustered cells (0.25 mL) were mixed with an 0.75 mL of fresh SIM in 24-well dishes containing 12 mm diameter round glass coverslips. Cells were incubated for 2-3 hours to allow for adherence to coverslips and to increase the percentage of mitotic cells. Cells were then fixed using a treatment of 4% paraformaldehyde (10 min) or ice-cold methanol (5 min).

Cells were washed 3 times (5 min) with wash buffer (0.1% Triton X-100 in PBS), followed by a 1 hour incubation with block buffer (0.1% Triton X-100 and 1% BSA in PBS). Primary antibodies were then incubated with slides overnight at 4 °C. Following primary antibody incubation, slides were washed 3 times with block buffer. Secondary antibodies (Jackson ImmunoResearch) diluted 1:250 in block buffer were then added and incubated at room temperature for 2 hours. Antibodies were removed and slides were washed 4 times with wash buffer. Finally, coverslips were inverted and mounted using Vectashield® HardSet reagent (Vector Laboratories, Burlingame, CA, USA) and stored at 4 °C prior to imaging.

Antibodies used were as follows: mouse anti-FLAG (1:500; Sigma), rat anti- α -tubulin (1:500; Abcam), rabbit anti-Mud (1:1000), and rabbit anti-PH3 (1:2000, Abcam). γ -tubulin antibodies were obtained from Sigma (1:500, rabbit) and Abcam (1:1500, mouse). The anti-Yorkie and anti-Pins antibodies were generous gifts from Dr. Kenneth Irvine (Rutgers University, HHMI) and Dr. Chris Doe (University of Oregon, HHMI), respectively. Imaging was performed using a Nikon Eclipse Ti-S inverted fluorescence microscope and collected under oil immersion at 60X magnification. All secondary antibodies (preabsorbed and non-crossreactive) were obtained from Jackson ImmunoResearch and used at 1:250 dilutions.

RNAi design and treatment: RNAi primer designs were obtained using SnapDragon web-based service (<http://www.flyrnai.org/snapdragon>). Primer sets that amplify segments of ~200-600 base pairs within the coding sequence of

desired targets were optimized for efficiency and specificity and designed with T7 promoter sequence recognition tags. Targeted sequences were designed to universally recognize all possible isoforms for desired transcript. PCR-amplified target sequences were transcribed to yield double-stranded RNA using the Megascript® T7 kit (Ambion, Austin, TX, USA) following the recommended protocol.

For RNAi treatment, S2 cells were seeded in 6-well dishes at 1×10^6 cells per well in 1 ml of serum-free Schneider growth media and incubated with 10 μ g of respective RNAi. After 1 hour, 2 mL of serum-containing media were added and cells were incubated for an additional 3 days prior to subsequent assays.

Protein purification: Mud and Pins sequences were PCR amplified from an S2 cell cDNA library with BamHI/Sall (Mud) or BglII/Sall (Pins) restriction sites, enzyme digested, and ligated into pGEX and pBH4 plasmid backbones to generate GST and 6xHis fusions, respectively. Mutation of Mud^{S1868} was carried out using standard PCR protocols. Plasmids were transformed into BL21(DE3) *E. coli* (Invitrogen) and cultures were grown at 37°C in standard LB supplemented with 100 μ g/mL ampicillin. At OD₆₀₀ ~ 0.7, cultures were induced with 1mM Isopropyl β -D-1-thiogalactopyranoside and grown for an additional 4 hours. Protein purification was carried out using sequential NINTA affinity, anion exchange, and size exclusion chromatographies. Proteins were concentrated using Vivaspin concentrators (Sigma Aldrich, St. Louis, MO), flash frozen in liquid

nitrogen, and stored at -80°C in storage buffer (20mM Tris, pH 8, 100mM NaCl, and 2mM DTT).

GST pulldown assay: GST-tagged constructs were absorbed to glutathione agarose for 30 minutes at room temperature and subsequently washed 3 times with PBS. Subsequently, desired concentrations of prey proteins were added for 3 hours at 4°C with constant rocking in wash buffer (20mM Tris, pH 8; 100mM NaCl; 1mM DTT with 0.5% NP-40 or without for *in cis* Mud^{CC}/Mud^{PBD} binding experiments). Reactions were washed 4 times in respective wash buffers, and resolved samples were analyzed using coomassie blue staining.

In vitro kinase assays: Active, recombinant human LATS1 kinase domain (orthologous to *Drosophila* Warts), purified from Sf9 insect cells, was purchased from SignalChem. Purified Mud^{CC} constructs (50 μg) and LATS1 (1 μg) were diluted in ice-cold assay buffer (20mM Tris, pH 7.4, 100mM NaCl, 1mM DTT, 10mM MgCl₂, and 10 μM ATP). To initiate reaction, [γ -³²P]ATP (5 μCi) was added to each reaction and incubated at 30°C for 30 minutes. Reactions were quenched by addition of SDS loading buffer. Samples were resolved by SDS-PAGE and dried gels were analyzed using Kodak BioMax MS film in a Konica SRX-101A developer.

Imaginal wing disc analysis: Imaginal wing discs were dissected from wandering third instar larvae in PBS. Discs were fixed in 4% paraformaldehyde at room

temperature for 20 minutes with rocking. Following fixation, discs were washed three times in wash buffer (0.3% Triton X-100 in PBS) and then once at RT for 20 minutes with rocking. Discs were blocked in block buffer (0.3% Triton X-100 + 1% BSA in PBS) for 1 hour at room temperature. Phalloidin-568 (1:5) and primary antibodies in block buffer were incubated with rocking at 4°C for 24-48 hours. Discs were washed and treated with secondary antibodies in block buffer for 2 hours. Washed discs were mounted in Vectashield Mounting Medium for Fluorescence or 80% glycerol and stored at 4°C until imaged. Antibodies used were as follows: mouse γ -tubulin (1:500), rabbit Mud (1:1000), rabbit phosphohistone-H3 (1:1000), and rat Pins (1:500).

ACKNOWLEDGMENTS

This work was supported by a grants from the National Institutes of Health: R01-GM108756 (C.A.J.) and R25-HG007630 (D.S. via UNM Post-baccalaureate Research and Education Program).

CHAPTER 2

Diverse mitotic functions of the cytoskeletal crosslinking protein Shortstop suggest a role in Dynein/Dynactin activity

From Molecular Biology of the Cell 28: 2555-2568

Evan B. Dewey and Christopher A. Johnston

ABSTRACT

Proper assembly and orientation of the bipolar mitotic spindle is critical to the fidelity of cell division. Mitotic precision fundamentally contributes to cell fate specification, tissue development and homeostasis, and chromosome distribution within daughter cells. Defects in these events is thought to contribute to several human diseases. The underlying mechanisms that function in spindle morphogenesis and positioning remain incompletely defined, however. Here we describe diverse roles for the actin-microtubule crosslinker, Shortstop (Shot), in mitotic spindle function in *Drosophila*. Shot localizes to mitotic spindle poles and its knockdown results in an unfocused spindle pole morphology and a disruption of proper spindle orientation. Loss of Shot also leads to chromosome congression defects, cell cycle progression delay, and defective chromosome segregation during anaphase. These mitotic errors trigger apoptosis in *Drosophila* epithelial tissue, and blocking this apoptotic response results in a marked induction of the EMT marker MMP-1. The Actin-binding domain of Shot directly interacts with Actin-related protein-1 (Arp-1), a key component of the Dynein/Dynactin complex. Knockdown of Arp-1 phenocopies Shot loss universally, whereas chemical disruption of F-actin does so selectively. Our work highlights novel roles for Shot in mitosis and suggests a mechanism involving Dynein/Dynactin activation.

INTRODUCTION

The cytoskeleton, consisting of microtubules (MTs), intermediate filaments, and filamentous actin filaments (F-actin), vitally contributes to diverse cellular processes including signal transduction, intracellular transport, chromosome segregation, and cytokinesis (Fletcher and Mullins, 2010). MTs and F-actin each undergo dynamic assembly and disassembly processes, both during interphase as well as throughout cell division. Coordination between the actin cytoskeleton and MTs is important for the establishment of cell polarity, where movement along microtubules promotes cortical localization of polarity cues that are subsequently stabilized by the cortical F-actin network (Li and Gundersen, 2008). During mitosis, actin and MTs cooperatively orchestrate several important cell shape changes necessary for division. For example, central spindle MTs promote Rho activation at the cell equator necessary for polymerization of the F-actin dense cytokinetic ring (Ramkumar and Baum, 2016). In turn, cortical actin plays an important role in mitotic spindle assembly and orientation in many systems (Sandquist et al., 2011). Thus, F-actin and MTs can be considered partners in regulating key cellular processes.

To aid in their coordination, several protein families can provide direct physical interactions between cytoskeletal components that stabilize their structural integrities and generate dynamic forces (Huber et al., 2015). Spectraplakins, members of the spectrin protein superfamily, are an evolutionarily conserved class of cytoskeletal crosslinking proteins (Suozzi et al., 2012). These large proteins contain multiple modular domains that together

confer the capability of physical association with all three cytoskeletal components (Figure 1A). Most spectraplakins contain tandem N-terminal Calponin Homology (CH) domains that bind F-actin (referred to here as the actin-binding domain, ABD) and C-terminal Growth Arrest Specific Protein 2 (GAS2) and SxIP domains that bind to the lattice and plus-ends of MTs, respectively (Applewhite et al., 2010; Suozzi et al., 2012). The central spectrin repeats not only provide physical separation of actin and MT binding regions, but are also considered to provide structural flexibility that may be important for accommodating the dynamic nature of the crosslinked components and contribute to Shot autoinhibition (Applewhite et al., 2013).

Owing to their unique cytoskeletal crosslinking capacity, spectraplakins have been shown to participate in diverse cellular functions. The mammalian Microtubule actin crosslinking factor 1 (MACF1), also called Actin crosslinking factor 7 (ACF7), plays a crucial role in endodermal cell migration during wound healing, a process which required both actin and MT binding functionalities (Kodama et al., 2003). Further studies in skin epidermis indicated an important role for ACF7 in maintaining proper dynamics of actin-based focal adhesions through physical coupling with MTs (Wu et al., 2008). Interestingly, ACF7 is capable of crosslinking and orienting non-centrosomal MTs to F-actin in regulating focal adhesion dynamics during migration of cultured human epithelial cells (Ning et al., 2016). A similar function has recently been described in specifying the anterior-posterior axis during *Drosophila* embryonic development (Nashchekin et al., 2016).

Studies on *Drosophila* Shortstop (Shot), the lone ACF7 orthologue in flies, have demonstrated a role in neuron axon development. Axons from both sensory and motor neurons in flies lacking Shot prematurely “stop short”; axon navigation requires an intact actin-binding functionality of Shot (Bottenberg et al., 2009; Lee and Kolodziej, 2002b; Sanchez-Soriano et al., 2009). Furthermore, terminal arborization at neuromuscular junctions is defective, a result that is caused by improper MT organization (Prokop et al., 1998). Shot cytoskeletal crosslinking activity is required for proper photoreceptor development as well (Mui et al., 2011). Recent studies have identified an interaction with Patronin, a MT minus-end-binding protein, which together promote MT polarization required for apical-basal epithelial polarity as well as the oocyte anterior-posterior axis (Khanal et al., 2016; Nashchekin et al., 2016). Studies in *Drosophila* S2 cells have provided molecular insights into its role in dynamic cytoskeletal organization. GAS2 domain-mediated MT interactions are critical for stabilization against lateral movements. Cross-linking to actin filaments via the ABD maintains this MT stabilizing effect (Applewhite et al., 2010). Interestingly, GAS2-mediated MT binding is autoinhibited prior to Shot activation at the MT plus end via the SxIP motif, and MT binding itself is dependent on an intact F-actin network (Applewhite et al., 2013).

These studies highlight a conserved role of spectraplakins in dynamic cytoskeletal cross-talk involved in cell migration and morphogenesis. However, these studies have all been conducted in non-dividing cells, and thus the role of spectraplakins in cell division is unclear. Here we have investigated the mitotic

functions of Shot in *Drosophila* S2 cells and the imaginal wing disc epithelium. We find that knockdown of Shot expression results in diverse mitotic defects including unfocused spindle poles, defective spindle orientation, and compromised chromosome movements. Interestingly, the processes altered following Shot loss are all known to require activity of the Dynein/Dynactin complex. We find that an intact Shot^{ABD} is both necessary and sufficient for direct *in vitro* interaction with Actin-related Protein-1 (Arp-1), an integral component of the Dynactin complex structure required for Dynein activation (Kardon and Vale, 2009), and knockdown of Arp-1 universally phenocopies the loss of Shot in dividing cells. Chemical disruption of F-actin, however, only partially resembles the effects of Shot knockdown. Using *Drosophila* wing disc epithelia as an *in vivo* tissue model, we show that loss of Shot causes induction of apoptosis, the prevention of which generates an EMT-like phenotype. Collectively, our results demonstrate novel mitotic functions of Shot and suggest these are, at least partially, dependent on interaction with the Dynactin complex as opposed to its known F-actin crosslinking activity during interphase.

RESULTS

Shot localizes to mitotic spindle poles and microtubules

We first examined the localization of Shot in mitotic S2 cells using fluorophore-tagged transgenes containing specific modular domains of the protein (Figure 1A). Full-length Shot fused to GFP (GFP:ShotA) predominantly localized to mitotic spindle poles (Figure 1B). GFP:ShotA signal was also

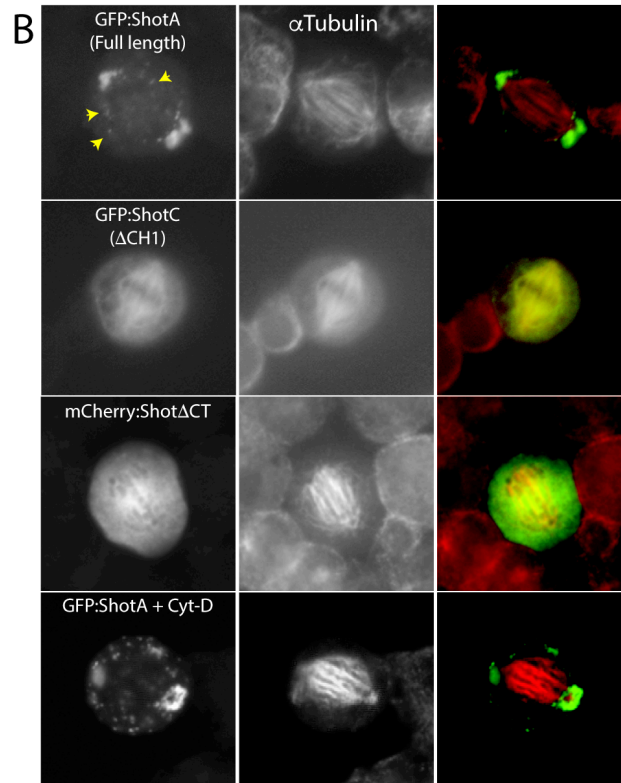
noticeable in small puncta found localized along spindle MTs, including at or near the MT plus ends, suggesting Shot may have mitotic functions not only at spindle poles but also at MT tips similar to non-dividing cells (Applewhite et al., 2010). Interestingly, a splice isoform of Shot with a unique N-terminal sequence that also lacks the calponin homology 1 (CH1) domain, a critical part of the actin-binding domain (ABD) (termed GFP:ShotC herein), localized throughout the mitotic spindle itself, likely mediated through intact microtubule binding domains (MBDs) in the C-terminus (Figure 1B). Recombinant removal of the C-terminal, MT-binding SxIP motifs (mCherry:Shot Δ CT) resulted in a mostly diffuse cytoplasmic localization (Figure 1B). In contrast to exclusion of the complete ABD sequence in ShotC, treatment of cells with the mycotoxin Cytochalasin-D (Cyt-D), which disrupts existing F-actin filaments and prevents further assembly, did not affect Shot localization at spindle poles or MTs either positively or negatively (Figure 1B). Altogether, these results suggest that spindle poles represent a major site of Shot localization during mitosis, with a smaller fraction localizing to spindle MTs, and that both actin- and MT-binding domains are required despite being independent of F-actin.

Shot directly binds the Dynactin component Arp-1.

The persistence of Shot's spindle pole localization following Cyt-D treatment suggested its ABD may have additional interactions beyond F-actin filaments crucial to its mitotic function. We reasoned that Shot may operate at spindle poles through interaction with actin-related protein-1 (Arp-1), the key

filamentous component of the Dynein-activating Dynactin complex (Kardon and Vale, 2009). Dynactin localizes to spindle poles in diverse cell types where it contributes to bipolar spindle assembly (Gaglio et al., 1997; Quinyne et al., 1999). Additionally, cortically localized Dynactin contacts spindle MT asters to generate forces that determine spindle orientation (Kotak et al., 2012; Siller and Doe, 2008; Siller et al., 2005). β III-spectrin, a member of the spectrin family from which spectraplakins evolved (Suozzi et al., 2012), directly binds Arp-1 to activate Dynein/Dynactin-mediated vesicular transport. This interaction occurs through the tandem CH domains of β III-spectrin and is disrupted in spinocerebellar ataxia 5 (Clarkson et al., 2010; Holleran et al., 2001; Ikeda et al., 2006). To examine this hypothesis directly, Shot tandem CH domains, the effective ABD, were expressed in *E. coli* as a GST fusion and immobilized on glutathione agarose resin. Arp-1 was expressed with an N-terminal His tag and purified via Ni²⁺-NTA and size exclusion chromatographies. His-Arp1 directly bound GST-Shot^{ABD} in pulldown experiments (Figure 1C). Binding required both CH domains, as the CH2 alone was insufficient for Arp-1 interaction. Binding was significantly reduced in an L238A mutant, which is located within the canonical actin-binding region of CH1 (Levine et al., 1992). An L340P mutation found within CH2, which is analogous to the allelic β III-spectrin mutation in cerebral ataxia (Clarkson et al., 2010), completely abolished Shot^{ABD} binding to Arp-1 (Figure 1C). As an additional control, the C-terminus of Shot, which has no known actin-binding property, was used and showed no appreciable interaction with Arp-1. These results demonstrate the ability of the Shot^{ABD} to directly bind a key

component of the Dynactin complex and establish a possible molecular mechanism for direct involvement in Dynein-dependent processes during mitosis.



C

			GST:	GST:	
	GST:	GST:	ABD	ABD	GST:
GST	ABD	CH2	L238A	L340P	CT

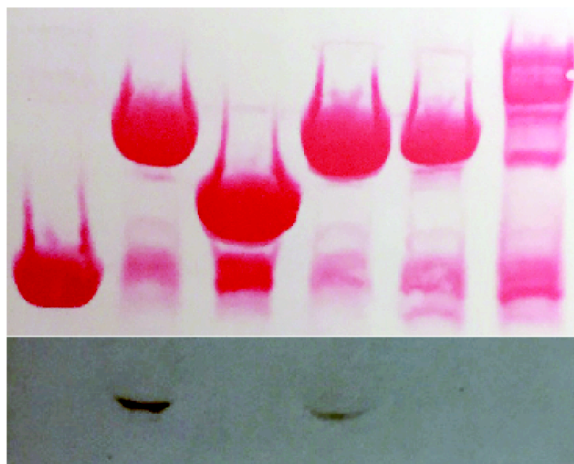


Figure 1. Shot localizes to mitotic spindle poles and directly binds Arp-1. (A) Domain diagram illustrates the modular structure of Shot. Tandem Calponin homology (CH) domains bind F-actin filaments; Spectrin repeats provide the core central structure; EF Hand (EFH) domain has no described function; Growth arrest specific protein 2 (GAS2) domain binds microtubule lattices; SxIP motif binds EB1 for microtubule +TIP localization. (B) Full-length ShotA localizes primarily to mitotic poles, with additional puncta found along spindle microtubules (*yellow arrows*). ShotC, lacking the CH1 domain due to alternative splicing, localizes throughout the mitotic spindle. Deletion of the C-terminal SxIP motifs (ShotDCT) results in primarily diffuse cytoplasmic localization. Treatment with Cyt-D does not reduce nor enhance ShotA pole localization. (C) His-Arp-1 directly interacts with GST-Shot^{ABD} (comprising CH1-CH2 domains); the CH2 domain alone is insufficient for Arp-1 binding. ABD mutations L238A and L340P reduce and completely ablate Arp-1 binding, respectively. Shot C-terminus (amino acids 5071-5501) does not bind Arp-1. GST alone is also devoid of binding.

Shot is required for proper mitotic spindle orientation.

Our previous work identified a role for cortical actin in spindle orientation mediated through Frizzled/Dishevelled (Fz/Dsh), which induces Rho-dependent actin polymerization through non-canonical signaling (Johnston et al., 2013). Similar results were demonstrated in other reports investigating Wnt-dependent spindle positioning (Cabello et al., 2010; Castanon et al., 2012), as well as those highlighting a generalized role of actin in this process (Kunda and Baum, 2009; Nestor-Bergmann et al., 2014). We thus examined the role of Shot in spindle positioning as a potential novel component of this mitotic process. Polarized cortical crescents of Dsh were induced using the cell adhesion protein Echinoid as previously described, to which spindle orientation at metaphase was measured (Figure S1 and 2A) (Johnston et al., 2009). Whereas control cells orient their spindle preferentially toward the center of the Ed:Dsh crescent, treatment with dsRNA (RNAi) targeted against the coding region of Shot randomized spindle orientation (Figure S1). We next examined whether Shot^{RNAi} could also perturb spindle orientation relative to Pins, a spindle-positioning cue not known to directly influence cortical actin, using the same reconstitution

system. Indeed, Shot^{RNAi} disrupted Pins-mediated spindle positioning similarly to that seen with Dsh (Figure 2A,B), suggesting Shot plays a more generalized role in this process. Because Pins likely represents a more universal spindle orientation cue (Lu and Johnston, 2013), and it has a more robust activity in the induced polarity assay, we chose to focus our efforts on it for the remainder of our studies.

We next examined the structure-function relationship of Shot-dependent spindle orientation using a set of recombinant rescue constructs. Cells were treated with RNAi directed against the 3'-UTR of Shot to reduce endogenous expression and transfected with RNAi-resistant Shot transgenes as potential rescue constructs. As shown in Figure 2C, full-length Shot (ShotA) was able to rescue Pins-mediated spindle orientation. In contrast, a Shot isoform lacking the N-terminal actin-binding domain (ShotC) was incapable of rescue. Removing the C-terminal MT-associating 'SxIP' motifs (ShotDCT) also prevented rescue activity (Figure 2C). These results demonstrate that Shot, and more specifically both its actin- and MT-binding regions, is necessary during cell division for proper positioning of the mitotic spindle.

Several studies have demonstrated a role for the actin cortex in mitotic spindle assembly and orientation, a role seemingly conserved from yeast to human cells (Kunda and Baum, 2009). To determine the role of F-actin in our Ed:Pins-based S2 cell system, we treated cells with Cyt-D; acute treatment resulted in spindle orientation randomization, indicating that cortical actin is necessary for Pins function in this system (Figure 2B). Treatment with Arp-1^{RNAi}

also uncoupled spindle orientation from Ed:Pins, as did treatment with RNAi directed against the Dynein heavy chain Dhc64C (Figure 2B). We confirmed that both Shot and Dhc64C RNAi constructs were highly effective at protein knockdown using western blot analysis (Figure S2), although no suitable antibody was identified for examining Arp-1 levels. We also performed double Shot^{RNAi}/Arp-1^{RNAi} and Shot^{RNAi}/Dhc64C^{RNAi} treatments and found these to be statistically indistinguishable from any single RNAi condition (Figure 2D). Whether Shot functions through F-actin filaments or Arp-1 to regulate spindle positioning cannot be completely deduced, although localization of ShotA, the only isoform that supports spindle orientation, is F-actin-independent in mitotic cells (Figure 1B), and loss of Shot is not synthetic with Arp-1 or Dhc64C loss, suggesting Arp-1 may be more relevant to its function.

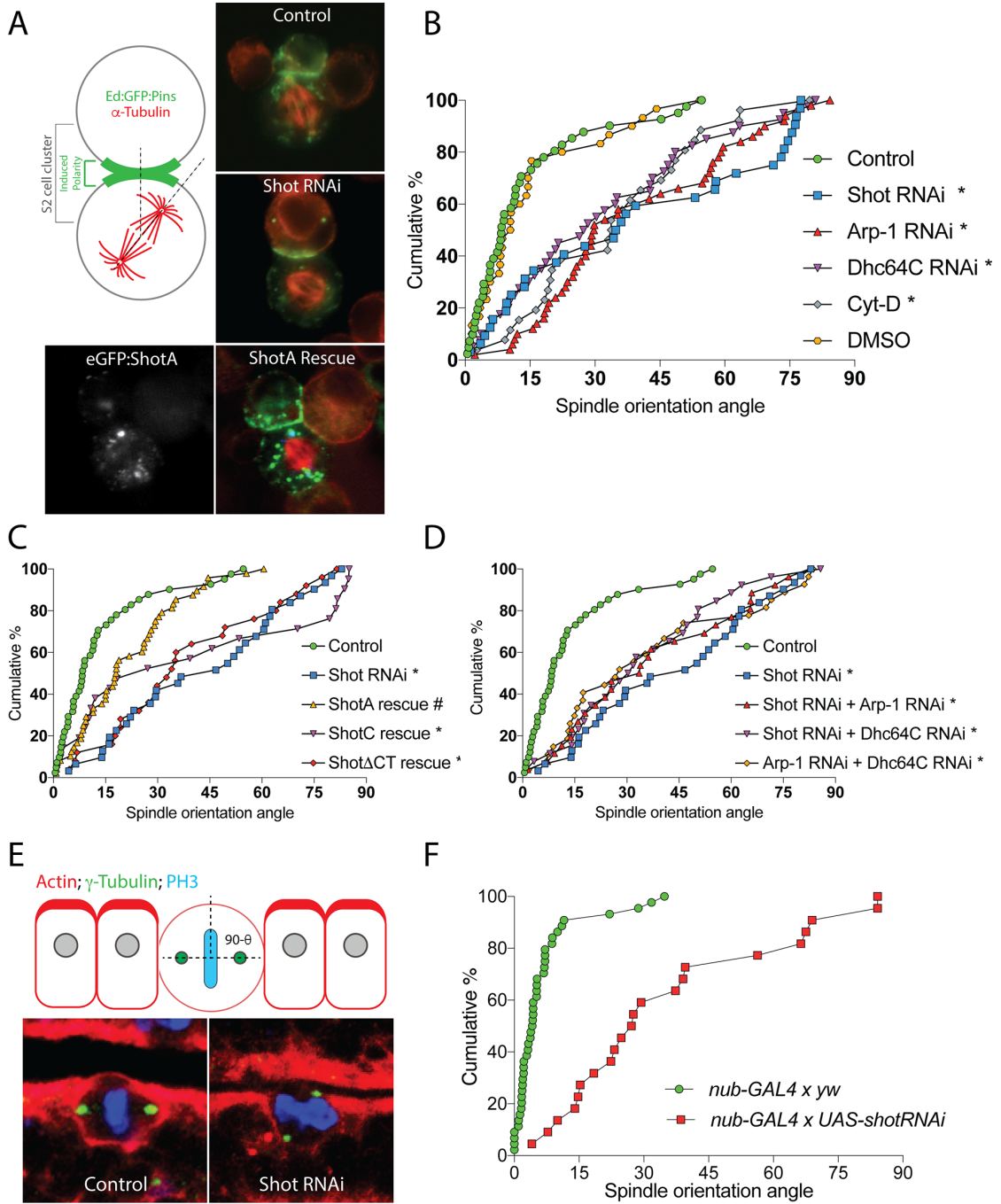


Figure 2. Shot is required for mitotic spindle orientation. (A) S2 cells transfected with Ed:GFP:Pins (or Ed:FLAG:Pins pseudo-colored green for ShotA rescue) were induced to form small (2-3 cells) clusters that cortically polarize Pins at sites of cell contact. The orientation of the mitotic spindle (marked by α -tubulin in red) was measured relative to the center of the induced Pins crescent. Representative images are shown for Control, Shot^{RNAi}-mediated loss of spindle orientation, and ShotA rescue of the Shot^{RNAi} phenotype. (B) Graph of cumulative percentage of measurements versus spindle angle demonstrating the loss of activity following RNAi directed against Shot, Arp-1, or Dhc64C. Treatment of cells with Cyt-D also prevents proper spindle orientation, whereas DMSO was without effect. Symbols represent individual measurements taken from at least three independent experiments. *, p<0.05 compared to Control (ANOVA, Tukey's post-hoc test). (C) Expression of RNAi-resistant Shot rescue transgenes demonstrates the necessity of both actin- and MT-binding functions in spindle orientation. ShotA, but not ShotC or ShotDCT, is capable of rescuing Ed:Pins-mediated spindle orientation in the absence of endogenous Shot expression (generated with RNAi against the Shot 3'-UTR). Symbols represent individual measurements taken from at least three independent experiments. *, p<0.05 compared to Control; #, p<0.05 compared to Shot^{RNAi} (ANOVA, Tukey's post-hoc test). (D) Combined treatment with Shot, Arp-1, and Dhc64C RNAi does not differ from any single RNAi treatment alone. Symbols represent individual measurements taken from at least three independent experiments. *, p<0.05 compared to Control (ANOVA, Tukey's post-hoc test). (E) Epithelial cells of the *Drosophila* imaginal wing disc normally orient spindles parallel to actin-dense folds. Shown are representative images for Control and Shot^{RNAi}-expressing cells. (F) Cumulative percentage graph depicting the magnitude of spindle orientation loss following Shot^{RNAi} expression. Shot^{RNAi} expression caused a significant reduction in spindle orientation accuracy. $p < 0.05$, Student's *t* test.

Shot is required for bipolar spindle assembly.

To determine if Shot affects other aspects of spindle function beyond spatial orientation, we examined spindle assembly following Shot knockdown. Shot^{RNAi} treatment resulted in a significant increase in cells with abnormal spindle morphology. Specifically, one or both spindle poles were often unfocused with K-fibers splayed at their ends despite the presence of an intact, γ -tubulin positive centrosome, with Shot^{RNAi} inducing a 2.05-fold increase in K-fiber spread distance (Figure 3B). The number of spindle poles was not significantly altered by Shot loss, and the predominant phenotype could be described as bipolar, unfocused spindles (Figure 3A). We next performed rescue experiments to determine the structure-activity relationship of Shot-dependent pole focusing. As with spindle orientation, full-length Shot (ShotA) expression conferred a significant rescue effect, whereas constructs lacking the ABD (ShotC) or MT

binding domain (Shot Δ CT) were devoid of rescue activity for spindle pole focusing (Figure 3B). Cells treated with Cyt-D had a smaller but significant increase in unfocused spindle poles (1.67-fold increase). Treatment with Arp-1^{RNAi} and Dhc64C^{RNAi} resulted in a 1.99- and 1.74-fold increase in pole distance, respectively (Figure 3B). As with spindle orientation, double RNAi treatments of Shot together with either Arp-1 or Dhc64C (or Arp-1 and Dhc64C together) did not result in further worsening of pole focusing (Figure 3B), suggesting these factors may function together within the same pathway. Thus, Shot is critical for proper spindle pole focusing, potentially through interactions with F-actin, Dynein/Dynactin, or both. Several studies have demonstrated that normal spindle pole focusing occurs through overlapping activities of minus-end microtubule motors, including the Dynein/Dynactin complex (Gaglio et al., 1996; Goshima et al., 2005; Maiato et al., 2004; Merdes et al., 2000; Morales-Mulia and Scholey, 2005; Walczak et al., 1998). Although cortical actin has been shown to contribute to centrosome dynamics and spindle assembly in some systems (Carreno et al., 2008; Kunda et al., 2008; Moulding et al., 2007; Sandquist et al., 2011), additional evidence suggests its main role is cell rounding, rather than a direct role *per se*, and is therefore dispensable in isolated, non-confined cells (Lancaster et al., 2013). Furthermore, normal bipolar spindles can form in cell extracts that are likely devoid of F-actin filaments (Heald et al., 1996).

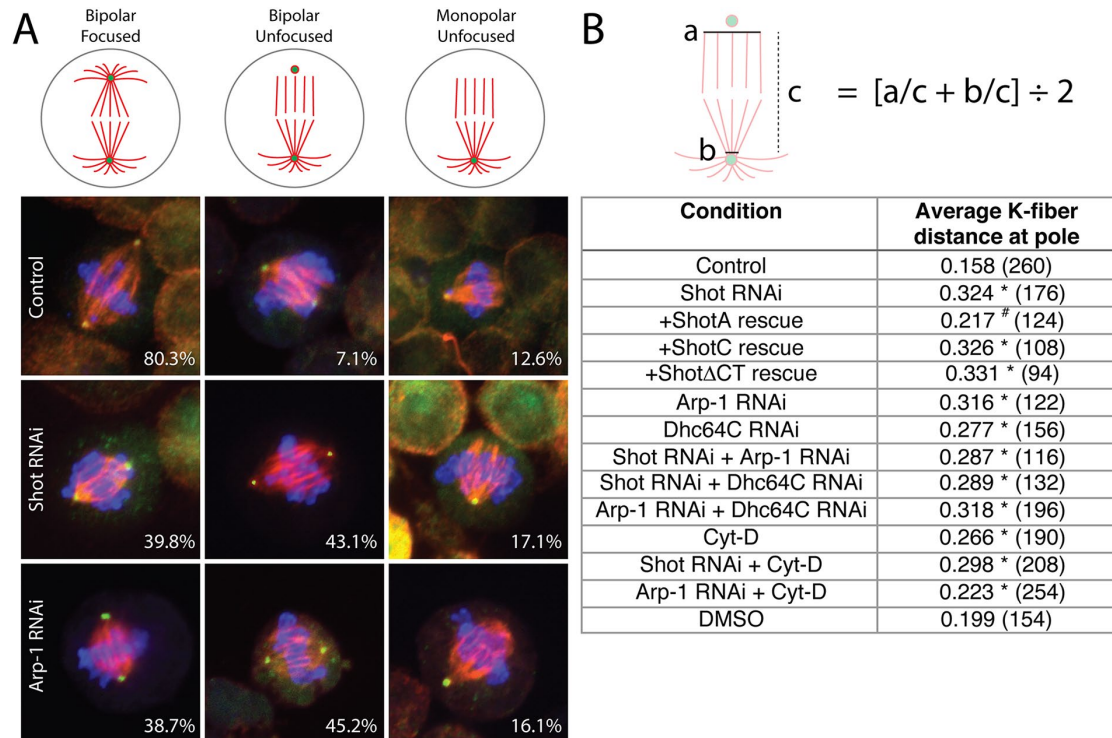


Figure 3. Shot is required for focusing of mitotic spindle poles. (A) Three significant phenotypes were observed for spindle morphology: ‘Bipolar Focused’ as normal, ‘Bipolar Unfocused’ in which one or both poles are unfocused although two g-tubulin positive centrosomes are still present, and ‘Monopolar Unfocused’ in which one unfocused pole is devoid of a g-tubulin positive centrosome. Representative images are shown for Control, Shot^{RNAi}-treated, and Arp-1^{RNAi}-treated S2 cells with a-tubulin marked red, g-tubulin marked green, and PH3 marked blue. Shot^{RNAi} and Arp-1^{RNAi} each lead to a selective increase in ‘Bipolar Unfocused’ spindles at the expense of ‘Bipolar Focused’. (B) Table summarizing all conditions tested. Data represent the average width of both spindle poles divided by spindle length. Numbers in parentheses are the total number of cells measured for each condition. Only ShotA was capable of rescuing spindle pole focusing. Shot^{RNAi} was indistinguishable from both Arp-1^{RNAi} and Dhc64C^{RNAi}. Double RNAi treatments were not significantly worse than single RNAi treatments, nor was combination treatment with Cyt-D. Statistical analyses were performed with ANOVA followed by Tukey’s post-hoc test (*, p<0.05 compared to Control; #, p<0.05 compared to Shot^{RNAi}).

Shot is required for timely chromosome congression necessary for anaphase onset.

To identify additional mitotic functions of Shot, particularly those known to depend on Dynactin/Dynein activity, we next examined chromosome congression (Sharp et al., 2000; Yang et al., 2007). Following nuclear envelope breakdown,

microtubule plus ends search and capture chromosome kinetochores, which must then be correctly congressed to the metaphase plate and properly aligned to ensure timely cell cycle progression and accurate segregation at anaphase. Complete congression of polar chromosomes to the spindle equator requires a coordinated effort of Aurora kinases, the CENP-E kinesin motor, and Dynein (Kim et al., 2010). Dynein is necessary to oppose polar ejection forces (PEFs), generated by plus-end directed kinesin motors, allowing for a net minus-end movement of chromosomes along astral microtubules to spindle poles (Barisic et al., 2014). Whereas control S2 cells typically did not show chromosomal congression defects (15.4%, n=156), Shot^{RNAi} treatment resulted in cells frequently having non-congressed, pole-localized chromosomes at metaphase (43.5%, n=184), which were visualized using the histone-like centromere marker, Centromere Identifier (*Drosophila* ortholog of CENP-A), fused to GFP (GFP:CID) (Figure 4A). RNAi directed against Arp-1 resulted in a similar congression defect (41.3%, n=184) as did treatment with Dhc64C^{RNAi} (54.3%, n=280). In contrast, Cyt-D treatment did not significantly increase the incidence of defective congression relative to control (18.5%, n=173), suggesting this Shot phenotype is strictly independent of F-actin interactions. Furthermore, Shot^{RNAi}/Arp-1^{RNAi} and Shot^{RNAi}/Dhc64C^{RNAi} double knockdowns did not significantly differ from any single RNAi treatment condition (49.6%, n=354 and 51.5%, n=518, respectively).

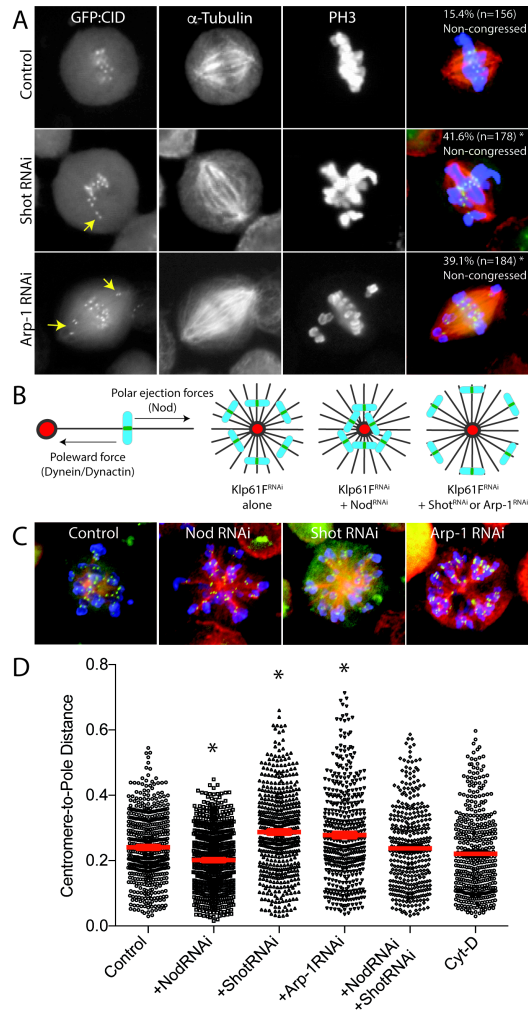


Figure 4. Shot is required for poleward congression of mitotic chromosomes. (A) S2 cells stably expressing GFP:CID were treated with Control, Shot^{RNAi} or Arp-1^{RNAi} and visualized using antibodies against α -tubulin (red) and PH3 (blue). Shot^{RNAi} and Arp-1^{RNAi} each significantly increase the percent of cells with non-congressed chromosomes (*, $p < 0.05$; ANOVA with Tukey's post hoc test). Percent of cells with non-congressed chromosomes for additional conditions not shown: Dhc64C^{RNAi}=54.3% (n=280)*, Shot^{RNAi}+Arp-1^{RNAi}=49.7% (n=312)*, Shot^{RNAi}+Dhc64C^{RNAi}=51.5% (n=518)*, Arp-1^{RNAi}+Dhc64C^{RNAi}=50.8% (n=354)*, and Cyt-D=18.5% (n=173) *not significant*. Double RNAi treatments did not significantly differ from single RNAi treatments. (B) Schematic depicting Klp61F^{RNAi}-mediated monopolar spindle assay. Chromosomes move along monopolar asters by means of two opposing forces: a plus-end 'Polar ejection force' generated by the chromokinesin Nod, and a minus-end 'Poleward force' generated by Dynein/Dynactin. Loss of PEF or Poleward forces is predicted to result in a decrease or increase in pole-to-chromosome distance, respectively. (C) Representative images for selective experimental conditions illustrate monopolar microtubules marked with α -tubulin (red), mitotic chromosomes marked with PH3 (blue), and centromeres marked with GFP:CID (green). (D) Plots for all data collected across each experimental condition. Whereas Nod^{RNAi} decreased centromere-to-pole distance, both Shot^{RNAi} and Arp-1^{RNAi} result in an increase in this metric. Co-treatment with Nod^{RNAi} and Shot^{RNAi} resulted in an intermediate distance. Cyt-D was without significantly effect. *, $p < 0.05$; ANOVA with Tukey's post hoc test.

To quantify this effect more precisely, we induced monopolar spindles using RNAi against Klp61F, the *Drosophila* orthologue of the Eg5 kinesin required for separation of duplicated centrosomes and spindle bipolarity (Sawin et al., 1992), and measured the distance from GFP:CID-positive centromeres to the center of this single pole (Figure 4B). Shot^{RNAi} and Arp-1^{RNAi} caused similar and statistically significant increases in this centromere-pole distance relative to control (Figure 4C,D). Increased distance from the pole is consistent with overwhelming PEFs in the absence of minus-end movements through Dynein (Barisic et al., 2014). To test this, we treated cells with RNAi against the PEF-generating chromokinesin, Nod. As expected, treatment with Nod^{RNAi} alone reduced the centromere-pole distance, consistent with unopposed Dynein function. Under double knockdown conditions, Shot^{RNAi} suppressed the effects of Nod^{RNAi}, yielding an intermediate distance similar to control cells (Figure 4D). Finally, treatment of cells with Cyt-D did not significantly affect chromosome distance relative to control, again indicating that F-actin does not play an essential role in this process under these experimental conditions. These findings collectively suggest a model in which Shot aids in Dynein-mediated chromosome forces that permit poleward transport, presumably through an interaction with Arp-1.

Proper chromosome congression and alignment are necessary for timely anaphase onset and mitotic exit. Once chromosomes congress and become bi-oriented at the metaphase plate, Dynein-mediated forces are used to remove

components of the spindle assembly checkpoint (SAC) from kinetochores, triggering anaphase onset, and to subsequently help separate sister chromatids to their respective spindle poles during anaphase (Bader and Vaughan, 2010; Howell et al., 2001). To determine whether Shot has a role in cell cycle timing, we measured the time from NEB to anaphase onset using live-cell imaging of S2 cells expressing GFP:CID and α -tubulin:mCherry. Anaphase onset in control cells occurred 47.8 ± 18.9 (n=8) minutes following NEB. Knockdown of Shot, Arp-1, or Dhc64C each resulted in significant delay of anaphase onset, with the majority of cells experiencing metaphase arrest (5 out of 7; 5 out of 9; and 8 out of 9 respectively, Figure 5B). Overall, Shot^{RNAi} increased NEB-anaphase timing to 143.8 ± 63.05 (n=7) minutes, whereas Arp-1^{RNAi} and Dhc64C^{RNAi} had similar average timings of 126.4 ± 63.05 (n=9) and 176.4 ± 10.7 (n=9) minutes to anaphase onset (Figure 5). Cells arrested in metaphase failed to enter anaphase even after 180 minutes, the time point at which we stopped imaging due to photobleaching and concerns of phototoxicity, and likely suggest these numbers may underrepresent the magnitude of the anaphase delay in RNAi-treated cells. To corroborate these live-cell results, we also measured the mitotic index in respective fixed cell populations: control cells 2.1% (n=3488), Shot^{RNAi} cells 9.1% (n=2539), Arp-1^{RNAi} cells 8.6% (n=2361), and Dhc64C^{RNAi} cells 8.8% (n=3014). These results are consistent with previous reports (Morales-Mulia and Scholey, 2005) and further substantiate the effects of Shot loss on mitotic exit. To differentiate between the potential roles of F-actin and Arp-1 in Shot-dependent cell cycle progression, we examined effects of Cyt-D on anaphase timing. In

contrast to Arp-1 loss, treatment with Cyt-D did not significantly affect NEB-anaphase timing (29.4 ± 8.6 minutes, $n=12$, Figure 5B). We also examined RNAi against β -spectrin, which also binds Arp-1 but for the purpose of vesicular traffic in non-dividing cells. This treatment did not significantly increase cell cycle timing, indicating specificity in Arp-1 binding interactions.

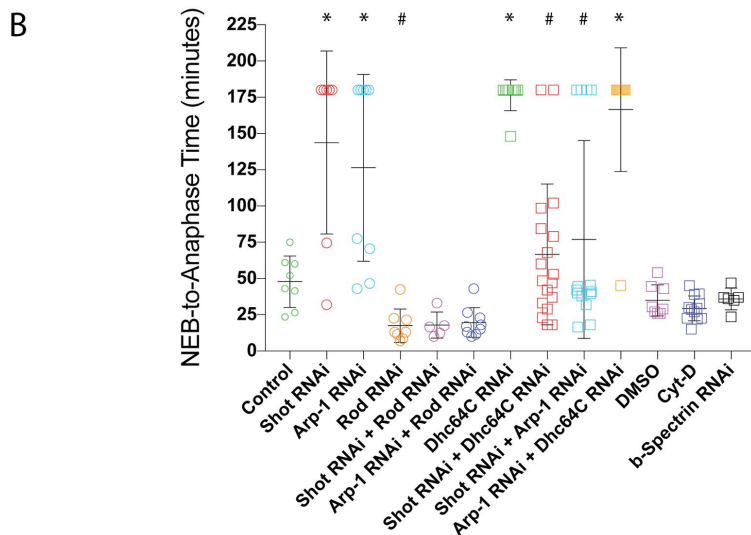
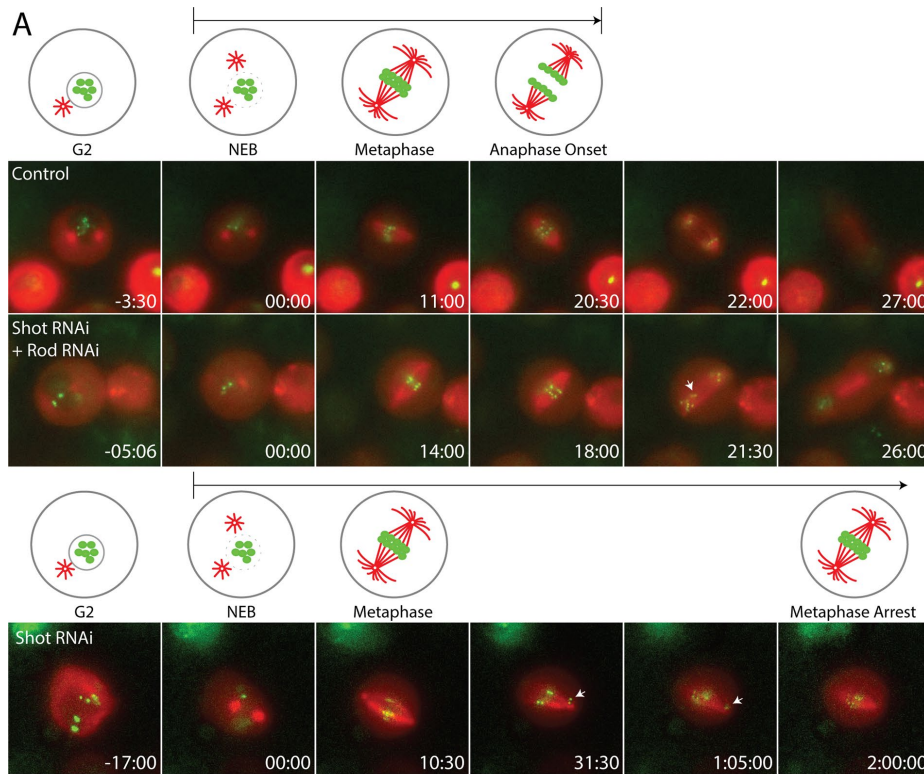


Figure 5. Shot loss activates the SAC to delay mitotic exit. (A) Live-cell imaging was conducted on S2 cells stably expressing inducible GFP::CID and mCherry::a-Tubulin. Images are shown from representative movies of Control, Shot^{RNAi} treated, and Shot^{RNAi}/Rod^{RNAi} co-treated cells at indicated time points relative to NEB. Whereas Control and double mutant cells progress to anaphase within ~20 minutes, Shot^{RNAi}-treated cells frequently undergo metaphase arrest. The arrow in Shot^{RNAi}/Rod^{RNAi} anaphase image indicates a lagging chromosome. The arrows in metaphase images of Shot^{RNAi} highlight a non-congressed chromosome that remains at the spindle pole. (B) Plot of NEB-to-anaphase timing for all movies taken from indicated experimental conditions. Shot^{RNAi}, Arp-1^{RNAi}, and Dhc64C^{RNAi} each induces a significant delay that results from cells frequently arresting in metaphase. Loss of the SAC component Rod suppressed both the Shot^{RNAi}- and Arp-1^{RNAi}-mediated metaphase arrest phenotype. Combined treatments of Shot^{RNAi}/Arp-1^{RNAi} or Shot^{RNAi}/Dhc64C^{RNAi} caused a suppression of metaphase arrest seen in single RNAi conditions, whereas Arp-1^{RNAi}/Dhc64C^{RNAi} dual treatment did not differ from either treatment alone. Cyt-D treatment did not affect cell cycle timing, nor did RNAi against the spectrin protein, bIII-spectrin. Data points are measured from individual cell divisions representing at least 3 independent experiments. *, p<0.05 compared to Control, #, p<0.05 compared to Shot^{RNAi} alone; ANOVA with Tukey's post hoc test.

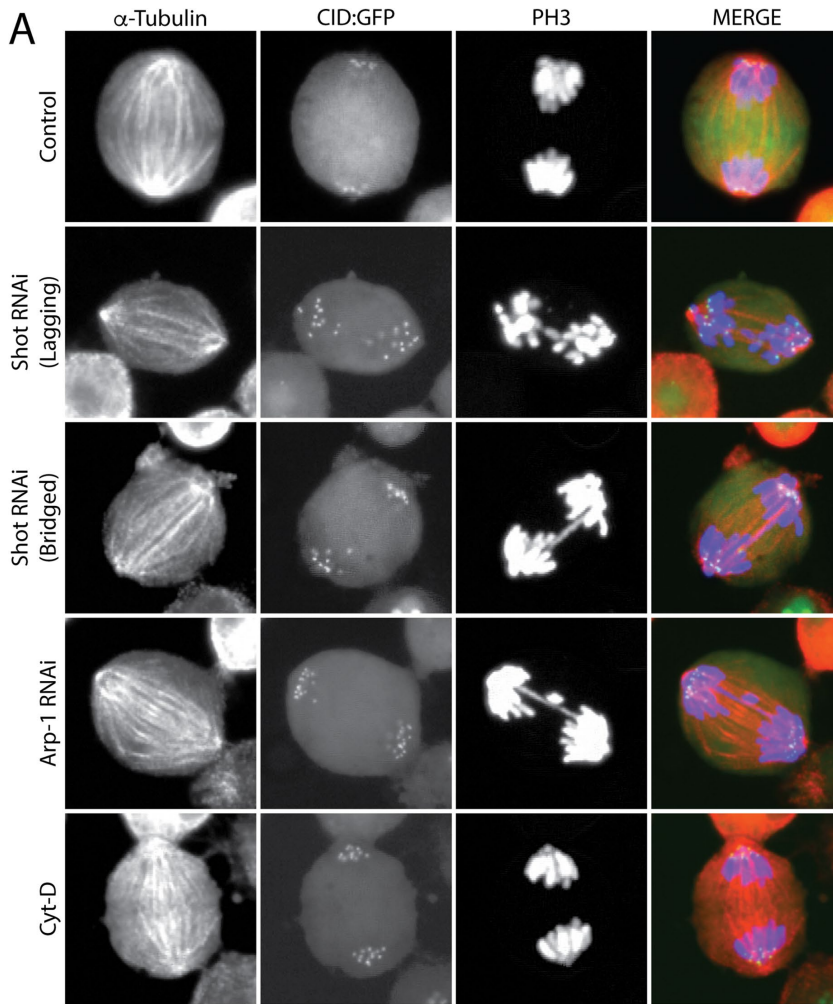
To ascertain whether activation of the SAC was responsible for this delay we used RNAi against Rod, a member of the RZZ complex and key component of the SAC (Basto et al., 2000). Indeed, Rod^{RNAi} suppressed the effects of both Shot^{RNAi} and Arp1^{RNAi} by shortening anaphase onset timing to a level similar to Rod^{RNAi} alone, which was slightly hastened compared to control cells (Figure 5). These results suggest that Shot functions together with Arp-1 to promote Dynein-mediated cell cycle timing by aiding in the proper silencing of the SAC necessary for mitotic checkpoint inactivation and anaphase transition. Surprisingly, when cells were treated with a combination of Shot^{RNAi} and Arp-1^{RNAi} (or Shot^{RNAi} and Dhc64C^{RNAi}) the anaphase onset delay seen in each single RNAi treatments was suppressed, and only a minority of cells in these conditions experienced metaphase arrest (Figure 5B). Concordantly, the mitotic index in the Shot/Arp-1 double knockdown was significantly reduced (4.1%, n=3600), while the Shot/Dhc double knockdown caused an even more complete reversal (2.8%, n=3383). Treatment with an Arp-1^{RNAi}/Dhc64C^{RNAi} combination did not, however, differ

from single RNAi treatments in either metric, indicating the loss of cell cycle arrest in Shot double knockdowns is not due to non-specific effects such as RNA toxicity.

Shot is required for proper chromosome segregation during anaphase but not for cytokinesis.

In addition to delaying anaphase onset, we next examined whether loss of Shot might also impact chromosome segregation once anaphase commences. We again used S2 cells stably expressing GFP:CID to quantify the incidence of chromosome segregation errors. Control cells showed a moderate incidence of lagging or bridged chromosomes (23.7%, n=169). Shot^{RNAi} treatment significantly increased segregation defects (42.4%, n=172; Figure 6). Arp-1^{RNAi} and Dhc64C^{RNAi} treatments resulted in similar effects (63.9%, n=161 and 49.8%, n=241, respectively), although the effects of Arp-1^{RNAi} were more prominent (Figure 6). Cyt-D, however, did not lead to significant chromosome segregation errors (23.1%, n=186), nor did it alter the effects of Shot^{RNAi} and Arp-1^{RNAi} when treated in combination (Figure 6B). These results collectively suggest that Shot participates in chromosome segregation independent of F-actin, and may rather function in Dynein/Dynactin-mediated poleward forces (Sharp et al., 2000). Double RNAi treatment against Shot/Arp-1 or Shot/Dhc64C each resulted in elevated levels of segregation defects relative to single knockdowns (75.1%, n=218 and 81.6%, n=223, respectively, Figure 6B). We believe these results are a direct result of the loss of metaphase arrest described above for these

conditions. Loss of Shot, Arp-1, or Dhc alone likely triggers anaphase delay due to defective chromosome congression and alignment. Slippage from the SAC under these double RNAi treatments could thus explain the high rates of segregation errors.



B

Condition	% cells with lagging or bridged chromosomes (n)	ANOVA: *,p<0.05 to Control #,p<0.05 to ShotRNAi
Control	23.7 (169)	-
Shot RNAi	42.4 (172)	*
Arp-1 RNAi	63.9 (161)	*,#
Dhc64C RNAi	49.8 (241)	*
Shot RNAi + Arp-1 RNAi	75.1 (354)	*,#
Shot RNAi + Dhc64C RNAi	81.6 (223)	*,#
Arp-1 RNAi + Dhc64C RNAi	58.3 (240)	*
Shot RNAi + Cyt-D	43.1 (174)	*
Arp-1 RNAi + Cyt-D	54.3 (162)	*
Cyt-D	23.1	#

Figure 6. Shot loss induces chromosome segregation defects. (A) GFP:CID-expressing S2 cells were fixed and marked with α -tubulin (red) and PH3 (blue) antibodies. Representative images are shown for indicated conditions. Control and Cyt-D-treated cells undergo mostly normal anaphase chromosome segregation, whereas Shot^{RNAi} and Arp-1^{RNAi} both induce lagging and bridged chromosomes. (B) Table shows quantification of defective segregation phenotype for all conditions tested. Treatment with Arp-1^{RNAi} or Dhc64C^{RNAi} had resulted in phenotypes similar to Shot^{RNAi}, although Arp-1^{RNAi} effects are significantly stronger. Cyt-D treatment, however, did not affect chromosome segregation, nor did it potentiate either Shot^{RNAi} or Arp-1^{RNAi} effects. Although combination RNAi treatment against Arp-1 and Dhc64C was not worse than either alone, concomitant loss of Shot and Arp-1 or Shot and Dhc64C was significantly worse than either condition alone. *, p<0.05 compared to Control, #, p<0.05 compared to Shot^{RNAi} alone; ANOVA with Tukey's post hoc test.

Finally, in order to assess the role of Shot and Arp-1 in cytokinesis, we quantified the percentage of binucleated S2 cells with the understanding that failed cytokinesis results in retention of both daughter nuclei in the original mother cell. Control cells were 1.18% binucleated (n=1348). RNAi against Shot or Arp-1 each resulted in a small but insignificant increase in binucleated cells to 2.28% (n=1097) and 2.98% (n=1508), respectively, suggesting that neither of these components is critical for completing cytokinesis. In contrast, treatment with Cyt-D to ablate cortical F-actin, which is a well-established component of the cleavage furrow and contractile ring (Glotzer, 2005), resulted in a significant increase to 43.7% (n=958) binucleated cells. Thus, Shot plays an important role in chromosome dynamics and mitotic exit, but does not appear to regulate the actomyosin ring function during cleavage furrow ingression and cytokinesis.

Shot is required for proper epithelial cell divisions in vivo.

Having elucidated several novel mitotic functions of Shot *in vitro*, we sought to investigate how Shot participates in proper development of an animal tissue *in vivo*. To do so, we used imaginal wing discs from third instar *Drosophila* larvae, the predecessors to the adult wing structure that represent an excellent

epithelial cell model and have been used extensively in the study of tissue growth and homeostasis (Hariharan, 2015). We first examined whether Shot participates in spindle orientation in this tissue. Wing discs display a characteristic pattern of actin-rich folds, and we have shown that adjacent cells normally orient their spindles parallel to these folds (Figure 2E) (Dewey et al., 2015a). We expressed shRNA against Shot using *Nubbin-GAL4* (*nub>GAL4*) that drives expression ubiquitously in the wing disc pouch. Shot^{RNAi} randomized spindle orientation (Figure 2E,F), demonstrating its role in oriented cell division is relevant in animal tissue. The effects of Shot^{RNAi} were similar in magnitude to RNAi against Mud, a previously identified spindle-orienting component in these cells (Dewey et al., 2015a; Nakajima et al., 2013). Recent studies have shown that centrosome loss (following RNAi against SAS-4) also disrupts spindle orientation in wing discs (Poulton et al., 2014), whereas supernumerary centrosomes induce only a mild disruption (Sabino et al., 2015). Despite abnormal spindle positioning, centrosome numbers in wing discs expressing Shot^{RNAi} were not altered, with all cells containing two g-tubulin positive structures, consistent with results from S2 cells.

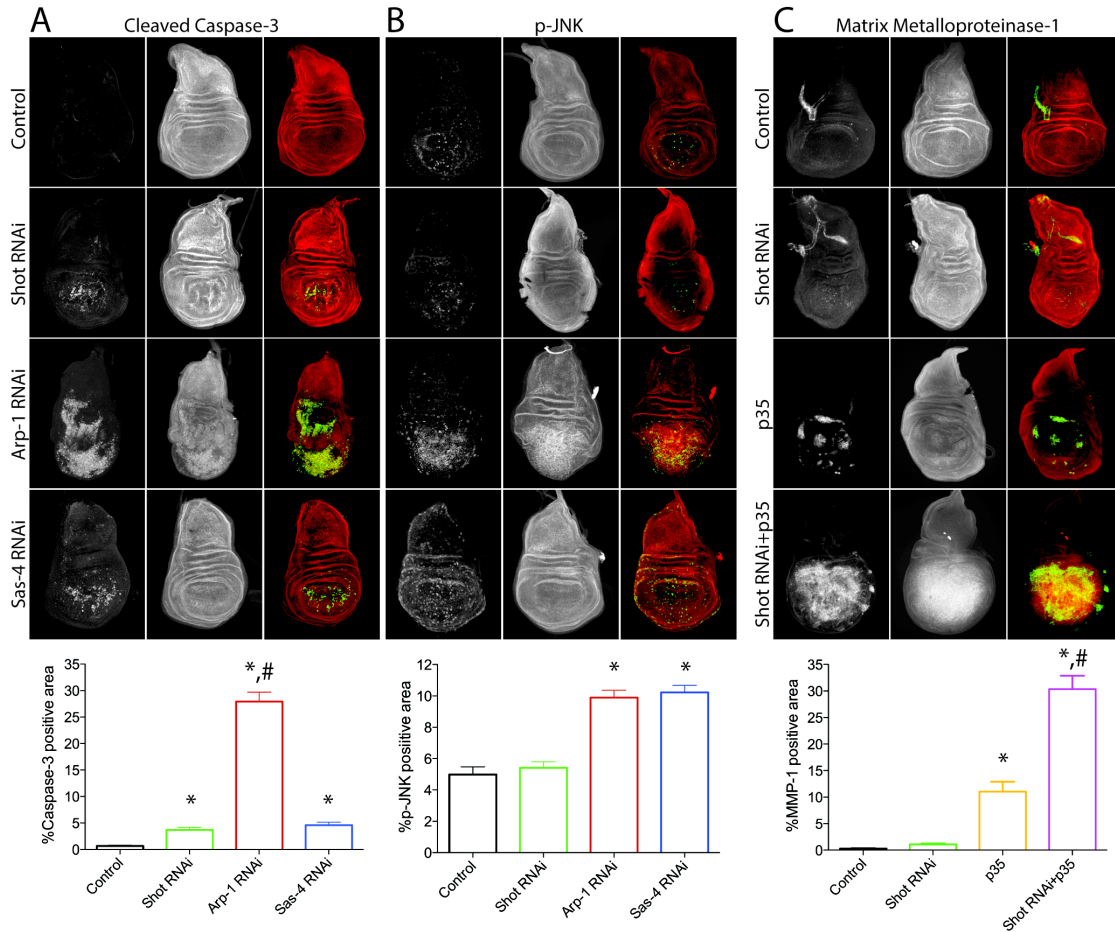


Figure 7. Shot loss activates apoptosis in *Drosophila* epithelia and leads to disruption of tissue morphology. (A) Imaginal wing discs were dissected from late stage L3 larvae, fixed, and stained for Cleaved Caspase-3 (green) and AlexaFluor-568-Phalloidin (red) to stain F-actin. Shot^{RNAi} causes an increase in apoptotic cells similar in magnitude to Sas-4^{RNAi}. Arp-1^{RNAi} induces a strikingly more significant apoptotic response. Shot^{RNAi} and, more so, Arp-1^{RNAi} often lead to noticeable alterations in the morphology of F-actin folds. *, p < 0.05 compared to Control and #, p < 0.05 compared to Shot^{RNAi}, ANOVA. (B) Imaginal wing discs were dissected from late stage L3 larvae, fixed, and stained for phosphorylated-JNK (green) and AlexaFluor-568-Phalloidin (red). Whereas Shot^{RNAi} does not increase p-JNK levels, Arp-1^{RNAi} and Sas-4^{RNAi} cause a similar degree of increase. *, p < 0.05 compared to Control, ANOVA. (C) Imaginal wing discs were dissected from late stage L3 larvae, fixed, and stained for Matrix Metalloproteinase (green) and AlexaFluor-568-Phalloidin (red). Shot^{RNAi} alone does not significantly affect MMP-1, whereas expression of the anti-apoptotic protein p35 leads to a moderate increase. Co-expression of Shot^{RNAi} and p35 leads to a dramatic and synergistic increase in MMP-1 expression as well as significant deformation in F-actin morphology. *, p < 0.05 compared to Control and # < 0.05 compared to p35, ANOVA.

We next sought to determine the consequences of Shot loss on tissue development. We first examined apoptosis using cleaved caspase-3 as a molecular marker. Expression of Shot^{RNAi} resulted in an increased apoptosis similar to other genes that have recently shown to induce apoptosis in wing discs, including the centrosomal protein Sas-4 (Figure 7A) (Poulton et al., 2014). In contrast to Sas-4, however, loss of Shot did not increase the expression of phosphorylated (activated) JNK, suggesting a JNK-independent mode of cell death (Figure 7B). Interestingly, Arp-1^{RNAi} also induced apoptosis; however, its effects were significantly more dramatic than any of the other conditions examined (Figure 7A). Shot^{RNAi}, and to an even greater extent Arp-1^{RNAi}, also caused morphological abnormalities in the F-actin dense folds of the wing pouch, indicating that their loss is detrimental to the overall tissue architecture (Figure 7A). To understand the importance of cell death in these contexts, we expressed the apoptosis inhibitor, p35. We also generated double transgenic lines that express p35 simultaneously with Shot^{RNAi}. We quantified the area of tissue expressing Matrix metalloproteinase-1 (MMP-1), a key marker of epithelial-mesenchymal transition (EMT), under these conditions. Expression of p35, but not Shot^{RNAi} alone, resulted in induction of MMP-1 expression. Co-expression of p35 with Shot^{RNAi} resulted in a marked and synergistic expression of MMP-1 (Figure 7C). These results indicate that although apoptosis following Shot loss can lead to mild defects in epithelial tissue architecture, it is likely a response to prevent more substantive alterations should Shot defective cells be allowed to persist.

DISCUSSION

Spectraplakins are large, modular scaffolds that facilitate dynamic crosslinking interactions between components of the cellular cytoskeleton. These proteins have well-established roles in facilitating cell migration, organizing multicellular tissue structures, and maintaining MT organization (Applewhite et al., 2010; Suozzi et al., 2012). Although remarkably diverse, these functions all contribute to activities that primarily operate in non-dividing cells. We have shown here that Shot, the lone *Drosophila* spectraplakins gene, also plays an important role in mitotic cells. Specifically, loss of Shot results in a multifaceted phenotype characterized by unfocused mitotic spindle poles, misaligned spindles, and defective chromosome dynamics. Shot loss frequently leads to metaphase arrest, which is likely due to activation of the spindle assembly checkpoint. These diverse mitotic processes all share a common trait in their dependence on the force-generating MT motor protein Dynein (Prosser and Pelletier, 2017; Raaijmakers et al., 2013). Importantly, disruption of F-actin leads to deficits in spindle morphology and orientation, but does not alter chromosome dynamics or cell cycle timing, demonstrating that interactions with F-actin are insufficient to completely describe the Shot phenotype. Conversely, all Shot phenotypes are mimicked by loss of Arp-1, an essential component of the Dynein-activating Dynactin complex, as well as loss of Dhc itself. The actin-binding domain of Shot directly interacts with Arp-1 *in vitro*, defining a physical link with the Dynactin complex. Finally, Shot loss induces significant cell death *in vivo*, and preventing this apoptotic response leads to marked expression of MMP-1 and epithelial

disorganization, both classic hallmarks of EMT. We propose that Shot, in addition to its traditional role as an actin-MT crosslinking agent, serves as an important regulator of mitotic Dynein/Dynactin activity to help ensure the fidelity and accuracy of cell division.

Shot participates in mitotic spindle assembly and orientation: The role of F-actin in mitotic spindle assembly and positioning has been studied in a variety of cellular systems (Lancaster and Baum, 2014; Sandquist et al., 2011). In budding yeast, cortical actin plays an important role in centrosome guidance into the developing bud that aids in satisfying the spindle orientation checkpoint process that triggers mitotic exit (Gachet et al., 2001; Yin et al., 2000). A similar modality contributes to bipolar spindle formation in mammalian cells: the F-actin cortex is necessary for centrosome separation and orientation after NEB through a myosin II-dependent connection with astral MTs (Rosenblatt et al., 2004). Chemical disruption of cortical actin induces spindle orientation defects in mammalian cell culture (Thery et al., 2005; Toyoshima and Nishida, 2007). Recent studies have shown that external forces controlling cell shape can dictate spindle assembly and positioning (Fink et al., 2011; Lancaster et al., 2013; Petridou and Skourides, 2014). The Ezrin-Radixin-Moesin (ERM) family of proteins, which associate with the F-actin-rich cortex, represents a likely candidate for mediating this effect by ensuring cortical localization of core spindle orientation machinery (Hebert et al., 2012; Kiyomitsu and Cheeseman, 2013; Machicoane et al., 2014).

Arp-1 (or more generally the Dynactin complex) is also an important component of spindle assembly and positioning. Dynactin is essential for spindle orientation in *Drosophila* neural stem cells, where it is thought to exert cortical forces on spindle poles to establish proper positioning as part of a complex with Dynein and Mud/NuMA (Bowman et al., 2006; Siller et al., 2006; Siller and Doe, 2008). Studies in HeLa cells have shown that NuMA is necessary for asymmetric cortical Dynactin localization (including Arp-1 itself), which is critical for proper spindle positioning (Kiyomitsu and Cheeseman, 2012). In fact, this cortical localization of Dynactin is sufficient for orienting the spindle in these cells (Kotak et al., 2012). Dynactin also plays a critical role in spindle assembly, particularly in the organization of spindle poles (Gaglio et al., 1997; Merdes et al., 2000; Merdes et al., 1996; Morales-Mulia and Scholey, 2005; Quintyne et al., 1999).

These parallel effects of F-actin and Arp-1/Dynactin on spindle morphology and orientation complicate the interpretation of this Shot phenotype. Shot interacts with both F-actin and Arp-1, and Shot loss has similar effects on spindle assembly and orientation as both Cyt-D treatment and Arp-1^{RNAi}. Thus, a complete molecular picture of Shot function in these processes will require further investigation. It is worth noting that Cyt-D treatment did not disrupt Shot localization in metaphasic S2 cells, a result consistent with a model in which Arp-1 plays a more important role in Shot mitotic function. Furthermore, concomitant loss of Shot and either Arp-1 or Dhc did not further potentiate the effects of either alone suggesting they operate in a common pathway. Mitotic spindle poles represent one prominent site for Shot localization, and we suggest that Shot, a

large structural protein, could physically connect cortical actin with astral MTs as a means of spindle capturing, an important and conserved feature of spindle positioning (Huisman and Segal, 2005; Johnston et al., 2009). Alternatively, but not mutually exclusive, Shot interaction with Arp-1 at spindle poles could directly participate in Dynactin/Dynein activity to ensure proper focusing of MTs and the force generation created by minus-end motor activity.

Molecular model for how Shot regulates Dynein function: MT motor proteins participate in diverse cellular events. In contrast to the relatively large family of plus-end directed kinesin motor proteins, cytoplasmic Dynein represents the sole minus-end directed motor within the cell (note that at least one unique member of the kinesin family also has minus-end directionality). Yet, the diversity of cellular functions involving Dynein easily matches that of the much larger kinesin superfamily. How then can this single, yet functionally diverse Dynein motor be properly regulated across its range of activities? Furthermore, Dynein/Dynactin alone is a non-processive motor, raising the question of how processive function can be achieved. These apparent problems are solved by the existence of a large group of 'adaptor' proteins, which together regulate both the localization and processive activity of the Dynein/Dynactin complex (Kardon and Vale, 2009). Dynactin itself is a large, multi-protein complex, including its core Arp-1 filament, that aids in Dynein localization, cargo assembly, and minus-end movement (Kardon and Vale, 2009). The adaptor protein BICD2 forms a tripartite complex with Dynein and Dynactin, the formation of which stabilizes binding of the Dynein tail to Arp-1 (Urnavicius et al., 2015). Dynactin binding induces

conformational changes in the Dynein motor domains that ultimately lead to processive minus-end movements (McKenney et al., 2014; Zhang et al., 2017). A diverse set of these adaptor proteins may, therefore, provide spatiotemporal and functionally-specific activation of Dynein activity. One such adaptor, Spindly, targets Dynein to kinetochores and is necessary for the poleward removal of the RZZ/Mad2 complex that silences SAC signaling (Griffis et al., 2007). Spindly binds Dynactin; however, it associates with the Pointed-End Complex rather than the Arp-1 filament (Gama et al., 2017). The ability of Shot to directly associate with the Arp-1 component of Dynactin suggests it may serve an adaptor role as well, ultimately leading to enhanced Dynein activity. Results presented herein suggest this may be particularly important in Dynein-dependent chromosome transport to spindle poles, as Shot loss leads to deficits in both chromosome congression and segregation ultimately delaying cell cycle progression (Figs. 4-6).

The mitotic arrest induced by Shot loss is phenocopied by reduction of Arp-1 or Dhc, and Inhibition of the SAC by knockdown of Rod suppresses both Shot^{RNAi}- and Arp-1^{RNAi}-mediated arrest. Interestingly, concomitant loss of Shot and Arp-1 or Shot and Dhc prevents effects on both mitotic arrest and index. Although the molecular basis for this effect is not immediately obvious, we speculate it could be due to a reduced efficiency and/or sustainability of the SAC resulting from less stable kinetochore MTs in the absence of Shot. Shot is known to function in stabilizing interphase microtubules (Applewhite et al., 2010). Unstable MTs could compromise kinetochore associations; however, this would

be predicted to increase SAC signaling (Tauchman et al., 2015). A more plausible model could be that certain SAC components are not properly localized in the double mutant cells, allowing anaphase transition despite chromosome congression and/or alignment errors. The MT-associated KMN network plays an important role in the recruitment of key SAC components (Varma and Salmon, 2012), the efficiency of which may be compromised in the absence of Shot. Why this effect is only seen in double RNAi (Shot/Arp-1 or Shot/Dhc) and not following Shot^{RNAi} alone remains unclear. Knockdown of both Arp-1 and Dhc does not suppress metaphase arrest, however, indicating that escape from mitotic arrest is dependent on Shot knockdown. The inability to arrest is not without consequences, as both Shot/Arp-1 and Shot/Dhc64C double RNAi treated cells exhibited extremely high rates of chromosome segregation defects.

bIII-spectrin, a gene in the spectrin superfamily from which spectraplakins proteins like Shot are thought to have evolved (Suozzi et al., 2012), localizes to the Golgi membranes and is thought to enhance Dynein-mediated vesicle transport. Similar to Shot, bIII-spectrin interacts with Arp-1 via its N-terminal ABD, and this interaction is ablated by a L253P mutation (corresponding to Shot L340P used herein) associated with Spinocerebellar ataxia type 5 leading to impaired vesicular transport in cerebellar axons (Clarkson et al., 2010; Holleran et al., 2001; Holleran et al., 1996; Lorenzo et al., 2010). In contrast to their common N-terminal ABDs, spectrins differ from spectraplakins in that they lack a MT-binding domain at the C-terminus and instead contain a phospholipid-binding Pleckstrin homology (PH) domain (Suozzi et al., 2012). Association of this C-terminal PH

domain with acidic lipids on transport vesicles allows bIII-spectrin to thus tether cargo to the motile Dynein/Dynactin complex bound at the N-terminal ABD via Arp-1 (Johansson et al., 2007). Moreover, this effect can be reconstituted *in vitro* in a manner that suggests bIII-spectrin, through its interaction with Arp-1, is sufficient for processive Dynein-mediated vesicle transport (Muresan et al., 2001). An analogous mechanism may underlie Shot aiding Dynein-mediated events during mitosis. For example, focusing of mitotic spindle poles is thought to be achieved through a multistep process, wherein processive Dynein motility allows for the transport of bundled K-fibers along centrosomal MTs (C-MTs) in a poleward direction (Goshima et al., 2005). This process is thought to rely on crosslinking factors that can tether C-MT-bound Dynein/Dynactin to the K-fiber MT bundles. Shot could accomplish this through simultaneous interactions with Arp-1 at its N-terminus and K-fiber MTs at its C-terminus. This would be consistent with both the general requirement of Shot in pole focusing as well as the dependence on its intact actin- and MT-binding domains (Figure 4), although the precise mechanism will require further investigation.

Importance of Shot in tissue organization and possible tumor suppression:

Knockdown of Shot *in vivo* results in an apoptotic response in imaginal wing disc epithelia. Interestingly, loss of Arp-1 in this tissue leads to a significantly greater level of apoptosis, demonstrating a strict requirement of this Dynactin component to epithelial cell viability. The precise mechanism by which Shot loss induces apoptosis is not yet elucidated, due in part to the pleiotropic mitotic errors that occur in its absence. Shot loss causes spindle misorientation in wing discs, and

studies have shown that loss of planar spindle orientation leads to apoptosis of daughter cells that are basally extruded from the epithelial layer (Nakajima et al., 2013). Recent studies have also shown that loss of several centrosomal proteins known to participate in spindle assembly lead to apoptosis in this tissue (Poulton et al., 2014). It should be noted that centrosome loss under these conditions also leads to spindle misorientation, complicating a direct mechanistic interpretation. Thus, further investigations will be necessary to determine the relative contributions of defective spindle assembly and orientation in the apoptotic response seen following Shot loss. Unlike loss of other genes well known to participate in spindle assembly and orientation (Nakajima et al., 2013; Poulton et al., 2014), Shot loss does not appear to significantly upregulate p-JNK levels, suggesting apoptosis is induced through an alternative pathway (Figure 7). Although JNK signaling has a clear canonical role in apoptosis, alternative pathways likely play a role in apoptotic induction (Strasser et al., 2000), and, furthermore, JNK signaling has been shown to play an activating role in cell proliferation under certain conditions such as compensatory growth (Mollereau and Ma, 2016).

Whatever the cause of apoptosis following Shot knockdown, results from p35 expression highlight the importance of this response in maintaining tissue architecture. Although Shot^{RNAi} expression alone results in a mild loss of organization within the wing pouch, co-expression with p35 to prevent the apoptotic response lead to a much more striking disorganization of tissue structure (Figure 7). Moreover, this genotype caused a marked induction of the

EMT marker MMP-1. What the relative contributions of Shot's mitotic functions are to these defects will be an important future question to resolve. Also of interest will be to evaluate the tumorigenic potential of this tissue, perhaps using recently established tumor models in *Drosophila* (Gonzalez, 2013).

MATERIALS AND METHODS

Fly stocks:

The following stocks were obtained from the Bloomington Stock Center: VALIUM TRiP lines for *shot*^{RNAi} (stock # 28336), *arp-1*^{RNAi} (stock # 32032), and *sas-4*^{RNAi} (stock # 35049), as well as *UAS-p35* (stock # 5072) and *nubbin*^{GAL4} (stock # 25754). The double transgenic line *UAS-p35/UAS-p35;shot*^{RNAi}/*shot*^{RNAi} was generated using a *Cyo/Br;TM2/TM6* double balancer line (generous gift from Dr. Richard M. Cripps, UNM).

S2 cell maintenance, RNAi treatments, and transient transfection:

Schneider S2 cells (Invitrogen) were grown in Schneider's insect media (Sigma) supplemented with 10% heat-inactivated fetal bovine serum (SIM). Cells were passaged every 3–4 days and stocks were maintained at 25°C in the absence of CO₂. For transient transfections (see below), 1-2 × 10⁶ cells were placed in six-well culture dishes for 30 min in 3 ml of SIM. Cells were then transfected with 1 µg total DNA using the Effectene reagent system according to manufacturer protocols (QIAGEN). Following 24–36 hr incubation, transgene expression was induced by the addition of CuSO₄ (500 µM) for 24-48 hr.

We used the following constructs for S2 cell transfections: Ed:GFP:Pins, Ed:GFP:Dsh, Ed:FLAG:Pins, ShotADCT:mCherry, and GAL4 were expressed using the copper-inducible pMT vector. ShotA:GFP, and ShotC:GFP were cloned in the pUAST vector and expressed via cotransfection of pMT-GAL4. All Shot constructs, as well as the pMT-GAL4 plasmid, were generous gifts from Drs. Stephen Rogers and Derek Applewhite (UNC, Chapel Hill and Reed College, respectively).

Primers used for RNAi construction were designed using the SnapDragon web-based service (<http://www.flyrnai.org/snapdragon>), and all primer synthesis was carried out by Invitrogen. Primer sets that amplify segments of ~200–600 base pairs within the coding or 3'-UTR sequence of desired targets were optimized for efficiency and specificity and synthesized with T7 promoter sequence recognition tags. Targeted sequences were designed to universally recognize all possible isoforms for desired transcript. PCR-amplified target sequences were transcribed to yield double-stranded RNA using the Megascript T7 kit (Ambion) following the recommended protocol.

For RNAi treatment, S2 cells were seeded in six-well dishes at 1×10^6 cells per well in 1 ml of serum-free Schneider growth media and incubated with 10 μ g of desired RNAi. After 1 hr, 2 ml of SIM was added, and cells were incubated for an additional 5 days prior to subsequent assays. Cells were typically supplemented with an additional 0.5-1 ml of SIM following day 3 to avoid excessive evaporation.

For the Echinoid-based “induced polarity” assay, cells were harvested, pelleted, and resuspended in fresh SIM supplemented with CuSO_4 . Cells were then placed in a new six-well dish and rotated at ~ 175 rpm for 2–3 hr, allowing for stochastic cell collisions that lead to cell-cell contacts and cluster formation (Johnston et al., 2009). Cyt-D treatments were done with 3 mg/mL of the drug dissolved in DMSO, with an equal volume of DMSO alone serving as a vehicle control.

Immunostaining and S2 live-cell imaging:

Following transfection and RNAi treatments, S2 cells were mixed with fresh SIM in 24-well dishes containing 12 mm diameter round glass coverslips. Cells were incubated for 2–3 hr to allow for adherence to coverslips and to increase the percentage of mitotic cells. Cells were then fixed using a treatment of 4% paraformaldehyde for 10 min. Fixed cells were washed three times (5 min each) with wash buffer (0.1% Triton X-100 in PBS), followed by a 1-hr incubation with block buffer (0.1% Triton X-100 and 1% BSA in PBS). Primary antibodies diluted in block buffer were then incubated with slides overnight at 4°C. Following primary antibody incubation, slides were washed three times with block buffer. Secondary antibodies were then added and incubated at room temperature for 2 hr. Antibodies were removed and slides were washed four times with wash buffer. Finally, coverslips were inverted and mounted using EverBrite Hardset reagent (VWR) and stored at 4°C prior to imaging.

Antibodies used were as follows: mouse anti-FLAG (1:500; Sigma), rat anti- α -tubulin (1:500; Sigma Aldrich), and rabbit anti-PH3 (1:1,000; Abcam). γ -tubulin antibodies were obtained from Sigma (1:500, rabbit) and GeneTex (1:2,000, mouse). Imaging was performed using Nikon Eclipse Ti-S and Olympus IX83 inverted fluorescence microscopes and collected under oil immersion at 60 \times magnification. All secondary antibodies (preabsorbed and non-crossreactive) were obtained from Jackson ImmunoResearch and used at 1:250 dilutions.

For live-cell experiments, movies were acquired using S2 cells stably expressing an inducible GFP:CID (a generous gift from Dr. Gary Karpen, UC Berkeley), which we subsequently stably transfected with inducible mCherry- α -tubulin (selected for using puromycin resistance) to generate a stable double transgenic S2 cell line. Cells were treated with Control or RNAi as described in the previous section. Upon completion of RNAi treatment, cells were settled at a density of 2 million/mL into Nunc Lab-Tek II 4-chambered coverglass chambers pre-coated with poly-L-lysine. After settling for 1 hour, chambers were placed onto an Olympus IX-83 inverted epifluorescent microscope and appropriate cells were located and imaged at either 30 second or 1 minute intervals using a Hamamatsu Orca-Flash 4.0LT camera, with three z-stacks taken at each interval. If cells (e.g. Shot^{RNAi} treated) did not enter anaphase after 3 hours the experiment was stopped and recorded as 180 min. data point. This was done due to significant photobleaching and the potential for phototoxicity. Movies were converted to AVI or MOV files and analyzed using ImageJ.

Protein purification:

The Shot ABD (CH1+CH2 domains, amino acids 149-368), CH2 domain alone (amino acids 264-365), and C-terminus (amino acids 5071-5501) were PCR amplified from a pUAST-Shot construct and cloned into the pGEX vector using 5'-BamHI and 3'-XhoI restriction sites to generate GST-Shot fusion constructs. Full-length Arp-1 was PCR amplified from an S2 cell cDNA library and cloned into pBH4 using 5'-BamHI and 3'-XhoI restriction sites to generate a 6xHis-Arp-1 fusion construct. All constructs were transformed into the BL21(DE3) strain of *E. coli* for recombinant protein expression and grown in standard Laurie Broth supplemented with 100 µg/mL ampicillin.

GST-Shot^{ABD} and GST-Shot^{CH2} were grown at 37°C to an OD₆₀₀ ~ 0.8, and protein expression was induced with 1 mM isopropyl β-D-1-thiogalactopyranoside (IPTG) for 3-4 hrs. GST-Shot^{CT} was grown at 30°C to an OD₆₀₀ ~ 0.6 and induced with 0.2 mM IPTG overnight at 20°C. Cells were harvested by centrifugation (5000 × g for 10 min) and bacterial pellets were resuspended in PBS and flash frozen in liquid nitrogen. Cells were lysed using a Branson digital sonifier and clarified by centrifugation (12,000 × g for 30 min). Cell lysates were aliquoted and stored at -80°C until use.

His-Arp-1 expression was induced similarly to GST-Shot^{CT}, except that cells were resuspended in N1 buffer (50 mM Tris, pH 8, 500 mM NaCl, and 10 mM imidazole). Following lysis and clarification, the His-Arp-1 supernatant was incubated with Nickel-NTA resin for 3 hours at 4°C with constant rotation. Resin was washed extensively with both N1 buffer and Wash buffer (N1 + 30 mM

imidazole). Bound proteins were eluted and collected in Elution buffer (20 mM Tris, pH 8, 200 mM NaCl, and 300 mM imidazole). This sample was dialyzed overnight at 4°C in buffer (20 mM Tris, pH 8, 200 mM NaCl, and 2 mM DTT), concentrated, and stored at -80°C prior to use. This crude preparation produced minimal amounts of soluble His-Arp-1, although they were sufficient for detection using an anti-His antibody in western blotting.

GST pulldown assay:

Equivalent amounts of GST-fused Shot constructs were absorbed to glutathione agarose for 30 min at room temperature and washed three times with PBS to remove unbound protein. Subsequently, His-Arp-1 was added for 3 hr at 4°C with constant rocking in wash buffer (PBS supplemented with 0.5% Triton X-100 and 1 mM DTT). Reactions were washed four times in wash buffers, and resolved samples were analyzed by western blot using mouse anti-His primary and bovine anti-mouse HRP secondary antibodies (ThermoFisher and Santa Cruz Biotechnologies).

Imaginal wing disc analysis:

Imaginal wing discs were dissected from wandering third instar larvae in PBS. Discs were fixed in 4% paraformaldehyde at room temperature for 20 min with rocking. Following fixation, discs were quickly washed three times in wash buffer (PBS supplemented with 0.3% Triton X-100) and then once at room temperature for 20 min with rocking. Discs were blocked in block buffer (wash

buffer supplemented with 1% BSA) for 1 hr at room temperature. Phalloidin-568 (1:50, Thermo Fisher) and primary antibodies in block buffer were incubated with constant rocking at 4°C for 24–48 hr. Subsequently, discs were washed and treated with secondary antibodies in block buffer for 2 hr at room temperature. Washed discs were mounted in Vectashield Mounting Medium for Fluorescence or 80% glycerol and stored at 4°C until imaged. Imaging was performed on a Zeiss LSM780 confocal microscope. Antibodies used were as follows: mouse γ -tubulin (1:500), rabbit phosphohistone-H3 (1:1,000), rabbit cleaved caspase-3 (1:500, Cell Signaling Technology), mouse MMP-1 (1:100, Developmental Studies Hybridoma Bank), and rabbit phospho-JNK (1:1,000, Promega).

Area quantification of wing disc maximum intensity projections was done using thresholding and the 'thresholdcolour' plugin in ImageJ. The area of the wing pouch was first taken using the polygon selection tool and recorded in pixels. The extraneous portions of the disc (the hinge and the notum that lie outside of the Nubbin expression pattern) were then removed using the 'Clear Outside' command. Then using the 'Threshold Colour' command, only pixels displaying green were selected. Using the 'Threshold' command, pixels positive for signal were selected and background was excluded. The number of positive pixels were then calculated using the 'Analyze Particles' command setting the minimum detectable pixel size to 2 square pixels, and displaying results. The number of pixels obtained was then normalized to a percent area measurement by dividing it by the size of the wing pouch obtained earlier.

ACKNOWLEDGMENTS

We thank Johnston lab members for helpful and insightful discussions. This work was supported by a grant from the National Institutes of Health: R01-GM108756 (C.A.J.).

Chapter 3

Mechanisms of Apoptosis Induced by Loss of Shortstop in *Drosophila*

Wing Disc Epithelial Tissue

ABSTRACT

Tissue development and homeostasis hinge on the ability for cells to divide properly in order to generate new tissue and replace old tissue effectively. Many proteins have been identified that govern the cell division process, with their loss affecting tissue development and homeostasis. These proteins have further been implicated in many disease phenotypes. Given the importance of cell division for growth and maintenance of tissue, surprisingly little is known about how tissues work to correct and respond to defects that may arise in these processes. Here we characterize a mechanism of how cells cope with loss of a particular regulator of cell division, the actin-microtubule crosslinker Shortstop (Shot). We show that Shot loss causes DNA damage in the form of double strand breaks (DSBs) and that these worsen when the spindle assembly checkpoint (SAC), which works to prevent breaks stemming from improper chromosomal segregation, is compromised. We show Shot loss likely works through p53 and the DNA damage response (DDR), with tissues attempting to repair DNA and inducing apoptosis in cells where DNA damage is too severe to be repaired. We show this mechanism is discrete from loss of another cell division regulator, Sas-4, and identify several genes through RNAseq that are distinct to Shot loss. This work highlights the unique, tissue-wide responses cell division regulators can illicit when lost, and underscores the need to characterize these mechanisms in order to better understand how tissues respond to loss of particular regulators.

INTRODUCTION

Development and maintenance of epithelial tissue is a highly complex process, requiring precise coordination of cell divisions to ensure and preserve properly patterned structures. Aberrant divisions due to mis-regulation or loss of key regulators can cause defects in growth and cellular differentiation, leading to severely malformed tissues and even embryonic death (Vorhagen and Niessen, 2014; Zhong and Zhou, 2017). Additionally, cell divisions are key to tissue maintenance in adult organisms, with irregular divisions sometimes initiating tumor and even cancerous formations (Bonello and Peifer, 2019; Tellkamp et al., 2014). During embryonic and adult cell divisions, cells must: 1. undergo proper polarization, 2. form and orient their mitotic spindles correctly, and 3. Coordinate chromosome movements such as congression and segregation (Butler and Wallingford, 2017; Dewey et al., 2015c; Knoblich, 2008; Lara-Gonzalez et al., 2012; Lu and Johnston, 2013; O'Connell and Khodjakov, 2007; Soto et al., 2019). Loss of polarity resulting from improper regulation of polarity proteins and abnormal spindle formation can lead to loss of cell identity and potentially to epithelial-to-mesenchymal transitions, a hallmark of many cancers (Hanahan and Weinberg, 2011). Incorrect spindle formation and mis-regulation or loss of chromosomal movement proteins and/or kinetochore proteins can additionally cause DNA damage through chromosomal breaks and even aneuploidy (whole chromosome mis-segregation events)(Duro and Marston, 2015; Lara-Gonzalez et al., 2012; O'Connell and Khodjakov, 2007; Soto et al., 2019). These defects

result in chromosome instability, another hallmark of cancer (Hanahan and Weinberg, 2011). The consequences of defects in oriented cell division are thus key to understanding both faults in development and formation of tissue, as well as in cancer/tumor formation in differentiated tissues.

In *Drosophila*, studies of oriented cell divisions in various cells and tissues have identified key regulators and the phenotypes associated with their loss. For example, analyses of *Drosophila* neuroblasts have characterized the importance of a properly oriented division to differentiation (Doe, 2008), whereas investigations of *Drosophila* imaginal wing and eye discs have highlighted how oriented divisions affect epithelial development (Hariharan and Bilder, 2006; Herranz et al., 2016). Defects in polarity, spindle formation, and chromosome movements all result in various outcomes depending on the components of oriented cell division that are affected. Some genes or genes result in massive cell death, while others result in excessive or stagnant growth (Cabernard and Doe, 2009; Dewey and Johnston, 2017; Dewey et al., 2015b; Poulton et al., 2014, 2017). Given the different effects of loss and/or mutation of particular regulators of oriented cell division, as well as differing results based on tissue/cell types, it is important to characterize the phenotypes of each regulator in order to accurately assess its effects and mechanisms of action stemming from its loss or mutation.

Previously, we have shown that one such regulator of oriented cell divisions, Shortstop (Shot), likely acts differently from another regulator, Sas-4 (Dewey and Johnston, 2017). While Sas-4 served to activate Jun-N-terminal

kinase (JNK) signaling in response to acentrosomy, Shot was suggested not to function predominantly through JNK, since the levels of active JNK (pJNK) observed in Shot RNAi discs were comparable to those in control discs. We believe this disparity was caused primarily through differences in defects caused by loss of each gene, and we proposed to define these differences and ascertain components of the mechanism by which wing disc epithelia respond to Shot RNAi. Here we show that Shot RNAi causes significantly increased double strand DNA breaks (DSBs) compared to Sas-4 RNAi and that this difference leads to distinct response pathways for each. Loss of the DNA damage repair protein, p53, affects the tissue response to Shot RNAi, but not to Sas-4 RNAi. Using RNA sequencing of the distinct area of the wing disc tissue driving RNAi, we find genes upregulated in the response to Shot RNAi that are not found in Sas-4 RNAi tissue, genes that are implicated in DNA damage response (DDR). These results not only illustrate that tissues can respond to the loss of distinct cell division regulators through differing mechanisms, but highlight the need to catalog specific tissue responses to loss of various regulators during investigations of cell division.

RESULTS

Shot RNAi Causes DSBs in Imaginal Wing Discs

Given that Shot RNAi-mediated apoptosis in *Drosophila* imaginal in wing discs may be JNK independent and that Shot RNAi in S2 cells caused significant lagging and bridged chromosomes in anaphase (Dewey and Johnston, 2017),

the possibility that Shot loss causes DNA damage in wing discs via double stranded breaks (DSBs) was analyzed. In discs stained for a phosphorylated variant of histone H2A that marks DSBs (pH2Av), Shot RNAi induces a higher level of DSBs, whereas Sas-4 RNAi has no significant effect (Figure 1A).

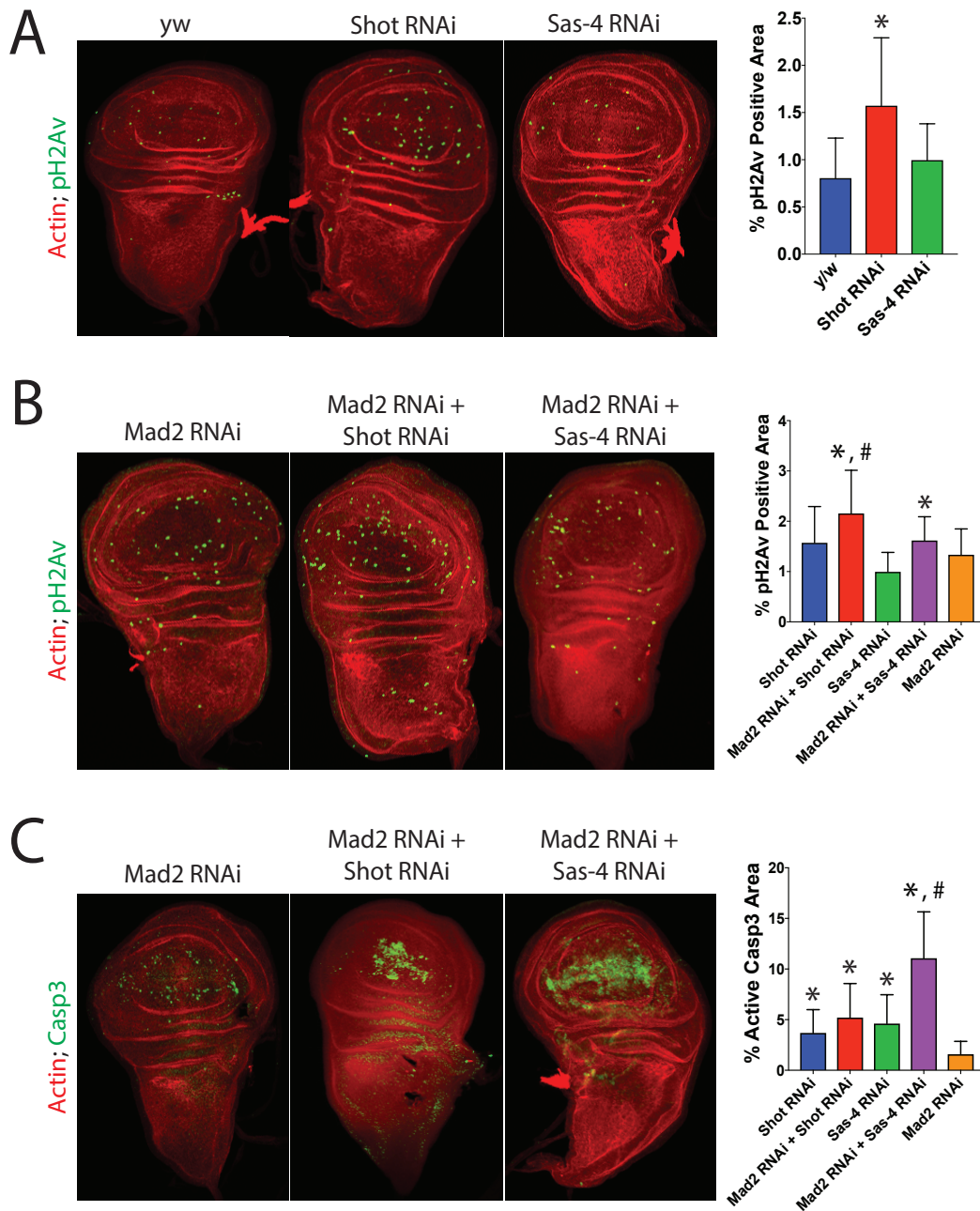


Figure 1. Shot loss causes DSBs in imaginal wing discs; levels of DSBs, but not apoptosis, are increased when SAC is disrupted. (A) Imaginal wing discs were dissected from late stage L3 larvae, fixed, and stained for phospho-Histone H2Av (pH2Av; green) to stain DSBs and AlexaFluor-568 Phalloidin to stain F-actin. Shot RNAi causes an increase in DSBs compared to yw (* $p < 0.05$), while Sas-4 RNAi does not cause an increase in DSBs compared to yw ($p > 0.999$). (B) RNAi against Mad2 (a SAC regulator) increases DSBs when coupled to Shot RNAi compared to Mad2 RNAi (* $p < 0.05$) and Shot RNAi alone (# $p < 0.05$), while coupling Mad2 RNAi to Sas-4 RNAi does not appreciably increase DSBs compared to Mad2 alone ($p = 0.801$). Note that all conditions except for Sas-4 RNAi are significant from yw ($p < 0.05$ for each). (C) Imaginal wing discs were dissected from late stage L3 larvae, fixed, and stained for active Caspase 3 (Casp3; green) to assess apoptosis and AlexaFluor-568 Phalloidin to stain F-actin. Mad2 RNAi + Sas-4 RNAi significantly increases apoptosis over both Mad2 RNAi (* $p < 0.05$) and Sas-4 RNAi (# $p < 0.05$) alone in line with previous findings (Poulton et al., 2014). Mad2 RNAi + Shot RNAi (avg Casp3 % area = 5.02) does not significantly ($p = 0.2911$) increase apoptosis compared to Shot RNAi alone (avg Casp3 % area = 3.67). Note that all conditions except for Mad2 RNAi are significant from yw ($p < 0.05$ for each).

Since the loss of SAC components inhibited Shot RNAi-induced mitotic arrest, likely resulting in quicker divisions but at a cost of improperly attached chromosomes (Dewey and Johnston, 2017), the DSB phenotype of Shot could be enhanced through knockdown of spindle assembly checkpoint (SAC) components. Accordingly, when coupled to Mad2 RNAi (a key component of the SAC), Shot RNAi increases DSBs in wing discs compared to treatments involving Shot RNAi, Mad2 RNAi, and Sas-4 RNAi + Mad2 RNAi, indicating that, compared to Sas-4 RNAi, Shot RNAi wing discs are more susceptible to DSBs when the SAC is inhibited in wing discs (Figure 1B). However, there is no increase in apoptosis as evidenced by active cleaved caspase 3 (Casp3) staining in Shot RNAi + Mad2 RNAi, though Sas-4 RNAi + Mad2 RNAi does trigger more apoptosis, as reported previously (Figure 1C) (Poulton et al., 2014).

Shot RNAi and Sas-4 RNAi tissues are differentially dependent on p53

A key mediator of DSB repair and DSB-induced apoptosis is the tumor suppressor p53 (Chen, 2016; Fridman and Lowe, 2003; Mello and Attardi, 2018).

Given that Shot RNAi caused significantly higher DSBs compared to both yw and Sas-4 RNAi, the possibility that Shot RNAi promoted p53 activity, rather than stimulated JNK activity as in Sas-4 RNAi. After combining both Shot RNAi and Sas-4 RNAi with p53 RNAi and staining for Casp3, pJNK, and pH2Av, Sas-4 RNAi + p53 RNAi shows significant differences in Casp3, pJnk, and pH2Av area compared to either Sas-4 RNAi alone or p53 RNAi alone, indicating that Sas-4 RNAi is not dependent on p53 to mitigate its defects in wing disc epithelia development (Figure 2A). As an indication that Shot RNAi discs cells function through p53 to induce apoptosis, it might be expected that Shot RNAi + p53 RNAi would result in lower Casp3 area compared to Shot RNAi alone. However, under such conditions, Casp3 actually increases compared to Shot RNAi alone in these discs (Figure 2B). While initially puzzling, this result coincides with a previous finding by Villicana et al. 2013, in which expression of a dominant negative p53 coupled to RNAi against an inducer of DSBs (p52), causes cells to default to stress response apoptosis through JNK rather than to attempt DNA repair via p53 (Villicana et al., 2013). Accordingly, Shot RNAi + p53 RNAi discs had significantly increased pJNK, indicating a shift from p53-mediated DNA repair to JNK-mediated stress response (Figure 2B). Loss of p53 does not significantly affect the prevalence of DSBs induced by Shot RNAi, with no

significance from either Shot RNAi alone or *yw* (Fig 2B).

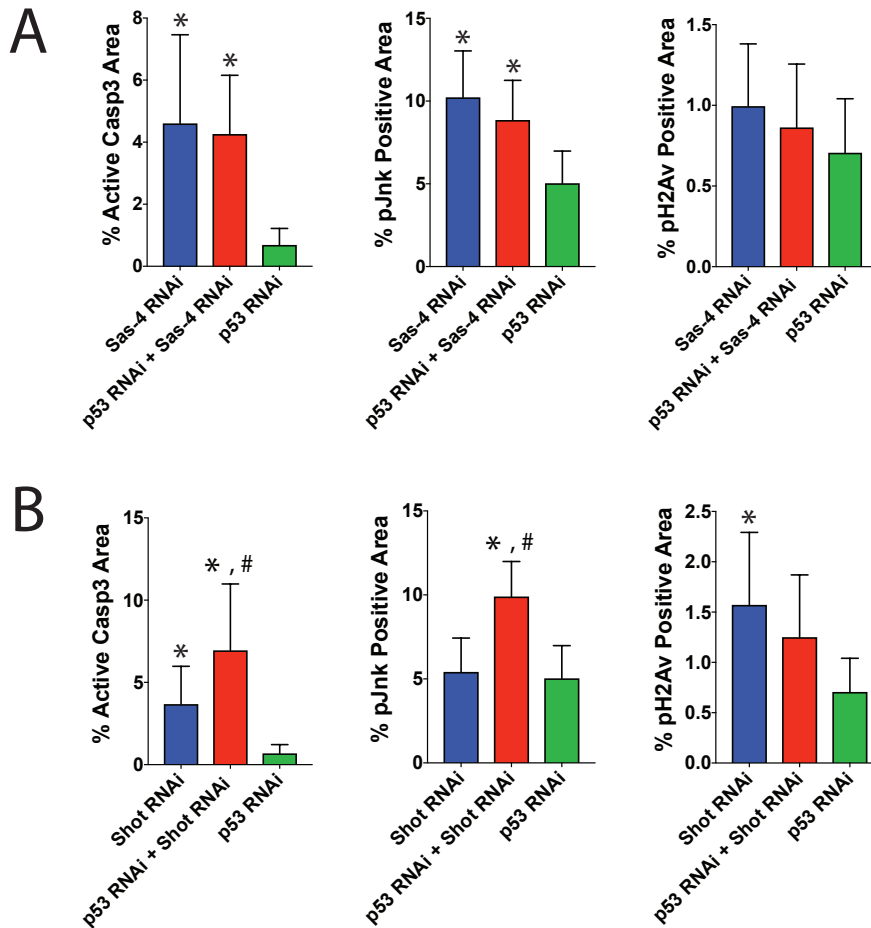


Figure 2. Loss of p53 affects Shot RNAi tissue; Sas-4 RNAi tissue is unaffected. (A) p53 RNAi, p53 RNAi + Sas-4 RNAi, and Sas-4 RNAi imaginal wing discs were dissected from late stage L3 larvae, fixed, and stained for cleaved caspase 3 (Casp3), active phospho-JNK (pJNK), and phospho-Histone H2Av (pH2Av) and assessed for overall area of each to determine apoptosis, Jnk activity, and DSBs, respectively, for each condition. Coupling of p53 RNAi to Sas-4 RNAi does not appear to have any affect relative to Sas-4 RNAi alone, indicating that Sas-4 RNAi tissue is not dependent on p53 (* $p < 0.05$ compared to p53 RNAi and *yw*). (B) p53 RNAi, p53 RNAi + Shot RNAi, and Shot RNAi imaginal wing discs were dissected from late stage L3 larvae, fixed, and stained for cleaved caspase 3 (Casp3), active phospho-JNK (pJNK), and phospho-Histone H2Av (pH2Av) and assessed for overall area of each to determine apoptosis, JNK activity, and DSBs, respectively, for each condition. Unlike Sas-4 RNAi, coupling of p53 RNAi to Shot RNAi does appear to affect these discs relative to Shot RNAi alone (* $p < 0.05$ compared to p53 RNAi and *yw*; # $p < 0.05$ compared to Shot RNAi). Both Casp3 (apoptosis) and pJNK (JNK activity) increase significantly compared to Shot RNAi alone, a unique phenotype owing to the inability to repair DSBs and switching instead to JNK-mediated apoptosis. These results suggest Shot RNAi tissue is dependent on p53.

RNAseq suggests Shot RNAi disc cells function to promote apoptosis through mechanisms distinct from Sas-4

To clarify the distinct mechanisms by which Shot RNAi wing discs cells mitigate mitotic defects compared to Sas-4 RNAi. RNA was extracted from yw, Shot RNAi, and Sas-4 RNAi discs to determine genes that are specifically up regulated in Shot RNAi that are not upregulated in Sas-4 RNAi. We found many genes that were differentially upregulated in Shot RNAi, but not in Sas-4 RNAi or yw (Figure 3A, top venn diagram). Of these genes we specifically looked for those implicated in cell cycle arrest, apoptosis, and DNA repair. We found four Shot RNAi upregulated genes that fit one or more of those criteria: Apoptotic-signal-regulating kinase 1 (Ask1), Growth arrest and DNA damage-inducible 45 (Gadd45), Spellchecker1 (Spel1), and Tousled-like kinase (Tlk, Figure 3A). We confirmed expression levels of each gene (except for Spel1) via quantitative PCR (qPCR, Figure 3B). Given the significance of Spel1 as both a DNA repair agent and a target of Gadd45, we decided it warranted continued experimentation (Duckett et al., 1999; Smith et al., 1994; Smith et al., 2000). These genes are implicated in the DNA damage response, and suggest how Shot RNAi disc cells could function to alleviate deficiencies stemming from aberrant cell divisions and specifically chromosome segregation defects.

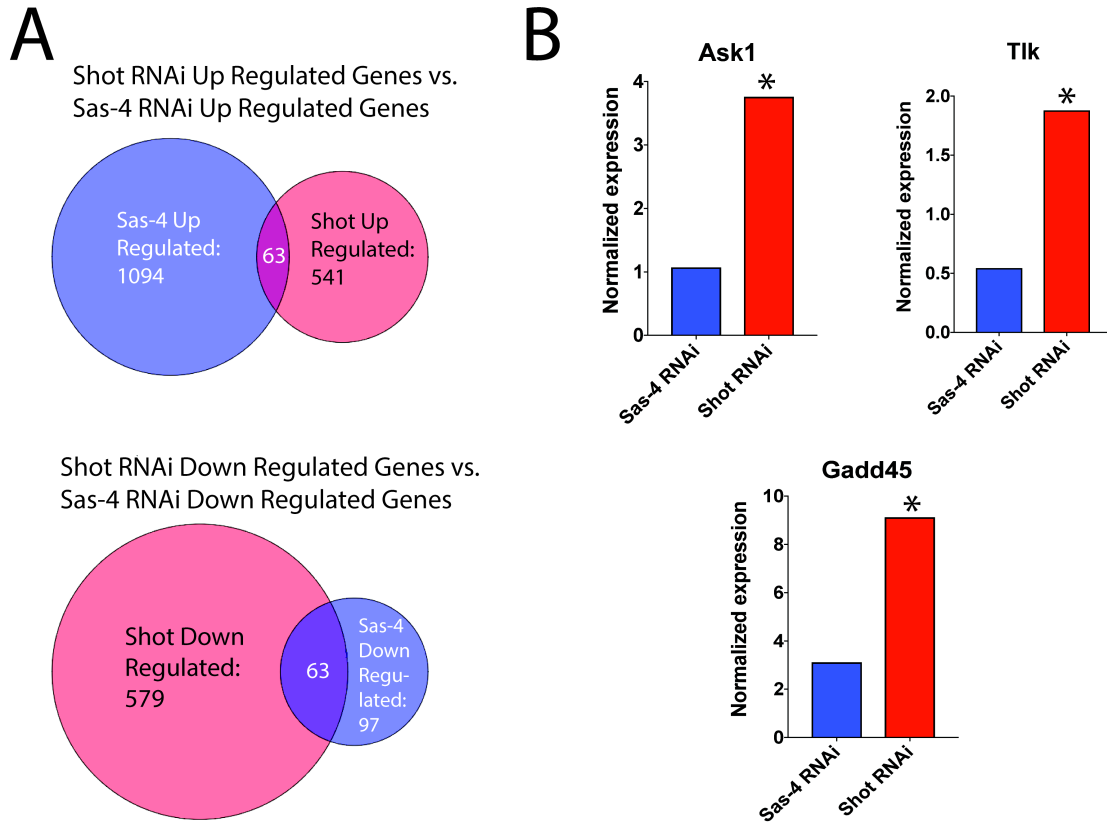


Figure 3. Differential Gene Expression in Shot RNAi and Sas-4 RNAi Imaginal Wing Pouch Tissue. (A) Venn diagrams of differential gene expression and overlap between Shot RNAi and Sas-4 RNAi imaginal wing pouch tissue. Top: Genes up-regulated compared to control (yw) in each condition. Bottom: Genes down-regulated compared to control (yw) in each condition. (B) Quantitative real-time PCR (qPCR) validation of differential gene expression for Shot RNAi-specific up-regulated genes. Ask1, Tlk, and Gadd45 all have significantly higher expression in Shot RNAi tissue than in Sas-4 RNAi tissue (* $p < 0.05$).

DISCUSSION

Shot has been shown previously to be involved in many aspects of cell division, specifically mediating proper chromosome segregation and proper tissue development (Dewey and Johnston, 2017). Sas-4 is another regulator of cell division that causes acentrosomy and defects in tissue development (Poulton et al., 2014). We show here that while RNAi against both Shot and Sas-4 causes apoptosis and defects in tissue development, they do so through differing mechanisms. This stems from Shot RNAi causing more DSBs than Sas-4, an

effect that is enhanced through loss of SAC components. Shot cells with DNA damage then function through p53 to attempt to repair these breaks, unlike Sas-4 RNAi, which instead functions to remove ascentrosomal cells through a JNK-mediated apoptotic response. Elimination of p53 coupled to loss of Shot switches cells from p53-mediated DNA repair to a stress response that involved JNK-mediated apoptosis, as reported previously (Villicana et al., 2013). Loss of p53 in Sas-4 RNAi discs has no effect on cell death however, indicating that Sas-4 RNAi does not trigger p53-mediated apoptosis. RNAseq reveals potential mediators of Shot RNAi specific cell responses, with many genes upregulated in Shot RNAi discs not upregulated in Sas-4 RNAi. Of these, we found several that were implicated in cell cycle arrest, apoptosis, and DNA repair. Our results illustrate that regulators of cell division cause distinct responses when lost, and that these responses likely stem from their initial defects.

Shot RNAi causes epithelial DSBs through improper chromosomal segregations

Proper chromosomal segregation is critical to maintaining genomic stability of cells. In both development and maintenance of epithelial tissues, cells must evenly divide DNA such that each new cell can express appropriate gene dosages. In anaphase, chromosome mis-segregations due to lagging and bridging events can lead to aneuploidy, either through extra copies of whole chromosomes in certain cells in the case of lagging or fragmented chromosomes in the case of bridging (Duro and Marston, 2015; Soto et al., 2019). Shot's role in this process is likely through interaction with the Dynein-Dynactin protein Arp1 as shown previously, and without Shot to stabilize Dynein-mediated chromosomal

segregation, lagging and bridging events frequently occur in S2 cells (Dewey and Johnston, 2017). This suggests that wing disc epithelia may exhibit an increase in DSBs when driving RNAi against Shot. Sas-4 however, has no known connection to dynein-mediated chromosomal segregation, and it has been shown in many tissue contexts that acentrosomal cells produce effective mitotic spindles through non-centrosomal MT-nucleating mechanisms to accurately segregate chromosomes (Basto et al., 2006; Poulton et al., 2017; Stevens et al., 2007). Our results with DSB marker expression in wing discs does contrast with results shown previously by Poulton et al., 2014, who indicate that Sas-4 RNAi causes increased DSBs (Poulton et al., 2014). It should be noted this group used a different antibody than we did, and additionally that their more recent study did not find DDR genes upregulated in response to Sas-4 RNAi (Poulton et al., 2019). Perhaps it could be that a certain DSB threshold is required to activate DDR, and either Sas-4 RNAi wing disc epithelia do not meet this threshold, or the response by cells to acentrosomy is more rapid owing to an inability to correct this defect (unlike DNA damage).

The DSBs caused by Shot RNAi are worsened when coupled to RNAi against the SAC component Mad2, however this does not cause increased cell death. It should be noted that while not significant, the average Casp3 area is higher in Mad2 RNAi + Shot RNAi discs (5.02%) compared to Shot RNAi alone (3.67%). This contrasts with Sas-4 RNAi + Mad2 RNAi, which does not have significantly more DSBs than Mad2 RNAi alone, but does show increased apoptosis in agreement with previous studies (Poulton et al., 2014). The

differences between Shot RNAi and Sas-4 RNAi provide insight into both the speed and means by which cells in these tissues respond to loss of each. In Shot RNAi discs, some cells likely arrest and attempt DNA repair, while others with more severe damage die immediately, unable to attempt repair. Acentrosomy in Sas-4 RNAi discs would be expected to increase when coupled to Mad2 RNAi due to a higher number of cells without duplicated centrosomes evading the SAC, and the resulting JNK-mediated apoptosis would be widespread, leading to the near doubling of cell death in these tissues.

Shot RNAi utilizes p53 to mediate DNA repair and apoptosis, Sas-4 uses JNK to respond to acentrosomy and induce apoptosis

Key to the alleviation of DSBs is p53, functioning as an important tumor suppressor and cellular regulator (Chen, 2016; Fridman and Lowe, 2003; Mello and Attardi, 2018). Loss of Shot in discs likely functions through p53 to promote DNA repair and may induce apoptosis in cells in which DNA damage is too severe. This mechanism was supported through a particular phenotype in Shot RNAi + p53 RNAi discs. Rather than decreasing apoptosis as was expected in this tissue, cells instead increased apoptosis, a result of an inability to attempt DNA repair, and instead converting to JNK-mediated apoptosis, in line with previous results (Villicana et al., 2013). In further support of this switch, pJNK increased significantly in Shot RNAi + p53 RNAi tissue (Figure 2B). As another example of the differing mechanisms between Shot RNAi and Sas-4 RNAi, Sas-4 RNAi does not exhibit any changes in apoptosis or JNK activity levels when coupled to p53 RNAi, indicating that p53 is not necessary in response to its loss.

This agrees with findings of Poulton et al., 2014 that p53 DN is not required for Sas-4 RNAi apoptosis (Poulton et al., 2014), as well as the same groups more recent findings that DDR genes are not upregulated in Sas-4 RNAi discs (Poulton et al., 2019), and is further supported by our finding that Sas-4 RNAi does not induce significant DSBs.

RNAseq-identified genes are likely involved in DDR in Shot RNAi

Several genes identified through RNAseq of Shot RNAi disc tissue have implications in DDR. These genes are each involved in one or more of three main processes as part of this response: DNA repair, cell cycle arrest, and apoptosis. Gadd45 has been shown to function in each of these processes in various ways. It has also been shown to be induced via p53 (Carrier et al., 1994; Zhan et al., 1998; Zhan et al., 1996), further implicating p53 in response to Shot RNAi. Through interactions with proliferating cell nuclear antigen (PCNA) and Spel1 (another gene implicated in Shot RNAi RNAseq), it can function to promote DNA repair (Smith et al., 1994; Smith et al., 2000). Gadd45 also induces G2/M arrest via binding to CyclinB/CDK1 complexes, inhibiting CDK1 function (Jin et al., 2002; Wang et al., 1999). If attempts to repair DNA fail, Gadd45 can cause apoptosis via JNK and/or another MAPK, p38 (Gupta et al., 2006; Hildesheim et al., 2002; Yoo et al., 2003). Given that Shot RNAi does not cause an increase in active JNK compared to control discs, it is likely that Gadd45 may instead predominantly activate p38 in this context. Ask1 may function in conjunction with Gadd45 to induce apoptosis in cells that cannot repair DNA (Papa et al., 2004; Zu et al., 2005). Ask1 can also function through both p38 and/or JNK to induce

apoptosis (Shiizaki et al., 2013), but again due to low active JNK in Shot RNAi discs may instead function mostly through p38.

Tlk is a major regulator of DNA dynamics throughout the cell cycle, and is involved in chromatin assembly, transcription, DNA repair, and chromosome condensation for efficient segregation in mitosis (Han et al., 2005; Sen and De Benedetti, 2006; Sunavala-Dossabhoy et al., 2003; Wang et al., 2007). Tlk has been shown to be regulated by the DDR signaling cascade kinases ATM and Chk1 to suppress its function, turning off Tlk activity to suppress transcription and chromatin assembly while DNA repair is attempted (Krause et al., 2003). Outside of this functionality, overexpression of Tlk (but not Tlk activity) was also recently shown to arrest cells at the G2/M checkpoint via activation of p38 in eye imaginal discs (Liaw and Chiang, 2019), where it has also been shown to cause a unique form of cell death not dependent on JNK activity (Zhang et al., 2016).

Spel1 is the MutS homolog in *Drosophila* and is involved in mismatch repair (MMR). Studies have implicated MutS proteins in sensing and signaling the DNA damage response via cell cycle arrest and induction of apoptosis through activation of the kinase ATM (Duckett et al., 1999). Spel1 could also directly be involved in DSB repair, as MMR proteins have been implicated in this process, facilitating the processing of intermediates in DSB repair and further providing surveillance and recognition of DNA lesions (Li et al., 2016).

Together, each of the identified genes responds to DNA damage caused by Shot RNAi. Future directions will characterize each of these genes' necessity in both Shot RNAi and Sas-4 RNAi contexts. While Sas-4 RNAi cells utilize a

JNK-mediated apoptosis pathway, Shot RNAi cells instead function through DDR, with proteins involved in MAPK cascade-induced apoptosis likely doing so through p38 rather than JNK. Stains for active p38 in Shot RNAi discs could potentially characterize this difference. Apoptosis could also be induced via p53. Further, Shot RNAi cells may induce cell cycle arrest, with evidence from other studies of Shot RNAi upregulated genes specifically implicating the G2/M transition. This could be assessed through measuring the prevalence of cyclin A in Shot RNAi discs, with a higher area of cyclin A suggesting a high number of cells lingering in G2.

MATERIALS AND METHODS

Fly stocks:

The following stocks were obtained from the Bloomington Stock Center: VALIUM TRiP lines for *shot*^{RNAi} (stock # 28336) and *sas-4*^{RNAi} (stock # 35049), as well as *nubbin*^{GAL4} (stock # 25754). Other stocks were obtained from the Vienna Drosophila Research Center: KK phiC31 lines for *mad2*^{RNAi} (stock # 106003), *p53*^{RNAi} (stock # 103001), *gadd45*^{RNAi} (stock # 100413), *ask1*^{RNAi} (stock # 110228), and *tlk*^{RNAi} (stock # 108036), as well as shRNA (VALIUM 20) line for *spe1*^{RNAi} (stock # 330106). The double transgenic lines *mad2*^{RNAi}/*mad2*^{RNAi}; *shot*^{RNAi}/*shot*^{RNAi}, *mad2*^{RNAi}/*mad2*^{RNAi}; *sas-4*^{RNAi}/*sas-4*^{RNAi}, *p53*^{RNAi}/*p53*^{RNAi}; *shot*^{RNAi}/*shot*^{RNAi}, and *p53*^{RNAi}/*p53*^{RNAi}; *sas-4*^{RNAi}/*sas-4*^{RNAi} were generated using a *Cyo/Br;TM2/TM6* double balancer line (generous gift from Dr. Richard M. Cripps, UNM).

S2 cell maintenance and RNAi treatments:

Schneider S2 cells stably expressing inducible GFP:CID and inducible mCherry- α -tubulin (Dewey and Johnston, 2017) were grown in Schneider's insect media (Sigma) supplemented with 10% heat-inactivated fetal bovine serum (SIM). Cells were passaged every 3–4 days and stocks were maintained at 25°C in the absence of CO₂. For RNAi treatment, 1-2 × 10⁶ cells were placed in six-well culture dishes in 3 ml of SIM and allowed to grow for 36-48 hrs. These cells were then seeded in six-well dishes at 1 × 10⁶ cells per well in 1 ml of serum-free Schneider growth media and incubated with 10 µg of desired RNAi. After 1 hr, 2 ml of SIM was added, and cells were incubated for an additional 5 days prior to subsequent assays. Cells were typically supplemented with an additional 0.5-1 ml of SIM following day 3 to avoid excessive evaporation.

Primers used for RNAi construction were designed using the SnapDragon web-based service (<http://www.flyrnai.org/snapdragon>), and all primer synthesis was carried out by Invitrogen. Primer sets that amplify segments of ~200–600 base pairs within the coding sequence of desired targets were optimized for efficiency and specificity and synthesized with T7 promoter sequence recognition tags. Targeted sequences were designed to universally recognize all possible isoforms for desired transcript. PCR-amplified target sequences were transcribed to yield double-stranded RNA using the Megascript T7 kit (Ambion) following the recommended protocol.

Immunostaining and S2 cell imaging:

Following transfection and RNAi treatments, S2 cells were mixed with fresh SIM in 24-well dishes containing 12 mm diameter round glass coverslips. Cells were incubated for 2–3 hr to allow for adherence to coverslips and to increase the percentage of mitotic cells. Cells were then fixed using a treatment of 4% paraformaldehyde for 10 min. Fixed cells were washed three times (5 min each) with wash buffer (0.1% Triton X-100 in PBS), followed by a 1-hr incubation with block buffer (0.1% Triton X-100 and 1% BSA in PBS). Primary antibodies diluted in block buffer were then incubated with slides overnight at 4°C. Following primary antibody incubation, slides were washed three times with block buffer. Secondary antibodies were then added and incubated at room temperature for 2 hr. Antibodies were removed and slides were washed four times with wash buffer. Finally, coverslips were inverted and mounted using EverBrite Hardset reagent (VWR) and stored at 4°C prior to imaging.

Antibodies used were as follows: rat anti- α -tubulin (1:500; Sigma Aldrich), and rabbit anti-PH3 (1:1,000; Abcam). Imaging was performed using an Olympus IX83 inverted fluorescence microscopes and collected under oil immersion at 60 \times magnification. All secondary antibodies (preabsorbed and non-crossreactive) were obtained from Jackson ImmunoResearch and used at 1:250 dilutions.

Imaginal wing disc analysis:

Imaginal wing discs were dissected from wandering third instar larvae in PBS. Discs were fixed in 4% paraformaldehyde at room temperature for 20 min with rocking. Following fixation, discs were quickly washed three times in wash buffer (PBS supplemented with 0.3% Triton X-100) and then once at room

temperature for 20 min with rocking. Discs were blocked in block buffer (wash buffer supplemented with 1% BSA) for 1 hr at room temperature. Phalloidin-568 (1:50, Thermo Fisher) and primary antibodies in block buffer were incubated with constant rocking at 4°C for 24–48 hr. Subsequently, discs were washed and treated with secondary antibodies in block buffer for 2 hr at room temperature. Washed discs were mounted in Vectashield Mounting Medium for Fluorescence or 80% glycerol and stored at 4°C until imaged. Imaging was performed on a Zeiss LSM780 confocal microscope. Antibodies used were as follows: rabbit cleaved caspase-3 (1:200, Cell Signaling Technology), rabbit phospho-JNK (1:1,000, Promega), and rabbit phospho-Histone H2Av (1:1000, Rockland). All secondary antibodies (preabsorbed and non-crossreactive) were obtained from Jackson ImmunoResearch and used at 1:250 dilutions.

Area quantification of wing disc maximum intensity projections was done using thresholding and the 'thresholdcolour' plugin in ImageJ. The area of the wing pouch was first taken using the polygon selection tool and recorded in pixels. The extraneous portions of the disc (the hinge and the notum that lie outside of the Nubbin expression pattern) were then removed using the 'Clear Outside' command. Then using the 'Threshold Colour' command, only pixels displaying green were selected. Using the 'Threshold' command, pixels positive for signal were selected and background was excluded. The number of positive pixels were then calculated using the 'Analyze Particles' command setting the minimum detectable pixel size to 2 square pixels, and displaying results. The

number of pixels obtained was then normalized to a percent area measurement by dividing it by the size of the wing pouch obtained earlier.

Imaginal wing disc RNAseq methods and qPCR analysis

Imaginal wing discs wing pouches from ~60 wandering larvae for *nub>GAL4* driven *yw*, *shot^{RNAi}*, and *sas-4^{RNAi}* were dissected and immediately lysed. RNA was extracted using the RNeasy Mini Kit (Qiagen) followed by digestion with RNase-free DNase (Qiagen). Total RNA was quantified using a Qubit Fluorometer (ThermoFisher Sci) and RNA quality was assessed using an Agilent 2100 Bioanalyzer. RNA sequencing was performed on three biological replicates using the Illumina Next Generation Sequencing platform (75 cycles) with a read depth of 20 million reads per library. Libraries were prepared using 500ng total RNA and a KAPA mRNA Hyper Prep kit (Roche). Raw reads were trimmed using Trimmomatic v0.36 and high-quality reads were mapped to the *Drosophila melanogaster* genome using STAR. Transcript expression was analyzed using featureCounts and differential gene expression analysis was performed using DESeq2 and EdgeR. Genes with an adjusted $p \leq 0.05$ with a \log_2 fold change <-1 or >1 were considered for further analysis.

Quantitative Real-time PCR (q-PCR)

RNA was extracted from imaginal wing discs as described above, and complementary DNA (cDNA) was synthesized using reverse transcriptase in 20 μ L reactions according to manufacturer's instructions with an iScript™ cDNA Synthesis Kit (Bio-Rad, #170-8891, Hercules, California, U.S.A.). The primers for

the candidate genes were designed for a single 100-350 bp region with the Integrated DNA Technologies OligoAnalyzer tool (www.idtdna.com)

ACKNOWLEDGMENTS

We thank Johnston lab members for helpful and insightful discussions. This work was supported by a grant from the National Institutes of Health: R01-GM108756 (C.A.J.).

REFERENCES

- Alves-Silva, J., Sanchez-Soriano, N., Beaven, R., Klein, M., Parkin, J., Millard, T.H., Bellen, H.J., Venken, K.J., Ballestrem, C., Kammerer, R.A., Prokop, A., 2012. Spectraplakins promote microtubule-mediated axonal growth by functioning as structural microtubule-associated proteins and EB1-dependent +TIPs (tip interacting proteins). *J Neurosci* 32, 9143-9158.
- Applewhite, D.A., Grode, K.D., Duncan, M.C., Rogers, S.L., 2013. The actin-microtubule cross-linking activity of *Drosophila* Short stop is regulated by intramolecular inhibition. *Mol Biol Cell* 24, 2885-2893.
- Applewhite, D.A., Grode, K.D., Keller, D., Zadeh, A.D., Slep, K.C., Rogers, S.L., 2010. The spectraplakin Short stop is an actin-microtubule cross-linker that contributes to organization of the microtubule network. *Mol Biol Cell* 21, 1714-1724.
- Atwood, S.X., Prehoda, K.E., 2009. aPKC phosphorylates Miranda to polarize fate determinants during neuroblast asymmetric cell division. *Curr Biol* 19, 723-729.
- Bader, J.R., Vaughan, K.T., 2010. Dynein at the kinetochore: Timing, Interactions and Functions. *Semin Cell Dev Biol* 21, 269-275.
- Baena-Lopez, L.A., Baonza, A., Garcia-Bellido, A., 2005. The orientation of cell divisions determines the shape of *Drosophila* organs. *Curr Biol* 15, 1640-1644.
- Barisic, M., Aguiar, P., Geley, S., Maiato, H., 2014. Kinetochore motors drive congression of peripheral polar chromosomes by overcoming random arm-ejection forces. *Nat Cell Biol* 16, 1249-1256.
- Basto, R., Gomes, R., Karess, R.E., 2000. Rough deal and Zw10 are required for the metaphase checkpoint in *Drosophila*. *Nat Cell Biol* 2, 939-943.
- Basto, R., Lau, J., Vinogradova, T., Gardiol, A., Woods, C.G., Khodjakov, A., Raff, J.W., 2006. Flies without centrioles. *Cell* 125, 1375-1386.
- Bell, G.P., Fletcher, G.C., Brain, R., Thompson, B.J., 2015. Aurora kinases phosphorylate Lgl to induce mitotic spindle orientation in *Drosophila* epithelia. *Curr Biol* 25, 61-68.
- Bellaiche, Y., Radovic, A., Woods, D.F., Hough, C.D., Parmentier, M.L., O'Kane, C.J., Bryant, P.J., Schweisguth, F., 2001. The Partner of Inscuteable/Discs-large complex is required to establish planar polarity during asymmetric cell division in *Drosophila*. *Cell* 106, 355-366.
- Betschinger, J., Mechtler, K., Knoblich, J.A., 2006. Asymmetric segregation of the tumor suppressor brat regulates self-renewal in *Drosophila* neural stem cells. *Cell* 124, 1241-1253.
- Bonello, T.T., Peifer, M., 2019. Scribble: A master scaffold in polarity, adhesion, synaptogenesis, and proliferation. *J Cell Biol* 218, 742-756.

- Bottenberg, W., Sanchez-Soriano, N., Alves-Silva, J., Hahn, I., Mende, M., Prokop, A., 2009. Context-specific requirements of functional domains of the Spectraplakins Short stop in vivo. *Mech Dev* 126, 489-502.
- Bouameur, J.E., Favre, B., Borradori, L., 2014. Plakins, a versatile family of cytolinkers: roles in skin integrity and in human diseases. *J Invest Dermatol* 134, 885-894.
- Bowman, S.K., Neumuller, R.A., Novatchkova, M., Du, Q., Knoblich, J.A., 2006. The *Drosophila* NuMA Homolog Mud regulates spindle orientation in asymmetric cell division. *Dev Cell* 10, 731-742.
- Butler, M.T., Wallingford, J.B., 2017. Planar cell polarity in development and disease. *Nat Rev Mol Cell Biol* 18, 375-388.
- Cabello, J., Neukomm, L.J., Gunesdogan, U., Burkart, K., Charette, S.J., Lochnit, G., Hengartner, M.O., Schnabel, R., 2010. The Wnt pathway controls cell death engulfment, spindle orientation, and migration through CED-10/Rac. *PLoS Biol* 8, e1000297.
- Cabernard, C., Doe, C.Q., 2009. Apical/basal spindle orientation is required for neuroblast homeostasis and neuronal differentiation in *Drosophila*. *Dev Cell* 17, 134-141.
- Carmena, A., Makarova, A., Speicher, S., 2011. The Rap1-Rgl-Ral signaling network regulates neuroblast cortical polarity and spindle orientation. *J Cell Biol* 195, 553-562.
- Carreno, S., Kouranti, I., Glusman, E.S., Fuller, M.T., Echard, A., Payre, F., 2008. Moesin and its activating kinase Slik are required for cortical stability and microtubule organization in mitotic cells. *J Cell Biol* 180, 739-746.
- Carrier, F., Smith, M.L., Bae, I., Kilpatrick, K.E., Lansing, T.J., Chen, C.Y., Engelstein, M., Friend, S.H., Henner, W.D., Gilmer, T.M., et al., 1994. Characterization of human Gadd45, a p53-regulated protein. *J Biol Chem* 269, 32672-32677.
- Castanon, I., Abrami, L., Holtzer, L., Heisenberg, C.P., van der Goot, F.G., Gonzalez-Gaitan, M., 2012. Anthrax toxin receptor 2a controls mitotic spindle positioning. *Nat Cell Biol*.
- Chen, H.J., Lin, C.M., Lin, C.S., Perez-Olle, R., Leung, C.L., Liem, R.K., 2006. The role of microtubule actin cross-linking factor 1 (MACF1) in the Wnt signaling pathway. *Genes Dev* 20, 1933-1945.
- Chen, J., 2016. The Cell-Cycle Arrest and Apoptotic Functions of p53 in Tumor Initiation and Progression. *Cold Spring Harb Perspect Med* 6, a026104.
- Chiyoda, T., Sugiyama, N., Shimizu, T., Naoe, H., Kobayashi, Y., Ishizawa, J., Arima, Y., Tsuda, H., Ito, M., Kaibuchi, K., Aoki, D., Ishihama, Y., Saya, H., Kuninaka, S., 2012. LATS1/WARTS phosphorylates MYPT1 to counteract PLK1 and regulate mammalian mitotic progression. *J Cell Biol* 197, 625-641.
- Clarkson, Y.L., Gillespie, T., Perkins, E.M., Lyndon, A.R., Jackson, M., 2010. Beta-III spectrin mutation L253P associated with spinocerebellar ataxia type 5 interferes with binding to Arp1 and protein trafficking from the Golgi. *Hum Mol Genet* 19, 3634-3641.

- Colombo, K., Grill, S.W., Kimple, R.J., Willard, F.S., Siderovski, D.P., Gonczy, P., 2003. Translation of polarity cues into asymmetric spindle positioning in *Caenorhabditis elegans* embryos. *Science* 300, 1957-1961.
- Couwenbergs, C., Labbe, J.C., Goulding, M., Marty, T., Bowerman, B., Gotta, M., 2007. Heterotrimeric G protein signaling functions with dynein to promote spindle positioning in *C. elegans*. *J Cell Biol* 179, 15-22.
- Cuenca, A.A., Schetter, A., Aceto, D., Kemphues, K., Seydoux, G., 2003. Polarization of the *C. elegans* zygote proceeds via distinct establishment and maintenance phases. *Development* 130, 1255-1265.
- David, N.B., Martin, C.A., Segalen, M., Rosenfeld, F., Schweisguth, F., Bellaiche, Y., 2005. *Drosophila* Ric-8 regulates Galphai cortical localization to promote Galphai-dependent planar orientation of the mitotic spindle during asymmetric cell division. *Nat Cell Biol* 7, 1083-1090.
- Dewey, E.B., Johnston, C.A., 2017. Diverse mitotic functions of the cytoskeletal cross-linking protein Shortstop suggest a role in Dynein/Dynactin activity. *Mol Biol Cell* 28, 2555-2568.
- Dewey, E.B., Sanchez, D., Johnston, C.A., 2015a. Warts Phosphorylates Mud to Promote Pins-Mediated Mitotic Spindle Orientation in *Drosophila*, Independent of Yorkie. *Curr Biol* 25, 2751-2762.
- Dewey, E.B., Sanchez, D., Johnston, C.A., 2015b. Warts phosphorylates mud to promote pins-mediated mitotic spindle orientation in *Drosophila*, independent of Yorkie. *Curr Biol* 25, 2751-2762.
- Dewey, E.B., Taylor, D.T., Johnston, C.A., 2015c. Cell Fate Decision Making through Oriented Cell Division. *J Dev Biol* 3, 129-157.
- Doe, C.Q., 2008. Neural stem cells: balancing self-renewal with differentiation. *Development* 135, 1575-1587.
- Du, Q., Macara, I.G., 2004. Mammalian Pins is a conformational switch that links NuMA to heterotrimeric G proteins. *Cell* 119, 503-516.
- Du, Q., Stukenberg, P.T., Macara, I.G., 2001. A mammalian Partner of inscuteable binds NuMA and regulates mitotic spindle organization. *Nat Cell Biol* 3, 1069-1075.
- Duckett, D.R., Bronstein, S.M., Taya, Y., Modrich, P., 1999. hMutSalph α - and hMutLalpha-dependent phosphorylation of p53 in response to DNA methylator damage. *Proc Natl Acad Sci U S A* 96, 12384-12388.
- Duro, E., Marston, A.L., 2015. From equator to pole: splitting chromosomes in mitosis and meiosis. *Genes Dev* 29, 109-122.
- Emoto, K., He, Y., Ye, B., Grueber, W.B., Adler, P.N., Jan, L.Y., Jan, Y.N., 2004. Control of dendritic branching and tiling by the Tricornered-kinase/Furry signaling pathway in *Drosophila* sensory neurons. *Cell* 119, 245-256.
- Etemad-Moghadam, B., Guo, S., Kemphues, K.J., 1995. Asymmetrically distributed PAR-3 protein contributes to cell polarity and spindle alignment in early *C. elegans* embryos. *Cell* 83, 743-752.
- Feng, Y., Irvine, K.D., 2007. Fat and expanded act in parallel to regulate growth through warts. *Proc Natl Acad Sci U S A* 104, 20362-20367.

- Fink, J., Carpi, N., Betz, T., Betard, A., Chebah, M., Azioune, A., Bornens, M., Sykes, C., Fetler, L., Cuvelier, D., Piel, M., 2011. External forces control mitotic spindle positioning. *Nat Cell Biol* 13, 771-778.
- Fletcher, D.A., Mullins, R.D., 2010. Cell mechanics and the cytoskeleton. *Nature* 463, 485-492.
- Fridman, J.S., Lowe, S.W., 2003. Control of apoptosis by p53. *Oncogene* 22, 9030-9040.
- Gachet, Y., Tournier, S., Millar, J.B., Hyams, J.S., 2001. A MAP kinase-dependent actin checkpoint ensures proper spindle orientation in fission yeast. *Nature* 412, 352-355.
- Gaglio, T., Dionne, M.A., Compton, D.A., 1997. Mitotic spindle poles are organized by structural and motor proteins in addition to centrosomes. *J Cell Biol* 138, 1055-1066.
- Gaglio, T., Saredi, A., Bingham, J.B., Hasbani, M.J., Gill, S.R., Schroer, T.A., Compton, D.A., 1996. Opposing motor activities are required for the organization of the mammalian mitotic spindle pole. *J Cell Biol* 135, 399-414.
- Galli, M., Munoz, J., Portegijs, V., Boxem, M., Grill, S.W., Heck, A.J., van den Heuvel, S., 2011. aPKC phosphorylates NuMA-related LIN-5 to position the mitotic spindle during asymmetric division. *Nat Cell Biol* 13, 1132-1138.
- Gama, J.B., Pereira, C., Simoes, P.A., Celestino, R., Reis, R.M., Barbosa, D.J., Pires, H.R., Carvalho, C., Amorim, J., Carvalho, A.X., Cheerambathur, D.K., Gassmann, R., 2017. Molecular mechanism of dynein recruitment to kinetochores by the Rod-Zw10-Zwilch complex and Spindly. *J Cell Biol*.
- Gho, M., Schweisguth, F., 1998. Frizzled signalling controls orientation of asymmetric sense organ precursor cell divisions in *Drosophila*. *Nature* 393, 178-181.
- Glotzer, M., 2005. The molecular requirements for cytokinesis. *Science* 307, 1735-1739.
- Gonzalez, C., 2007. Spindle orientation, asymmetric division and tumour suppression in *Drosophila* stem cells. *Nat Rev Genet* 8, 462-472.
- Gonzalez, C., 2013. *Drosophila melanogaster*: a model and a tool to investigate malignancy and identify new therapeutics. *Nat Rev Cancer* 13, 172-183.
- Gonzalez-Gaitan, M., Capdevila, M.P., Garcia-Bellido, A., 1994. Cell proliferation patterns in the wing imaginal disc of *Drosophila*. *Mech Dev* 46, 183-200.
- Goshima, G., Nedelec, F., Vale, R.D., 2005. Mechanisms for focusing mitotic spindle poles by minus end-directed motor proteins. *J Cell Biol* 171, 229-240.
- Gotta, M., Ahringer, J., 2001. Distinct roles for Galpha and Gbetagamma in regulating spindle position and orientation in *Caenorhabditis elegans* embryos. *Nat Cell Biol* 3, 297-300.
- Gotta, M., Dong, Y., Peterson, Y.K., Lanier, S.M., Ahringer, J., 2003. Asymmetrically distributed *C. elegans* homologs of AGS3/PINS control spindle position in the early embryo. *Curr Biol* 13, 1029-1037.

- Graybill, C., Prehoda, K.E., 2014. Ordered multisite phosphorylation of lethal giant larvae by atypical protein kinase C. *Biochemistry* 53, 4931-4937.
- Griffis, E.R., Stuurman, N., Vale, R.D., 2007. Spindly, a novel protein essential for silencing the spindle assembly checkpoint, recruits dynein to the kinetochore. *J Cell Biol* 177, 1005-1015.
- Grill, S.W., Gonczy, P., Stelzer, E.H., Hyman, A.A., 2001. Polarity controls forces governing asymmetric spindle positioning in the *Caenorhabditis elegans* embryo. *Nature* 409, 630-633.
- Grusche, F.A., Richardson, H.E., Harvey, K.F., 2010. Upstream regulation of the hippo size control pathway. *Curr Biol* 20, R574-582.
- Guo, C., Tommasi, S., Liu, L., Yee, J.K., Dammann, R., Pfeifer, G.P., 2007. RASSF1A is part of a complex similar to the *Drosophila* Hippo/Salvador/Lats tumor-suppressor network. *Curr Biol* 17, 700-705.
- Gupta, M., Gupta, S.K., Hoffman, B., Liebermann, D.A., 2006. Gadd45a and Gadd45b protect hematopoietic cells from UV-induced apoptosis via distinct signaling pathways, including p38 activation and JNK inhibition. *J Biol Chem* 281, 17552-17558.
- Han, Z., Riefler, G.M., Saam, J.R., Mango, S.E., Schumacher, J.M., 2005. The *C. elegans* Tousled-like kinase contributes to chromosome segregation as a substrate and regulator of the Aurora B kinase. *Curr Biol* 15, 894-904.
- Hanahan, D., Weinberg, R.A., 2011. Hallmarks of cancer: the next generation. *Cell* 144, 646-674.
- Hao, Y., Boyd, L., Seydoux, G., 2006. Stabilization of cell polarity by the *C. elegans* RING protein PAR-2. *Dev Cell* 10, 199-208.
- Hao, Y., Chun, A., Cheung, K., Rashidi, B., Yang, X., 2008. Tumor suppressor LATS1 is a negative regulator of oncogene YAP. *J Biol Chem* 283, 5496-5509.
- Hariharan, I.K., 2015. Organ Size Control: Lessons from *Drosophila*. *Dev Cell* 34, 255-265.
- Hariharan, I.K., Bilder, D., 2006. Regulation of imaginal disc growth by tumor-suppressor genes in *Drosophila*. *Annu Rev Genet* 40, 335-361.
- Heald, R., Tournebize, R., Blank, T., Sandaltzopoulos, R., Becker, P., Hyman, A., Karsenti, E., 1996. Self-organization of microtubules into bipolar spindles around artificial chromosomes in *Xenopus* egg extracts. *Nature* 382, 420-425.
- Hebert, A.M., DuBoff, B., Casaletto, J.B., Gladden, A.B., McClatchey, A.I., 2012. Merlin/ERM proteins establish cortical asymmetry and centrosome position. *Genes Dev* 26, 2709-2723.
- Hergovich, A., 2013. Regulation and functions of mammalian LATS/NDR kinases: looking beyond canonical Hippo signalling. *Cell Biosci* 3, 32.
- Hergovich, A., Stegert, M.R., Schmitz, D., Hemmings, B.A., 2006. NDR kinases regulate essential cell processes from yeast to humans. *Nat Rev Mol Cell Biol* 7, 253-264.
- Herranz, H., Eichenlaub, T., Cohen, S.M., 2016. Cancer in *Drosophila*: Imaginal Discs as a Model for Epithelial Tumor Formation. *Curr Top Dev Biol* 116, 181-199.

- Hildesheim, J., Bulavin, D.V., Anver, M.R., Alvord, W.G., Hollander, M.C., Vardanian, L., Fornace, A.J., Jr., 2002. Gadd45a protects against UV irradiation-induced skin tumors, and promotes apoptosis and stress signaling via MAPK and p53. *Cancer Res* 62, 7305-7315.
- Holleran, E.A., Ligon, L.A., Tokito, M., Stankewich, M.C., Morrow, J.S., Holzbaur, E.L., 2001. beta III spectrin binds to the Arp1 subunit of dynactin. *J Biol Chem* 276, 36598-36605.
- Holleran, E.A., Tokito, M.K., Karki, S., Holzbaur, E.L., 1996. Centractin (ARP1) associates with spectrin revealing a potential mechanism to link dynactin to intracellular organelles. *J Cell Biol* 135, 1815-1829.
- Hotz, M., Barral, Y., 2014. The Mitotic Exit Network: new turns on old pathways. *Trends Cell Biol* 24, 145-152.
- Hotz, M., Leisner, C., Chen, D., Manatschal, C., Wegleiter, T., Ouellet, J., Lindstrom, D., Gottschling, D.E., Vogel, J., Barral, Y., 2012. Spindle pole bodies exploit the mitotic exit network in metaphase to drive their age-dependent segregation. *Cell* 148, 958-972.
- Howell, B.J., McEwen, B.F., Canman, J.C., Hoffman, D.B., Farrar, E.M., Rieder, C.L., Salmon, E.D., 2001. Cytoplasmic dynein/dynactin drives kinetochore protein transport to the spindle poles and has a role in mitotic spindle checkpoint inactivation. *J Cell Biol* 155, 1159-1172.
- Huang, J., Wu, S., Barrera, J., Matthews, K., Pan, D., 2005. The Hippo signaling pathway coordinately regulates cell proliferation and apoptosis by inactivating Yorkie, the Drosophila Homolog of YAP. *Cell* 122, 421-434.
- Huber, F., Boire, A., Lopez, M.P., Koenderink, G.H., 2015. Cytoskeletal crosstalk: when three different personalities team up. *Curr Opin Cell Biol* 32, 39-47.
- Huisman, S.M., Segal, M., 2005. Cortical capture of microtubules and spindle polarity in budding yeast - where's the catch? *J Cell Sci* 118, 463-471.
- Ikeda, Y., Dick, K.A., Weatherspoon, M.R., Gincel, D., Armbrust, K.R., Dalton, J.C., Stevanin, G., Durr, A., Zuhlke, C., Burk, K., Clark, H.B., Brice, A., Rothstein, J.D., Schut, L.J., Day, J.W., Ranum, L.P., 2006. Spectrin mutations cause spinocerebellar ataxia type 5. *Nat Genet* 38, 184-190.
- Izumi, Y., Ohta, N., Hisata, K., Raabe, T., Matsuzaki, F., 2006. Drosophila Pins-binding protein Mud regulates spindle-polarity coupling and centrosome organization. *Nat Cell Biol* 8, 586-593.
- Jin, S., Tong, T., Fan, W., Fan, F., Antinore, M.J., Zhu, X., Mazzacurati, L., Li, X., Petrik, K.L., Rajasekaran, B., Wu, M., Zhan, Q., 2002. GADD45-induced cell cycle G2-M arrest associates with altered subcellular distribution of cyclin B1 and is independent of p38 kinase activity. *Oncogene* 21, 8696-8704.
- Johansson, M., Rocha, N., Zwart, W., Jordens, I., Janssen, L., Kuijl, C., Olkkonen, V.M., Neefjes, J., 2007. Activation of endosomal dynein motors by stepwise assembly of Rab7-RILP-p150Glued, ORP1L, and the receptor betaIII spectrin. *J Cell Biol* 176, 459-471.
- Johnston, C.A., Hirono, K., Prehoda, K.E., Doe, C.Q., 2009. Identification of an Aurora-A/PinsLINKER/Dlg spindle orientation pathway using induced cell polarity in S2 cells. *Cell* 138, 1150-1163.

- Johnston, C.A., Manning, L., Lu, M.S., Golub, O., Doe, C.Q., Prehoda, K.E., 2013. Formin-mediated actin polymerization cooperates with Mushroom body defect (Mud)-Dynein during Frizzled-Dishevelled spindle orientation. *J Cell Sci* 126, 4436-4444.
- Jorgensen, L.H., Mosbech, M.B., Faergeman, N.J., Graakjaer, J., Jacobsen, S.V., Schroder, H.D., 2014. Duplication in the microtubule-actin cross-linking factor 1 gene causes a novel neuromuscular condition. *Sci Rep* 4, 5180.
- Ka, M., Jung, E.M., Mueller, U., Kim, W.Y., 2014. MACF1 regulates the migration of pyramidal neurons via microtubule dynamics and GSK-3 signaling. *Dev Biol* 395, 4-18.
- Kardon, J.R., Vale, R.D., 2009. Regulators of the cytoplasmic dynein motor. *Nat Rev Mol Cell Biol* 10, 854-865.
- Kemphues, K.J., Priess, J.R., Morton, D.G., Cheng, N.S., 1988. Identification of genes required for cytoplasmic localization in early *C. elegans* embryos. *Cell* 52, 311-320.
- Khanal, I., Elbediwy, A., Diaz de la Loza Mdel, C., Fletcher, G.C., Thompson, B.J., 2016. Shot and Patronin polarise microtubules to direct membrane traffic and biogenesis of microvilli in epithelia. *J Cell Sci* 129, 2651-2659.
- Kim, Y., Holland, A.J., Lan, W., Cleveland, D.W., 2010. Aurora kinases and protein phosphatase 1 mediate chromosome congression through regulation of CENP-E. *Cell* 142, 444-455.
- Kiyomitsu, T., Cheeseman, I.M., 2012. Chromosome- and spindle-pole-derived signals generate an intrinsic code for spindle position and orientation. *Nat Cell Biol* 14, 311-317.
- Kiyomitsu, T., Cheeseman, I.M., 2013. Cortical dynein and asymmetric membrane elongation coordinately position the spindle in anaphase. *Cell* 154, 391-402.
- Knoblich, J.A., 2008. Mechanisms of asymmetric stem cell division. *Cell* 132, 583-597.
- Kodama, A., Karakesisoglou, I., Wong, E., Vaezi, A., Fuchs, E., 2003. ACF7: an essential integrator of microtubule dynamics. *Cell* 115, 343-354.
- Kolodziej, P.A., Jan, L.Y., Jan, Y.N., 1995. Mutations that affect the length, fasciculation, or ventral orientation of specific sensory axons in the *Drosophila* embryo. *Neuron* 15, 273-286.
- Kotak, S., Busso, C., Gonczy, P., 2012. Cortical dynein is critical for proper spindle positioning in human cells. *J Cell Biol* 199, 97-110.
- Kotak, S., Busso, C., Gonczy, P., 2013. NuMA phosphorylation by CDK1 couples mitotic progression with cortical dynein function. *EMBO J* 32, 2517-2529.
- Krause, D.R., Jonnalagadda, J.C., Gatei, M.H., Sillje, H.H., Zhou, B.B., Nigg, E.A., Khanna, K., 2003. Suppression of Tousled-like kinase activity after DNA damage or replication block requires ATM, NBS1 and Chk1. *Oncogene* 22, 5927-5937.
- Kunda, P., Baum, B., 2009. The actin cytoskeleton in spindle assembly and positioning. *Trends Cell Biol* 19, 174-179.

- Kunda, P., Pelling, A.E., Liu, T., Baum, B., 2008. Moesin controls cortical rigidity, cell rounding, and spindle morphogenesis during mitosis. *Curr Biol* 18, 91-101.
- Lancaster, O.M., Baum, B., 2014. Shaping up to divide: coordinating actin and microtubule cytoskeletal remodelling during mitosis. *Semin Cell Dev Biol* 34, 109-115.
- Lancaster, O.M., Le Berre, M., Dimitracopoulos, A., Bonazzi, D., Zlotek-Zlotkiewicz, E., Picone, R., Duke, T., Piel, M., Baum, B., 2013. Mitotic rounding alters cell geometry to ensure efficient bipolar spindle formation. *Dev Cell* 25, 270-283.
- Lara-Gonzalez, P., Westhorpe, F.G., Taylor, S.S., 2012. The spindle assembly checkpoint. *Curr Biol* 22, R966-980.
- Lechler, T., Fuchs, E., 2005. Asymmetric cell divisions promote stratification and differentiation of mammalian skin. *Nature* 437, 275-280.
- Lee, C.Y., Andersen, R.O., Cabernard, C., Manning, L., Tran, K.D., Lanskey, M.J., Bashirullah, A., Doe, C.Q., 2006a. *Drosophila* Aurora-A kinase inhibits neuroblast self-renewal by regulating aPKC/Numb cortical polarity and spindle orientation. *Genes Dev* 20, 3464-3474.
- Lee, C.Y., Robinson, K.J., Doe, C.Q., 2006b. Lgl, Pins and aPKC regulate neuroblast self-renewal versus differentiation. *Nature* 439, 594-598.
- Lee, S., Harris, K.L., Whittington, P.M., Kolodziej, P.A., 2000. short stop is allelic to kakapo, and encodes rod-like cytoskeletal-associated proteins required for axon extension. *J Neurosci* 20, 1096-1108.
- Lee, S., Kolodziej, P.A., 2002a. The plakin Short Stop and the RhoA GTPase are required for E-cadherin-dependent apical surface remodeling during tracheal tube fusion. *Development* 129, 1509-1520.
- Lee, S., Kolodziej, P.A., 2002b. Short Stop provides an essential link between F-actin and microtubules during axon extension. *Development* 129, 1195-1204.
- Levine, B.A., Moir, A.J., Patchell, V.B., Perry, S.V., 1992. Binding sites involved in the interaction of actin with the N-terminal region of dystrophin. *FEBS Lett* 298, 44-48.
- Li, R., Gundersen, G.G., 2008. Beyond polymer polarity: how the cytoskeleton builds a polarized cell. *Nat Rev Mol Cell Biol* 9, 860-873.
- Li, Z., Pearlman, A.H., Hsieh, P., 2016. DNA mismatch repair and the DNA damage response. *DNA Repair (Amst)* 38, 94-101.
- Liaw, G.J., Chiang, C.S., 2019. Inactive Tik associating with Tak1 increases p38 MAPK activity to prolong the G2 phase. *Sci Rep* 9, 1885.
- Lorenzo, D.N., Li, M.G., Mische, S.E., Armbrust, K.R., Ranum, L.P., Hays, T.S., 2010. Spectrin mutations that cause spinocerebellar ataxia type 5 impair axonal transport and induce neurodegeneration in *Drosophila*. *J Cell Biol* 189, 143-158.
- Lu, M.S., Johnston, C.A., 2013. Molecular pathways regulating mitotic spindle orientation in animal cells. *Development* 140, 1843-1856.
- Lu, M.S., Prehoda, K.E., 2013. A NudE/14-3-3 pathway coordinates dynein and the kinesin Khc73 to position the mitotic spindle. *Dev Cell* 26, 369-380.

- Machicoane, M., de Frutos, C.A., Fink, J., Rocancourt, M., Lombardi, Y., Garel, S., Piel, M., Echard, A., 2014. SLK-dependent activation of ERMs controls LGN-NuMA localization and spindle orientation. *J Cell Biol* 205, 791-799.
- Maiato, H., Rieder, C.L., Khodjakov, A., 2004. Kinetochore-driven formation of kinetochore fibers contributes to spindle assembly during animal mitosis. *J Cell Biol* 167, 831-840.
- Mao, Y., Mulvaney, J., Zakaria, S., Yu, T., Morgan, K.M., Allen, S., Basson, M.A., Francis-West, P., Irvine, K.D., 2011a. Characterization of a Dchs1 mutant mouse reveals requirements for Dchs1-Fat4 signaling during mammalian development. *Development* 138, 947-957.
- Mao, Y., Rauskolb, C., Cho, E., Hu, W.L., Hayter, H., Minihan, G., Katz, F.N., Irvine, K.D., 2006. Dachs: an unconventional myosin that functions downstream of Fat to regulate growth, affinity and gene expression in *Drosophila*. *Development* 133, 2539-2551.
- Mao, Y., Tournier, A.L., Bates, P.A., Gale, J.E., Tapon, N., Thompson, B.J., 2011b. Planar polarization of the atypical myosin Dachs orients cell divisions in *Drosophila*. *Genes Dev* 25, 131-136.
- Mao, Y., Tournier, A.L., Hoppe, A., Kester, L., Thompson, B.J., Tapon, N., 2013. Differential proliferation rates generate patterns of mechanical tension that orient tissue growth. *EMBO J* 32, 2790-2803.
- Mardin, B.R., Agircan, F.G., Lange, C., Schiebel, E., 2011. Plk1 controls the Nek2A-PP1gamma antagonism in centrosome disjunction. *Curr Biol* 21, 1145-1151.
- Mardin, B.R., Lange, C., Baxter, J.E., Hardy, T., Scholz, S.R., Fry, A.M., Schiebel, E., 2010. Components of the Hippo pathway cooperate with Nek2 kinase to regulate centrosome disjunction. *Nat Cell Biol* 12, 1166-1176.
- Mausser, J.F., Prehoda, K.E., 2012. Inscuteable regulates the Pins-Mud spindle orientation pathway. *PLoS One* 7, e29611.
- McKenney, R.J., Huynh, W., Tanenbaum, M.E., Bhabha, G., Vale, R.D., 2014. Activation of cytoplasmic dynein motility by dynactin-cargo adapter complexes. *Science* 345, 337-341.
- Mello, S.S., Attardi, L.D., 2018. Deciphering p53 signaling in tumor suppression. *Curr Opin Cell Biol* 51, 65-72.
- Menssen, R., Neutzner, A., Seufert, W., 2001. Asymmetric spindle pole localization of yeast Cdc15 kinase links mitotic exit and cytokinesis. *Curr Biol* 11, 345-350.
- Merdes, A., Heald, R., Samejima, K., Earnshaw, W.C., Cleveland, D.W., 2000. Formation of spindle poles by dynein/dynactin-dependent transport of NuMA. *J Cell Biol* 149, 851-862.
- Merdes, A., Ramyar, K., Vechio, J.D., Cleveland, D.W., 1996. A complex of NuMA and cytoplasmic dynein is essential for mitotic spindle assembly. *Cell* 87, 447-458.
- Mollereau, B., Ma, D., 2016. Rb-mediated apoptosis or proliferation: It's up to JNK. *Cell Cycle* 15, 11-12.

- Morales-Mulia, S., Scholey, J.M., 2005. Spindle pole organization in *Drosophila* S2 cells by dynein, abnormal spindle protein (Asp), and KLP10A. *Mol Biol Cell* 16, 3176-3186.
- Morisaki, T., Hirota, T., Iida, S., Marumoto, T., Hara, T., Nishiyama, Y., Kawasaki, M., Hiraoka, T., Mimori, T., Araki, N., Izawa, I., Inagaki, M., Saya, H., 2002. WARTS tumor suppressor is phosphorylated by Cdc2/cyclin B at spindle poles during mitosis. *FEBS Lett* 529, 319-324.
- Motegi, F., Zonies, S., Hao, Y., Cuenca, A.A., Griffin, E., Seydoux, G., 2011. Microtubules induce self-organization of polarized PAR domains in *Caenorhabditis elegans* zygotes. *Nat Cell Biol* 13, 1361-1367.
- Moulding, D.A., Blundell, M.P., Spiller, D.G., White, M.R., Cory, G.O., Calle, Y., Kempinski, H., Sinclair, J., Ancliff, P.J., Kinnon, C., Jones, G.E., Thrasher, A.J., 2007. Unregulated actin polymerization by WASp causes defects of mitosis and cytokinesis in X-linked neutropenia. *J Exp Med* 204, 2213-2224.
- Mui, U.N., Lubczyk, C.M., Nam, S.C., 2011. Role of spectraplakins in *Drosophila* photoreceptor morphogenesis. *PLoS One* 6, e25965.
- Munro, E., Nance, J., Priess, J.R., 2004. Cortical flows powered by asymmetrical contraction transport PAR proteins to establish and maintain anterior-posterior polarity in the early *C. elegans* embryo. *Dev Cell* 7, 413-424.
- Muresan, V., Stankewich, M.C., Steffen, W., Morrow, J.S., Holzbaur, E.L., Schnapp, B.J., 2001. Dynactin-dependent, dynein-driven vesicle transport in the absence of membrane proteins: a role for spectrin and acidic phospholipids. *Mol Cell* 7, 173-183.
- Nakajima, Y., Meyer, E.J., Kroesen, A., McKinney, S.A., Gibson, M.C., 2013. Epithelial junctions maintain tissue architecture by directing planar spindle orientation. *Nature* 500, 359-362.
- Nashchekin, D., Fernandes, A.R., St Johnston, D., 2016. Patronin/Shot Cortical Foci Assemble the Noncentrosomal Microtubule Array that Specifies the *Drosophila* Anterior-Posterior Axis. *Dev Cell* 38, 61-72.
- Nechiporuk, T., Klezovitch, O., Nguyen, L., Vasioukhin, V., 2013. Dlg5 maintains apical aPKC and regulates progenitor differentiation during lung morphogenesis. *Dev Biol* 377, 375-384.
- Nestor-Bergmann, A., Goddard, G., Woolner, S., 2014. Force and the spindle: mechanical cues in mitotic spindle orientation. *Semin Cell Dev Biol* 34, 133-139.
- Nguyen-Ngoc, T., Afshar, K., Gonczy, P., 2007. Coupling of cortical dynein and G alpha proteins mediates spindle positioning in *Caenorhabditis elegans*. *Nat Cell Biol* 9, 1294-1302.
- Ning, W., Yu, Y., Xu, H., Liu, X., Wang, D., Wang, J., Wang, Y., Meng, W., 2016. The CAMSAP3-ACF7 Complex Couples Noncentrosomal Microtubules with Actin Filaments to Coordinate Their Dynamics. *Dev Cell* 39, 61-74.
- Nipper, R.W., Siller, K.H., Smith, N.R., Doe, C.Q., Prehoda, K.E., 2007. Galphai generates multiple Pins activation states to link cortical polarity and spindle orientation in *Drosophila* neuroblasts. *Proc Natl Acad Sci U S A* 104, 14306-14311.

- O'Connell, C.B., Khodjakov, A.L., 2007. Cooperative mechanisms of mitotic spindle formation. *J Cell Sci* 120, 1717-1722.
- Oh, H., Irvine, K.D., 2008. In vivo regulation of Yorkie phosphorylation and localization. *Development* 135, 1081-1088.
- Papa, S., Zazzeroni, F., Bubici, C., Jayawardena, S., Alvarez, K., Matsuda, S., Nguyen, D.U., Pham, C.G., Nelsbach, A.H., Melis, T., De Smaele, E., Tang, W.J., D'Adamio, L., Franzoso, G., 2004. Gadd45 beta mediates the NF-kappa B suppression of JNK signalling by targeting MKK7/JNKK2. *Nat Cell Biol* 6, 146-153.
- Park, D.H., Rose, L.S., 2008. Dynamic localization of LIN-5 and GPR-1/2 to cortical force generation domains during spindle positioning. *Dev Biol* 315, 42-54.
- Petridou, N.I., Skourides, P.A., 2014. FAK transduces extracellular forces that orient the mitotic spindle and control tissue morphogenesis. *Nat Commun* 5, 5240.
- Petronczki, M., Knoblich, J.A., 2001. DmPAR-6 directs epithelial polarity and asymmetric cell division of neuroblasts in *Drosophila*. *Nat Cell Biol* 3, 43-49.
- Poulson, N.D., Lechler, T., 2010. Robust control of mitotic spindle orientation in the developing epidermis. *J Cell Biol* 191, 915-922.
- Poulton, J.S., Cuningham, J.C., Peifer, M., 2014. Acentrosomal *Drosophila* epithelial cells exhibit abnormal cell division, leading to cell death and compensatory proliferation. *Dev Cell* 30, 731-745.
- Poulton, J.S., Cuningham, J.C., Peifer, M., 2017. Centrosome and spindle assembly checkpoint loss leads to neural apoptosis and reduced brain size. *J Cell Biol* 216, 1255-1265.
- Poulton, J.S., McKay, D.J., Peifer, M., 2019. Centrosome Loss Triggers a Transcriptional Program To Counter Apoptosis-Induced Oxidative Stress. *Genetics*.
- Prokop, A., Uhler, J., Roote, J., Bate, M., 1998. The kakapo mutation affects terminal arborization and central dendritic sprouting of *Drosophila* motoneurons. *J Cell Biol* 143, 1283-1294.
- Prosser, S.L., Pelletier, L., 2017. Mitotic spindle assembly in animal cells: a fine balancing act. *Nat Rev Mol Cell Biol* 18, 187-201.
- Quintyne, N.J., Gill, S.R., Eckley, D.M., Crego, C.L., Compton, D.A., Schroer, T.A., 1999. Dynactin is required for microtubule anchoring at centrosomes. *J Cell Biol* 147, 321-334.
- Raaijmakers, J.A., Tanenbaum, M.E., Medema, R.H., 2013. Systematic dissection of dynein regulators in mitosis. *J Cell Biol* 201, 201-215.
- Raghavan, S., Bauer, C., Mundschaug, G., Li, Q., Fuchs, E., 2000. Conditional ablation of beta1 integrin in skin. Severe defects in epidermal proliferation, basement membrane formation, and hair follicle invagination. *J Cell Biol* 150, 1149-1160.
- Ramkumar, N., Baum, B., 2016. Coupling changes in cell shape to chromosome segregation. *Nat Rev Mol Cell Biol* 17, 511-521.

- Rauskolb, C., Sun, S., Sun, G., Pan, Y., Irvine, K.D., 2014. Cytoskeletal tension inhibits Hippo signaling through an Ajuba-Warts complex. *Cell* 158, 143-156.
- Repiso, A., Bergantinos, C., Serras, F., 2013. Cell fate respecification and cell division orientation drive intercalary regeneration in *Drosophila* wing discs. *Development* 140, 3541-3551.
- Roberts, S., Calautti, E., Vanderweil, S., Nguyen, H.O., Foley, A., Baden, H.P., Viel, A., 2007. Changes in localization of human discs large (hDlg) during keratinocyte differentiation are [corrected] associated with expression of alternatively spliced hDlg variants. *Exp Cell Res* 313, 2521-2530.
- Roper, K., Brown, N.H., 2003. Maintaining epithelial integrity: a function for gigantic spectraplakins isoforms in adherens junctions. *J Cell Biol* 162, 1305-1315.
- Rosenblatt, J., Cramer, L.P., Baum, B., McGee, K.M., 2004. Myosin II-dependent cortical movement is required for centrosome separation and positioning during mitotic spindle assembly. *Cell* 117, 361-372.
- Sabino, D., Gogendeau, D., Gambarotto, D., Nano, M., Pannetier, C., Dingli, F., Arras, G., Loew, D., Basto, R., 2015. Moesin is a major regulator of centrosome behavior in epithelial cells with extra centrosomes. *Curr Biol* 25, 879-889.
- Sanchez-Soriano, N., Goncalves-Pimentel, C., Beaven, R., Haessler, U., Ofner-Ziegenfuss, L., Ballestrem, C., Prokop, A., 2010. *Drosophila* growth cones: a genetically tractable platform for the analysis of axonal growth dynamics. *Dev Neurobiol* 70, 58-71.
- Sanchez-Soriano, N., Travis, M., Dajas-Bailador, F., Goncalves-Pimentel, C., Whitmarsh, A.J., Prokop, A., 2009. Mouse ACF7 and *drosophila* short stop modulate filopodia formation and microtubule organisation during neuronal growth. *J Cell Sci* 122, 2534-2542.
- Sandquist, J.C., Kita, A.M., Bement, W.M., 2011. And the dead shall rise: actin and myosin return to the spindle. *Dev Cell* 21, 410-419.
- Sawin, K.E., LeGuellec, K., Philippe, M., Mitchison, T.J., 1992. Mitotic spindle organization by a plus-end-directed microtubule motor. *Nature* 359, 540-543.
- Schaefer, M., Petronczki, M., Dorner, D., Forte, M., Knoblich, J.A., 2001. Heterotrimeric G proteins direct two modes of asymmetric cell division in the *Drosophila* nervous system. *Cell* 107, 183-194.
- Segalen, M., Johnston, C.A., Martin, C.A., Dumortier, J.G., Prehoda, K.E., David, N.B., Doe, C.Q., Bellaiche, Y., 2010. The Fz-Dsh planar cell polarity pathway induces oriented cell division via Mud/NuMA in *Drosophila* and zebrafish. *Dev Cell* 19, 740-752.
- Sen, S.P., De Benedetti, A., 2006. TLK1B promotes repair of UV-damaged DNA through chromatin remodeling by Asf1. *BMC Mol Biol* 7, 37.
- Sharp, D.J., Rogers, G.C., Scholey, J.M., 2000. Cytoplasmic dynein is required for poleward chromosome movement during mitosis in *Drosophila* embryos. *Nat Cell Biol* 2, 922-930.

- Shiizaki, S., Naguro, I., Ichijo, H., 2013. Activation mechanisms of ASK1 in response to various stresses and its significance in intracellular signaling. *Adv Biol Regul* 53, 135-144.
- Siller, K.H., Cabernard, C., Doe, C.Q., 2006. The NuMA-related Mud protein binds Pins and regulates spindle orientation in *Drosophila* neuroblasts. *Nat Cell Biol* 8, 594-600.
- Siller, K.H., Doe, C.Q., 2008. Lis1/dynactin regulates metaphase spindle orientation in *Drosophila* neuroblasts. *Dev Biol* 319, 1-9.
- Siller, K.H., Doe, C.Q., 2009. Spindle orientation during asymmetric cell division. *Nat Cell Biol* 11, 365-374.
- Siller, K.H., Serr, M., Steward, R., Hays, T.S., Doe, C.Q., 2005. Live imaging of *Drosophila* brain neuroblasts reveals a role for Lis1/dynactin in spindle assembly and mitotic checkpoint control. *Mol Biol Cell* 16, 5127-5140.
- Smith, C.A., Lau, K.M., Rahmani, Z., Dho, S.E., Brothers, G., She, Y.M., Berry, D.M., Bonneil, E., Thibault, P., Schweisguth, F., Le Borgne, R., McGlade, C.J., 2007. aPKC-mediated phosphorylation regulates asymmetric membrane localization of the cell fate determinant Numb. *EMBO J* 26, 468-480.
- Smith, M.L., Chen, I.T., Zhan, Q., Bae, I., Chen, C.Y., Gilmer, T.M., Kastan, M.B., O'Connor, P.M., Fornace, A.J., Jr., 1994. Interaction of the p53-regulated protein Gadd45 with proliferating cell nuclear antigen. *Science* 266, 1376-1380.
- Smith, M.L., Ford, J.M., Hollander, M.C., Bortnick, R.A., Amundson, S.A., Seo, Y.R., Deng, C.X., Hanawalt, P.C., Fornace, A.J., Jr., 2000. p53-mediated DNA repair responses to UV radiation: studies of mouse cells lacking p53, p21, and/or gadd45 genes. *Mol Cell Biol* 20, 3705-3714.
- Soto, M., Raaijmakers, J.A., Medema, R.H., 2019. Consequences of Genomic Diversification Induced by Segregation Errors. *Trends Genet* 35, 279-291.
- Srinivasan, D.G., Fisk, R.M., Xu, H., van den Heuvel, S., 2003. A complex of LIN-5 and GPR proteins regulates G protein signaling and spindle function in *C elegans*. *Genes Dev* 17, 1225-1239.
- Stevens, N.R., Raposo, A.A., Basto, R., St Johnston, D., Raff, J.W., 2007. From stem cell to embryo without centrioles. *Curr Biol* 17, 1498-1503.
- Strasser, A., O'Connor, L., Dixit, V.M., 2000. Apoptosis signaling. *Annu Rev Biochem* 69, 217-245.
- Sunavala-Dossabhoy, G., Li, Y., Williams, B., De Benedetti, A., 2003. A dominant negative mutant of TLK1 causes chromosome missegregation and aneuploidy in normal breast epithelial cells. *BMC Cell Biol* 4, 16.
- Suoizzi, K.C., Wu, X., Fuchs, E., 2012. Spectraplakins: master orchestrators of cytoskeletal dynamics. *J Cell Biol* 197, 465-475.
- Tauchman, E.C., Boehm, F.J., DeLuca, J.G., 2015. Stable kinetochore-microtubule attachment is sufficient to silence the spindle assembly checkpoint in human cells. *Nat Commun* 6, 10036.
- Tellkamp, F., Vorhagen, S., Niessen, C.M., 2014. Epidermal polarity genes in health and disease. *Cold Spring Harb Perspect Med* 4, a015255.

- Thery, M., Racine, V., Pepin, A., Piel, M., Chen, Y., Sibarita, J.B., Bornens, M., 2005. The extracellular matrix guides the orientation of the cell division axis. *Nat Cell Biol* 7, 947-953.
- Toji, S., Yabuta, N., Hosomi, T., Nishihara, S., Kobayashi, T., Suzuki, S., Tamai, K., Nojima, H., 2004. The centrosomal protein Lats2 is a phosphorylation target of Aurora-A kinase. *Genes Cells* 9, 383-397.
- Toyoshima, F., Nishida, E., 2007. Integrin-mediated adhesion orients the spindle parallel to the substratum in an EB1- and myosin X-dependent manner. *EMBO J* 26, 1487-1498.
- Urnavicius, L., Zhang, K., Diamant, A.G., Motz, C., Schlager, M.A., Yu, M., Patel, N.A., Robinson, C.V., Carter, A.P., 2015. The structure of the dynactin complex and its interaction with dynein. *Science* 347, 1441-1446.
- Varma, D., Salmon, E.D., 2012. The KMN protein network--chief conductors of the kinetochore orchestra. *J Cell Sci* 125, 5927-5936.
- Villicana, C., Cruz, G., Zurita, M., 2013. The genetic depletion or the triptolide inhibition of TFIID in p53-deficient cells induces a JNK-dependent cell death in *Drosophila*. *J Cell Sci* 126, 2502-2515.
- Vorhagen, S., Niessen, C.M., 2014. Mammalian aPKC/Par polarity complex mediated regulation of epithelial division orientation and cell fate. *Exp Cell Res* 328, 296-302.
- Walczak, C.E., Vernos, I., Mitchison, T.J., Karsenti, E., Heald, R., 1998. A model for the proposed roles of different microtubule-based motor proteins in establishing spindle bipolarity. *Curr Biol* 8, 903-913.
- Wang, C., Li, S., Januschke, J., Rossi, F., Izumi, Y., Garcia-Alvarez, G., Gwee, S.S., Soon, S.B., Sidhu, H.K., Yu, F., Matsuzaki, F., Gonzalez, C., Wang, H., 2011. An ana2/ctp/mud complex regulates spindle orientation in *Drosophila* neuroblasts. *Dev Cell* 21, 520-533.
- Wang, X.W., Zhan, Q., Coursen, J.D., Khan, M.A., Kontny, H.U., Yu, L., Hollander, M.C., O'Connor, P.M., Fornace, A.J., Jr., Harris, C.C., 1999. GADD45 induction of a G2/M cell cycle checkpoint. *Proc Natl Acad Sci U S A* 96, 3706-3711.
- Wang, Y., Liu, J., Xia, R., Wang, J., Shen, J., Cao, R., Hong, X., Zhu, J.K., Gong, Z., 2007. The protein kinase TOUSLED is required for maintenance of transcriptional gene silencing in *Arabidopsis*. *EMBO Rep* 8, 77-83.
- Wee, B., Johnston, C.A., Prehoda, K.E., Doe, C.Q., 2011. Canoe binds RanGTP to promote Pins(TPR)/Mud-mediated spindle orientation. *J Cell Biol* 195, 369-376.
- Werts, A.D., Roh-Johnson, M., Goldstein, B., 2011. Dynamic localization of *C. elegans* TPR-GoLoco proteins mediates mitotic spindle orientation by extrinsic signaling. *Development* 138, 4411-4422.
- Williams, S.E., Beronja, S., Pasolli, H.A., Fuchs, E., 2011. Asymmetric cell divisions promote Notch-dependent epidermal differentiation. *Nature* 470, 353-358.
- Wodarz, A., Ramrath, A., Kuchinke, U., Knust, E., 1999. Bazooka provides an apical cue for Inscuteable localization in *Drosophila* neuroblasts. *Nature* 402, 544-547.

- Wu, S., Huang, J., Dong, J., Pan, D., 2003. hippo encodes a Ste-20 family protein kinase that restricts cell proliferation and promotes apoptosis in conjunction with salvador and warts. *Cell* 114, 445-456.
- Wu, X., Kodama, A., Fuchs, E., 2008. ACF7 regulates cytoskeletal-focal adhesion dynamics and migration and has ATPase activity. *Cell* 135, 137-148.
- Yabuta, N., Mukai, S., Okada, N., Aylon, Y., Nojima, H., 2011. The tumor suppressor Lats2 is pivotal in Aurora A and Aurora B signaling during mitosis. *Cell Cycle* 10, 2724-2736.
- Yang, C.H., Lambie, E.J., Snyder, M., 1992. NuMA: an unusually long coiled-coil related protein in the mammalian nucleus. *J Cell Biol* 116, 1303-1317.
- Yang, Z., Tulu, U.S., Wadsworth, P., Rieder, C.L., 2007. Kinetochore dynein is required for chromosome motion and congression independent of the spindle checkpoint. *Curr Biol* 17, 973-980.
- Yin, H., Pruyne, D., Huffaker, T.C., Bretscher, A., 2000. Myosin V orientates the mitotic spindle in yeast. *Nature* 406, 1013-1015.
- Yoo, J., Ghiassi, M., Jirmanova, L., Balliet, A.G., Hoffman, B., Fornace, A.J., Jr., Liebermann, D.A., Bottinger, E.P., Roberts, A.B., 2003. Transforming growth factor-beta-induced apoptosis is mediated by Smad-dependent expression of GADD45b through p38 activation. *J Biol Chem* 278, 43001-43007.
- Yu, F., Morin, X., Cai, Y., Yang, X., Chia, W., 2000. Analysis of partner of inscuteable, a novel player of *Drosophila* asymmetric divisions, reveals two distinct steps in inscuteable apical localization. *Cell* 100, 399-409.
- Zhan, Q., Chen, I.T., Antinore, M.J., Fornace, A.J., Jr., 1998. Tumor suppressor p53 can participate in transcriptional induction of the GADD45 promoter in the absence of direct DNA binding. *Mol Cell Biol* 18, 2768-2778.
- Zhan, Q., Fan, S., Smith, M.L., Bae, I., Yu, K., Alamo, I., Jr., O'Connor, P.M., Fornace, A.J., Jr., 1996. Abrogation of p53 function affects gadd gene responses to DNA base-damaging agents and starvation. *DNA Cell Biol* 15, 805-815.
- Zhang, K., Foster, H.E., Rondelet, A., Lacey, S.E., Bahi-Buisson, N., Bird, A.W., Carter, A.P., 2017. Cryo-EM Reveals How Human Cytoplasmic Dynein Is Auto-inhibited and Activated. *Cell*.
- Zhang, Y., Cai, R., Zhou, R., Li, Y., Liu, L., 2016. Tousled-like kinase mediated a new type of cell death pathway in *Drosophila*. *Cell Death Differ* 23, 146-157.
- Zhao, B., Tumaneng, K., Guan, K.L., 2011. The Hippo pathway in organ size control, tissue regeneration and stem cell self-renewal. *Nat Cell Biol* 13, 877-883.
- Zhong, T., Zhou, J., 2017. Orientation of the Mitotic Spindle in the Development of Tubular Organs. *J Cell Biochem* 118, 1630-1633.
- Zhu, J., Wen, W., Zheng, Z., Shang, Y., Wei, Z., Xiao, Z., Pan, Z., Du, Q., Wang, W., Zhang, M., 2011. LGN/mlnsc and LGN/NuMA complex structures suggest distinct functions in asymmetric cell division for the

Par3/mInsc/LGN and Galphai/LGN/NuMA pathways. *Mol Cell* 43, 418-431.

Zu, K., Hawthorn, L., Ip, C., 2005. Up-regulation of c-Jun-NH2-kinase pathway contributes to the induction of mitochondria-mediated apoptosis by alpha-tocopheryl succinate in human prostate cancer cells. *Mol Cancer Ther* 4, 43-50.

